

إقرار

أنا الموقع أدناه مقدم الرسالة التي تحمل العنوان:

Negative Refractive Index- Semiconductor Circular Waveguide Fiber

أقر بأن ما اشتملت عليه هذه الرسالة إنما هي نتاج جهدي الخاص، باستثناء ما تمت الإشارة إليه حيثما ورد، وإن هذه الرسالة ككل، أو أي جزء منها لم يقدم من قبل لنيل درجة أو لقب علمي أو بحث لدى أية مؤسسة تعليمية أو بحثية أخرى.

DECLARATION

The work provided in this thesis, unless otherwise referenced, is the researcher's own work, and has not been submitted elsewhere for any other degree or qualification.

Student's name: **Abdalla Sami Saadeh**

اسم الطالب :

Signature:



التوقيع: عبد الله سامي إبراهيم سعد

Date: 27/07/2013

التاريخ: ٢٧/٧/٢٠١٣ م

Islamic University of Gaza
Deanery of Graduate Science
Faculty of Science
Department of Physics



**NEGATIVE REFRACTIVE INDEX –
SEMICONDUCTOR CIRCULAR
WAVEGUIDE FIBER**

By

Abdalla Sami Saadeh

Supervisor

Prof. Dr. Mohmmmed M. Shabat

**Submitted to the Faculty of Science as a partial Fulfillment of
the Master degree of Science program (M. Sc.) in Physics**

Palestine – Gaza

May- 2013



نتيجة الحكم على أطروحة ماجستير

بناءً على موافقة عمادة الدراسات العليا بالجامعة الإسلامية بغزة على تشكيل لجنة الحكم على أطروحة الباحث/ عبدالله سامي إبراهيم سعادة لنيل درجة الماجستير في كلية العلوم/ قسم الفيزياء وموضوعها:

Negative refractive index -semiconductor circular waveguide fiber

وبعد المناقشة العلنية التي تمت اليوم الأحد 30 رجب 1434هـ، الموافق 2013/06/09 الساعة التاسعة صباحاً بمبنى القدس، اجتمعت لجنة الحكم على الأطروحة والمكونة من:

..... MSA	مشرفاً ورئيساً	أ.د. محمد موسى شبات
..... عبدالله	مناقشاً داخلياً	د. سفيان عبد الرحمن تايه
..... عبدالله	مناقشاً خارجياً	أ.د. علي حامد الأسطل

وبعد المداولة أوصت اللجنة بمنح الباحث درجة الماجستير في كلية العلوم/قسم الفيزياء.

واللجنة إذ تمنحه هذه الدرجة فإنها توصيه بتقوى الله ولزوم طاعته وأن يسخر علمه في خدمة دينه ووطنه.

والله ولي التوفيق،،،

عميد الدراسات العليا

.....
د. فؤاد علي العاجز
أ.د. فؤاد علي العاجز

- To my dear parents, brothers, and sisters for their support, continuous encouragement, and love.
- To my family for their great care and help.
- To my friends and relatives.
- To my homeland Palestine.

Abdalla Sami Saadeh

ACKNOWLEDGMENTS

In the name of Allah to whom provide my endless support, encouragement and help me to complete my thesis. I would like to express my deep thanks to all those who helped me greatly to overcome the obstacles.

I am extremely indebted to my supervisor Professor Dr. Mohammed. M. Shabat not only for his continuous efforts but also for his effective help. He worked day and night to help me to arrange and write my thesis. Also, I would like to express my deep thanks to Dr. Sofyan Taya who supported me and was always by my side. Also, I would like to thank Dr. Mazen Abadla too for his continues guidance during my research.

In fact, I would like to express my deepest appreciation to the wonderful staff of Physics Department at the Islamic University of Gaza.

Finally, I am deeply and forever indebted to my lovely parents and my wife for their support and encouragement through my entire life.

Palestine, Gaza

May, 2013

Abdalla Sami Saadeh

ABSTRACT

In this work, we will consider the electromagnetic waves propagation along the symmetric cylindrical fiber with left handed material (LHM) as the core layer bounded by a semiconductor clad layer. We will study the dispersion properties in the considered optical fiber for two cases. In the first case, we consider the leading diagonal elements of the semiconductor permittivity tensor are different from each other. In the second case, we consider as a special case, the elements are equal to each other.

In the two cases, the fast and slow modes will be studied in TE, TM, HE and EH mode polarizations. The dispersion relations for all modes will be obtained from Maxwell's equations. The total power flow in the structure within core and clad layers will be calculated in the general and in special cases for TE and TM mode polarizations. The dispersion curves for TE, TM, HE and EH modes will be studied for different parameters of the structure.

List of Figure Captions

CHAPTER ONE

- Figure 1.1:** Wave pulse moving at constant speed .4
- Figure 1.2:** Light reflection at different cases with a) $n_1 < n_2$, $\theta_1 > \theta_c$ and b) $n_1 > n_2$, $\theta_1 < \theta_c$ and c) $n_1 > n_2$, $\theta_1 \geq \theta_c$ (TIR). 12
- Figure 1.3:** Fiber consists of a cylindrical central core clad by a material. 14
- Figure 1.4:** Light rays impinging on the core -cladding interface at an angle greater than the critical angle are trapped inside the core of the fiber. 15
- Figure 1.5:** Permittivity-permeability ($\epsilon - \mu$) and refractive index (n) diagram for all materials. 17
- Figure 1.6:** Orientation of the electric and magnetic vectors of the intensity of the electromagnetic fields, \mathbf{E} and \mathbf{H} , with respect to the wave vector \mathbf{k} and Poynting vector \mathbf{S} for LHM and RHM. 18

CHAPTER TWO

- Figure 2.1:** Structure of the optical fiber with LHM core and dielectric clad 21
- Figure 2.2:** Optical fiber in a cylindrical coordinate system (r, θ, z) . 21
- Figure 2.3:** Zero- and first-order Bessel functions of the second kind with $m = 0, 1$. 27
- Figure 2.4:** Modified Bessel functions of first $I_m(x)$ and the second $K_m(x)$ kind with $m = 0, 1$. 28
- Figure 2.5:** Dispersion curves described the fast mode (AB curve), fast- slow mode (CF curve) and slow mode (PL curve). Fiber parameters: cladding $\epsilon_{cl} = 2.5$, $\mu_{cl} = 1$) $n_{cl} = \sqrt{\epsilon_{cl}\mu_{cl}}$, and fiber radius $a = 1cm$ after [25]. 40
- Figure 2.6:** Fast guided modes with curve AB- type at $m = 0, 1$ with fiber parameters $\epsilon_{cl} = 2.5$, $\mu_{cl} = 1$, and fiber radius $a = 1cm$ by [25]. 40
- Figure 2.7:** The fast-slow and slow low-order guided modes $m = 0, 1$. with fiber parameters : $\epsilon_{cl} = 2.5$, $\mu_{cl} = 1$, and fiber radius $a = 1cm$ by [25]. 41

CHAPTER THREE

- Figure 3.1:** Schematic for optical fiber with LHM core layer, semiconductor 46

clad..

CHAPTER FOUR

- Figure 4.1:** Dispersion relation for TM mode with different fractional area F . **69**
Fiber parameters $m = 0, \mu_{cl} = 1, a = 30\mu m, \omega_p / 2\pi = 10GHz,$
 $\nu / 2\pi = 3GHz$ and $\omega_c / 2\pi = 7GHz.$
- Figure 4.2:** Dispersion relation for TM mode with different core fiber radius a . **69**
Fiber parameters $m = 0, \mu_{cl} = 1, F = 0.56, \omega_p / 2\pi = 10GHz,$
 $\nu / 2\pi = 3GHz$ and $\omega_c / 2\pi = 7GHz.$
- Figure 4.3:** Dispersion relation for TE mode with different fractional area F . **70**
Fiber parameters $m = 0, \mu_{cl} = 1, \omega_p / 2\pi = 10GHz, a = 30\mu m$
 $\nu / 2\pi = 3GHz$ and $\omega_c / 2\pi = 7GHz.$
- Figure 4.4:** Dispersion relation for TE mode with different core fiber radius a . **71**
Fiber parameters $m = 0, \mu_{cl} = 1, \omega_p / 2\pi = 10GHz, \nu / 2\pi = 3GHz,$
 $F = 0.56$ and $\omega_c / 2\pi = 7GHz.$
- Figure 4.5:** Dispersion relation for HE mode with different fractional area F **72**
. Fiber parameters $m = 1, \mu_{cl} = 1, a = 30\mu m, \omega_p / 2\pi = 10GHz$
 $\nu / 2\pi = 3GHz$ and $\omega_c / 2\pi = 7GHz.$
- Figure 4.6:** Dispersion relation for HE mode with different core fiber radius a . **72**
Fiber parameters $m = 1, \mu_{cl} = 1, F = 0.56, \omega_p / 2\pi = 10GHz,$
 $\nu / 2\pi = 3GHz$ and $\omega_c / 2\pi = 7GHz.$
- Figure 4.7:** Dispersion relation for EH mode with different fractional area F **73**
Fiber parameters $m = 1, \mu_{cl} = 1, a = 30\mu m, \omega_p / 2\pi = 10GHz,$
 $\nu / 2\pi = 3GHz$ and $\omega_c / 2\pi = 7GHz.$
- Figure 4.8:** Dispersion relation for EH mode with different core fiber radius a **73**
Fiber parameters $m = 1, \mu_{cl} = 1, F = 0.56, \omega_p / 2\pi = 10GHz,$
 $\nu / 2\pi = 3GHz$ and $\omega_c / 2\pi = 7GHz.$
- Figure 4.9:** The total real part of the power flowing through the structure in TE **74**
mode versus the frequency with different value of core radius a .
Fiber parameters $F = 0.56, \mu_{cl} = 1, C = 1, \omega_p / 2\pi = 10GHz$
, $\nu / 2\pi = 3GHz$ and $\omega_c / 2\pi = 7GHz.$

- Figure 4.10:** The total imaginary part of the power flowing through the structure in TE mode versus the frequency with different values of core radius a . Fiber parameters $F = 0.56, \mu_{cl}=1, C=1, \omega_p/2\pi = 10GHz,$
 $\omega_c/2\pi = 7GHz$ and $\nu/2\pi = 3GHz$. **75**
- Figure 4.11:** The total real part of the power flowing through the structure in TE mode versus the frequency with different values of fractional area F ., Fiber parameters, $\mu_{cl}=1, C=1, \omega_p/2\pi = 10GHz, \omega_c/2\pi = 7GHz,$
 $\nu/2\pi = 3GHz$ and $a = 30\mu m$. **76**
- Figure 4.12:** The total imaginary part of the power flowing through the structure in TE mode versus the frequency with different values of fractional area F . Fiber parameters, $\mu_{cl}=1, C=1, \omega_p/2\pi = 10GHz,$
 $\omega_c/2\pi = 7GHz, \nu/2\pi = 3GHz$ and $a = 30\mu m$. **76**
- Figure 4.13:** The total real part of the power flowing through the structure in TE mode versus the propagation constant with different values of core radius a . Fiber parameters $F = 0.56, \mu_{cl}=1, C=1,$
 $\omega_p/2\pi = 10GHz, \omega_c/2\pi = 7GHz$ and $\nu/2\pi = 3GHz$. **77**
- Figure 4.14:** The total imaginary power flowing through the structure in TE modes versus the propagation constant with different values of core radius a . Fiber parameters $F = 0.56, \mu_{cl}=1, C=1,$
 $\omega_p/2\pi = 10GHz, \omega_c/2\pi = 7GHz$ and $\nu/2\pi = 3GHz$. **78**
- Figure 4.15:** The total real part of the power flowing through the structure in TM mode versus the frequency with different values of core radius a . Fiber parameters $F = 0.56, \mu_{cl}=1, C=1, \omega_p/2\pi = 10GHz, \nu/2\pi = 3GHz$ and
 $\omega_c/2\pi = 7GHz$. **79**
- Figure 4.16:** The total imaginary part of the power flowing through the structure in TM mode versus the frequency with different values of core radius a . Fiber parameters $F = 0.56, \mu_{cl}=1, C=1, \omega_p/2\pi = 10GHz,$
 $\omega_c/2\pi = 7GHz$ and $\nu/2\pi = 3GHz$. **79**
- Figure 4.17:** The total real part of the power flowing through the structure in TM mode versus the frequency with different value of fractional area F , Fiber parameters, $\mu_{cl}=1, C=1, \omega_p/2\pi = 10GHz, \omega_c/2\pi = 7GHz$ **80**

$$v/2\pi = 3\text{GHz} \text{ and } a = 30\mu\text{m}.$$

- Figure 4.18:** The total imaginary part of the power flowing through the structure in TM mode versus the frequency with different values of fractional area F . Fiber parameters $a = 30\mu\text{m}$, $\mu_{cl} = 1$, $C = 1$, $\omega_p/2\pi = 10\text{GHz}$, $\omega_c/2\pi = 7\text{GHz}$ and $v/2\pi = 3\text{GHz}$. 81
- Figure 4.19:** The total real part of the power flowing through the structure in TM mode versus the propagation constant with different values of core radius a . Fiber parameters $F = 0.56$, $\mu_{cl} = 1$, $A = 1$, $\omega_p/2\pi = 10\text{GHz}$, $\omega_c/2\pi = 7\text{GHz}$, $v/2\pi = 3\text{GHz}$ and $a = 30\mu\text{m}$. 82
- Figure 4.20:** The total imaginary part of the power flowing through the structure in TM mode versus the propagation constant with different values of core radius a . Fiber parameters $F = 0.56$, $\mu_{cl} = 1$, $A = 1$, $\omega_p/2\pi = 10\text{GHz}$, $\omega_c/2\pi = 7\text{GHz}$, $v/2\pi = 3\text{GHz}$ and $a = 30\mu\text{m}$. 82

CHAPTER FIVE

- Figure 5.1:** Dispersion curves describing the (fast- slow) mode curve AC ,fast mode with curve DF in the fiber. Fiber parameters $\mu_{cl} = 1$, $a = 50\mu\text{m}$, fractional area $F = 0.56$, $\omega_p/2\pi = 10\text{GHz}$, $\omega_c/2\pi = 1\text{GHz}$ and $v/2\pi = 2\text{GHz}$ that be divided in two region curves. 87
- Figure 5.2:** Fast-slow guided modes (desertion curve of AC type in Fig 2.2) at $m = 0,1$ Fiber parameters $\mu_{cl} = 1$, $a = 50\mu\text{m}$, fractional area $F = 0.56$, $\omega_p/2\pi = 10\text{GHz}$, $\omega_c/2\pi = 1\text{GHz}$ and $v/2\pi = 2\text{GHz}$. 88
- Figure 5.3:** Slow guided modes (desertion curve of DF type in Fig 2.2) at fiber parameters, $\mu_{cl} = 1$, $a = 50\mu\text{m}$, fractional area $F = 0.56$, $\omega_p/2\pi = 10\text{GHz}$, $\omega_c/2\pi = 1\text{GHz}$ and $v/2\pi = 2\text{GHz}$. 89
- Figure 5.4:** Dispersion relation for TM mode with different fractional area F . Fiber parameters $m = 0$, $\mu_{cl} = 1$, $a = 50\mu\text{m}$, $\omega_p/2\pi = 10\text{GHz}$, $\omega_c/2\pi = 1\text{GHz}$ and $v/2\pi = 2\text{GHz}$. 90
- Figure 5.5:** Dispersion relation for TM mode with different core radius a , $m = 0$ Fiber parameters $\mu_{cl} = 1$, fractional area $F = 0.56$, $\omega_p/2\pi = 10\text{GHz}$, $\omega_c/2\pi = 1\text{GHz}$ and $v/2\pi = 2\text{GHz}$. 90

- Figure 5.6:** Dispersion relation for TE mode with different fractional area F , $m = 0$ **91**
 Fiber parameters $\mu_{cl}=1, a = 50\mu m, \omega_p/2\pi = 10GHz, \omega_c/2\pi = 1GHz$
 and $\nu/2\pi = 2GHz$.
- Figure 5.7:** Dispersion relation for TE mode with different core radius a , $m = 0$. **92**
 Fiber parameters $\mu_{cl}=1$, fractional area $F = 0.56, \omega_p/2\pi = 10GHz,$
 $\omega_c/2\pi = 1GHz$ and $\nu/2\pi = 2GHz$.
- Figure 5.8:** Dispersion relation for HE mode with different fractional area F , **93**
 $m = 1$. Fiber parameters $\mu_{cl}=1, a = 50\mu m, \omega_p/2\pi = 10GHz, \omega_c/2\pi = 1GHz$
 and $\nu/2\pi = 2GHz$.
- Figure 5.9:** Dispersion relation for HE mode with different core radius a , $m = 1$. **93**
 Fiber parameters $\mu_{cl}=1$, fractional area unit cell $F = 0.56,$
 $\omega_p/2\pi = 10GHz, \omega_c/2\pi = 1GHz$ and $\nu/2\pi = 2GHz$.
- Figure 5.10:** Dispersion relation for EH mode with different fractional area F , **94**
 $m = 1$, Fiber parameter $\mu_{cl}=1, a = 50\mu m, \omega_p/2\pi = 10GHz,$
 $\omega_c/2\pi = 1GHz$ and $\nu/2\pi = 2GHz$.
- Figure 5.11:** Dispersion relation for EH mode with different core radius a , $m = 1$ **94**
 Fiber parameters $\mu_{cl}=1$, fractional area unit cell $F = 0.56,$
 $\omega_p/2\pi = 10GHz, \omega_c/2\pi = 1GHz$ and $\nu/2\pi = 2GHz$.
- Figure 5.12:** The total real part of the power flowing through the structure in **95**
 TE mode versus the frequency with different values of core radius
 a . Fiber parameters $F = 0.56, \mu_{cl}=1, C=1, \omega_p/2\pi = 10GHz,$
 $\omega_c/2\pi = 1GHz$ and $\nu/2\pi = 2GHz$.
- Figure 5.13:** The total imaginary part of the power flowing through the structure **96**
 in TE mode versus the frequency with different values of core radius'
 a . Fiber parameter $F = 0.56, \mu_{cl}=1, C=1, \omega_p/2\pi = 10GHz,$
 $\omega_c/2\pi = 1GHz$ and $\nu/2\pi = 2GHz$.
- Figure 5.14:** The total real part of the power flowing through the structure in **97**
 TE mode versus the propagation constant with different value of
 core radius a . Fiber parameters $F = 0.56, \mu_{cl}=1, C=1,$

$$\omega_p/2\pi = 10\text{GHz}, \omega_c/2\pi = 1\text{GHz} \text{ and } \nu/2\pi = 2\text{GHz}.$$

Figure 5.15: The total imaginary part of the power flowing through the structure in TE mode versus the propagation constant with different values of core radius a . Fiber parameter $F = 0.56$, $\mu_{cl}=1$, $C=1$, ,

$$\omega_p/2\pi = 10\text{GHz}, \omega_c/2\pi = 1\text{GHz} \text{ and } \nu/2\pi = 2\text{GHz}.$$

Figure 5.16: The total real part of the power flowing through the structure in TM mode versus the frequency with different values of core radius a . Fiber parameters $F = 0.56$, $\mu_{cl}=1$, $A=1$, ,

$$\omega_p/2\pi = 10\text{GHz}, \omega_c/2\pi = 1\text{GHz} \text{ and } \nu/2\pi = 2\text{GHz}.$$

Figure 5.17: The total imaginary part of the power flowing through the structure in TM mode versus the frequency with different values of core radius a . Fiber parameters $F = 0.56$, $\mu_{cl}=1$, $A=1$, $\omega_p/2\pi = 10\text{GHz}$,

$$\omega_c/2\pi = 1\text{GHz} \text{ and } \nu/2\pi = 2\text{GHz}.$$

Figure 5.18: The total real part of the power flowing through the structure TM in mode versus the propagation constant with different values of core radius a . Fiber parameters $F = 0.56$, $\mu_{cl}=1$, $A=1$,

$$\omega_p/2\pi = 10\text{GHz}, \omega_c/2\pi = 1\text{GHz} \text{ and } \nu/2\pi = 2\text{GHz}.$$

Figure 5.19: The total imaginary part of the power flowing through the structure in TM mode versus the propagation constant with different value of core radius a . Fiber parameters $F = 0.56$, $\mu_{cl}=1$, $A=1$,

$$\omega_p/2\pi = 10\text{GHz}, \omega_c/2\pi = 1\text{GHz} \text{ and } \nu/2\pi = 2\text{GHz}.$$

Figure 5.20: The total real part of the power flowing through the structure in TE mode versus the frequency with different values of fractional area F . Fiber parameters $a = 50\mu\text{m}$, $\mu_{cl}=1$, $C=1$, $\omega_p/2\pi = 10\text{GHz}$,

$$\omega_c/2\pi = 1\text{GHz} \text{ and } \nu/2\pi = 2\text{GHz}.$$

Figure 5.21: The total imaginary part of the power flowing through the structure in TE mode versus the frequency with different values of fractional area. Fiber parameters $a = 50\mu\text{m}$, $\mu_{cl}=1$, $C=1$, $\omega_p/2\pi = 10\text{GHz}$,

$$\omega_c/2\pi = 1\text{GHz} \text{ and } \nu/2\pi = 2\text{GHz}.$$

Figure 5.22: The total real part of the power flowing through the structure in TM mode versus the frequency with different values of fractional

area . Fiber parameter $a = 50\mu m$, $\mu_{cl} = 1$, $A = 1$, $\omega_p/2\pi = 10GHz$,
 $\omega_c/2\pi = 1GHz$ and $\nu/2\pi = 2GHz$.

Figure 5.23: The total imaginary part of the power flowing through the structure
in TM mode versus the frequency with different values of fractional
area F. Fiber parameters $a = 50\mu m$, $\mu_{cl} = 1$, $A = 1$, $\omega_p/2\pi = 10GHz$,
 $\omega_c/2\pi = 1GHz$ and $\nu/2\pi = 2GHz$.

103

Contents

CHAPTER ONE: INTRODUCTION TO OPTICAL WAVEGUIDES AND FIBERS

1.1. Introduction	1
1.2 .Light Propagation.....	2
1.2.1. Maxwell's Equations and Plane Waves.....	2
1.2.2. Wave Equation.....	4
1.2.3. Boundary Conditions at an Interface.....	6
1.2.4. Poynting's Vectors.....	7
1.3. Polarization.....	8
1.3.1. S- polarized light (TE mode)	8
1.3.2. P - polarized light (TM mode).....	9
1.4. Fiber Optics	9
1.4.1. History and Definition of Optical Fiber.....	10
1.4.2.Types of Optical Fibers.....	11
1.4.3.Total Internal Reflection (TIR).....	12
1.4.4. Structure of Optical Fiber	13
1.5 Left-handed materials (LHM).....	15
1.5.1.Introduction to LHM materials	15
1.5.2.Electromagnetic Properties of LHM materials	17

CHAPTER TWO : GUIDED MODES IN NEGATIVE REFRACTIVE INDEX FIBERS

2.1. Structure Analysis.....	20
2.2. Solution of Wave Equations in the Cylindrical Coordinate.....	21
2.3. Solution Of Maxwells Equations in Cylindrical Coordinate.....	22
2.4 . Expressions for $E_r, H_r, E_\theta, H_\theta$ Components.....	24
2.5. Expressions for E_z and H_z Components.....	25
2.5.1. Solutions in the Core Region $a \geq r > 0$	26
2.5.2. Solutions in the Clad Region $r > a$	28

2.6. Expressions for the E_z and H_z Components in Terms of Bessel Function.	29
2.6.1. Expressions for the $E_r, H_r, E_\theta, H_\theta$ in the Core Region $a \geq r > 0$	30
2.6.2. Expressions for the $E_r, H_r, E_\theta, H_\theta$ in the Clad Region $r > a$	31
2.7. Dispersion Equation of an Optical Fiber	31
2.8. Modes in Optical Fibers	36
2.8.1. Meridional Modes : $m = 0$	36
2.8.2. Skew Modes: $m \neq 0$	36
2.9. Numerical Results	38

CHAPTER THREE: MODES IN OPTICAL FIBERS WITH SEMICONDUCTOR CLADDING AND LHM CORE

3.1. Introduction to Semiconductors	42
3.2. Optical Properties of Semiconductor	43
3.2.1. Electromagnetic Energy	44
3.2.2. Maxwell's Equation	44
3.3. Structure Analysis	45
3.4. Solution of Maxwell's Equations in Clad region (Semiconductor)	46
3.5. Expressions for $E_r, H_r, E_\theta, H_\theta$ in the Clad Semiconductor	47
3.6. Dispersion Equation for Modes	48
3.6.1. TE Mode	48
3.6.2. TM Mode	51
3.6.3. Hybrid Mode	55
3.7. Optical Power for TE and TM Modes	59
3.7.1 TE mode	60
3.7.2 TM mode	62

CHAPTER FOUR: MODES IN OPTICAL FIBER WITH LHM CORE AND SEMICONDUCTOR CLAD; GENERAL CASE

4.1. Structure Analysis	65
4.2. The Dispersion Relations	66

4.3. Power Consideration	67
4.3.1. TE Mode Case.....	67
4.3.2. TM Mode Case	67
4.4. Numerical Results and Discussions.....	68

CHAPTER FIVE: MODES IN OPTICAL FIBER WITH LHM CORE AND SEMICNDUCTOR CLAD; SPECIAL CASE

5.1. Structure Analysis.....	83
5.2. The Dispersion Equations.....	84
5.2.1. TE and TM Mode.....	84
5.2.2. Hybrid Mode (HE and EH).....	85
5.3. Power Considerations.....	85
5.3.1. For TE Mode.....	85
5.3.2 . For TM Mode.....	86
5.4. Numerical Results.....	87

CHAPTER SIX : CONCLUSIONS

Applications.....	106
Advantages and Disadvantages.....	107
References.....	108

CHAPTER ONE

INTRODUCTION TO OPTICAL WAVEGUIDES AND FIBERS

In this chapter, the basic concepts and equations of electromagnetic wave theory required in the treatment of optical waveguides are presented. Maxwell's equations, wave equations, Boundary conditions and Poynting's Vector are described in section 1.2. TE and TM Polarizations are discussed in section 1.3. Optical fiber properties and its structure, advantages and disadvantages, Typs of optical fiber, and total internal reflection (TIR) are presented in section 1.4. Finally, left handed metamaterial (LHM) and their electromagnetic properties are explained in section 1.5.

1.1. Introduction

Communication implies transfer of information from one point to another. When it is necessary to transmit information, such as speech, images, or data, over a distance, one generally uses the concept of carrier wave communication. In such a system, the information sent modulates an electromagnetic wave such as a radio wave, microwave, or light wave, which acts as a carrier. This modulated wave is then transmitted to the receiver through a channel and the receiver demodulates it to retrieve the imprinted signal. This is due to the fact that, in any communication system employing electromagnetic waves as the carrier, the amount of information that can be sent increases as the frequency of the carrier is increased. The idea of using light waves for communication can be traced as far back as 1880 when Alexander Graham Bell [1] invented the photophone shortly after he invented the telephone in 1876. Hockham [2] in 1966 suggested that optical fibers based on silica glass could provide the necessary transmission medium if metallic and other impurities could be removed. In 1970 Kapron et al., [2] had successful by produced silica fibers with a loss of about 17 dB/km at a wavelength of 633 nm. Since then, the technology has advanced with tremendous rapidity. By 1985 [2] glass fibers were routinely produced with extremely low losses (< 0.2 dB/km). Along the path of the optical fiber are splices, which are permanent joints between sections of fibers, and repeaters that boost the signal and correct any distortion that may have occurred along the path of the fiber.

1.2. Light Propagation

1.2.1. Maxwell's Equations and Plane Waves

All the analysis of wave propagation is based on Maxwell's equations which govern the time dependence of the intensity of the electric and magnetic fields \mathbf{E} and \mathbf{H} , respectively. These two field vectors are often used to describe the electromagnetic fields. Maxwell's equations can be written as follows

1-Faraday's law [3]

$$\nabla \times \mathbf{E} = -\frac{\partial \mathbf{B}}{\partial t} \quad (1.1)$$

2-Ampere's law with Maxwell's correction, [3]

$$\nabla \times \mathbf{H} = \frac{\partial \mathbf{D}}{\partial t} + \mathbf{J} \quad (1.2)$$

3-Gauss's law [3].

$$\nabla \cdot \mathbf{D} = \rho \quad (1.3)$$

4- Non existance of magnetic monopole [3]

$$\nabla \cdot \mathbf{B} = 0 \quad (1.4)$$

The quantities \mathbf{D} and \mathbf{B} are called the electric displacement and the magnetic induction, respectively. The quantities ρ and \mathbf{J} are the electric charge density and the current density, respectively. In a medium with no free charges ($\rho = 0$) and no currents ($\mathbf{J} = 0$) Eq. (1.2) and Eq. (1.3) rewritten as:

$$\nabla \times \mathbf{H} = \frac{\partial \mathbf{D}}{\partial t} \quad (1.5)$$

$$\nabla \cdot \mathbf{E} = 0 \quad (1.6)$$

We can also introduce the electric permittivity ϵ and the magnetic permeability μ . These two parameters characterize the response of the material to an external electric and magnetic field as [4]:

$$\mathbf{D} = \epsilon \mathbf{E} + \mathbf{P} \quad (1.7)$$

$$\mathbf{B} = \mu \mathbf{H} + \mathbf{M} \quad (1.8)$$

where \mathbf{P} and \mathbf{M} are the electric and magnetic polarizations, respectively. When an electromagnetic field is present in a material, the electric field can perturb the motion of electrons and produce a dipole polarization \mathbf{P} . The application of a magnetic field \mathbf{H} to a material can induce a magnetization \mathbf{M} . For a plane wave, the electric and magnetic fields can be expressed as [5]:

$$\mathbf{E}(\mathbf{r}, t) = \mathbf{E}_0 e^{i(\mathbf{k} \cdot \mathbf{r} - \omega t)} \quad (1.9)$$

$$\mathbf{H}(\mathbf{r}, t) = \mathbf{H}_0 e^{i(\mathbf{k} \cdot \mathbf{r} - \omega t)} \quad (1.10)$$

where ω is the frequency of the field and \mathbf{k} is the wave vector, \mathbf{r} is the position vector, t is the time, and \mathbf{E}_0 and \mathbf{H}_0 define the amplitude and the direction of the vectors \mathbf{E} and \mathbf{H} respectively. Now, we substitute Eq. (1.7) and Eq. (1.8) into Maxwell's equations with the use of Eq. (1.9) and Eq. (1.10), Maxwell's equations become [6]:

$$\mathbf{k} \times \mathbf{E} = -\mu \frac{\partial \mathbf{H}}{\partial t} = \mu \omega \mathbf{H} \quad (1.11)$$

$$\mathbf{k} \times \mathbf{H} = \epsilon \frac{\partial \mathbf{E}}{\partial t} = -\epsilon \omega \mathbf{E} \quad (1.12)$$

$$\mathbf{k} \cdot \mathbf{E} = 0 \quad (1.13)$$

$$\mathbf{k} \cdot \mathbf{H} = 0 \quad (1.14)$$

Eq. (1.13) and Eq. (1.14) show that both the electric field vector \mathbf{E} and the magnetic field vector \mathbf{H} are perpendicular to the wave vector \mathbf{k} where $\mathbf{E} \perp \mathbf{k}$ and $\mathbf{H} \perp \mathbf{k}$. Also, from Eq. (1.11) and Eq. (1.12) we see that the electric and magnetic field vectors are perpendicular to each other, $\mathbf{E} \perp \mathbf{H}$. Thus, we obtain that the three vectors \mathbf{E} , \mathbf{H} , and \mathbf{k} form a triplet of mutually perpendicular vectors

By multiplying both sides of Eq. (1.11) by $\mathbf{k} \times \mathbf{E}$ we obtain

$$k^2 E^2 = (\mu \omega)^2 H^2 \quad (1.15)$$

Similarly, multiplying both sides of Eq. (1.12) by $\mathbf{k} \times \mathbf{H}$ to obtain

$$k^2 H^2 = (\epsilon\omega)^2 E^2 \quad (1.16)$$

Dividing Eq. (1.15) by Eq. (1.16), we obtain a relation between the absolute values of the intensities of the electric and magnetic fields

$$\mathbf{E} = \sqrt{\frac{\mu}{\epsilon}} \mathbf{H} \quad (1.17)$$

1.2.2. Wave Equation

Consider now wave pulse propagating in the x-direction as shown in figure 1.1. It is given by the relation

$$y = A \sin kx \quad (1.18)$$

where A is the wave amplitude.

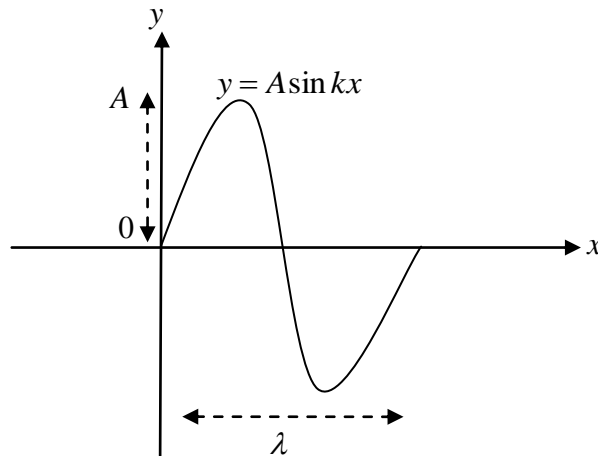


Figure 1.1 Wave pulse moving at constant speed.

The wave vector can be defined as :

$$k = \frac{2\pi}{\lambda} \quad (1.19)$$

And some relation to the pulse is given by

$$T = \frac{\lambda}{v} \quad (1.20)$$

$$f = \frac{1}{T} \quad (1.21)$$

$$\omega = \frac{2\pi}{T} = 2\pi f \quad (1.22)$$

where T is the periodic time, f is the frequency, ω is the angular frequency, λ is the wave length and v is the speed constant.

From Eq's. (1.1), (1.5), (1.7), and (1.8), we can derive the wave equation for the electric and magnetic fields. Applying the operator $\nabla \times$ to both sides of Eq. (1.1) we get:

$$\nabla \times (\nabla \times \mathbf{E}) = -\mu \frac{\partial}{\partial t} \nabla \times \mathbf{H} \quad (1.23)$$

The left-hand side of Eq. (1.23) can be simplified with use of the identity

$$\nabla \times (\nabla \times \mathbf{E}) = \nabla(\nabla \cdot \mathbf{E}) - \nabla^2 \mathbf{E} \quad (1.24)$$

The right-hand side of Eq. (1.23) can be rewritten using Eq's (1.5) and (1.7), finally the equation can be written as:

$$\nabla^2 \mathbf{E} = \mu \omega \frac{\partial^2 \mathbf{E}}{\partial t^2} \quad (1.25)$$

Using Eq. (1.9) into Eq. (1.25) the wave equation is written as [5,8]:

$$\nabla^2 \mathbf{E} + (nk)^2 \mathbf{E} = 0 \quad (1.26)$$

which is called the wave equation of the electric field \mathbf{E} , where n is the refractive index $n = \sqrt{\epsilon\mu}$. Similar equation can be obtained for the magnetic field \mathbf{H} by applying the operator $\nabla \times$ to both sides of Eq. (1.5)

$$\nabla \times (\nabla \times \mathbf{H}) = \epsilon \frac{\partial}{\partial t} \nabla \times \mathbf{E} \quad (1.27)$$

The left-hand side of Eq. (1.27) can be simplified with use of the identity

$$\nabla \times (\nabla \times \mathbf{H}) = \nabla(\nabla \cdot \mathbf{H}) - \nabla^2 \mathbf{H} \quad (1.28)$$

The right-hand side of Eq. (1.27) can be rewritten by using Eqs. (1.1 and 1.8), finally we obtain the equation

$$\nabla^2 \mathbf{H} = \varepsilon \omega \frac{\partial^2 \mathbf{H}}{\partial t^2} \quad (1.29)$$

Using Eq. (1.10) into Eq. (1.29) the wave equation is written as [5,8]:

$$\nabla^2 \mathbf{H} + (nk)^2 \mathbf{H} = 0 \quad (1.30)$$

which is called the wave equation to the magnetic field \mathbf{H} .

The fields \mathbf{E} and \mathbf{H} propagate through empty space with ($\varepsilon = \mu = 1$) with a speed equal to the velocity of light, c . However, in a medium with ε and μ different from 1, the electromagnetic fields propagate with a velocity v as:

$$v = \frac{c}{\sqrt{\varepsilon\mu}} = \frac{c}{n} \quad (1.31)$$

1.2.3. Boundary Conditions at an Interface

At the interface between two media, the following boundary conditions are satisfied as [3,5]:

$$\vec{n} \cdot (\mathbf{B}_2 - \mathbf{B}_1) = 0 \quad (1.32)$$

$$\vec{n} \cdot (\mathbf{D}_2 - \mathbf{D}_1) = 0 \quad (1.33)$$

$$\vec{n} \times (\mathbf{E}_2 - \mathbf{E}_1) = 0 \quad (1.34)$$

$$\vec{n} \times (\mathbf{H}_2 - \mathbf{H}_1) = 0 \quad (1.35)$$

Here, \vec{n} is the unit vector perpendicular to the plane surface and indices (1, 2) refer to the first and (second) medium. The Eq's (1.32)–(1.35) follow directly from Maxwell's equations. They play a key role in our analysis of propagation of electromagnetic waves through various structures. From Eqs. (1.34) and (1.35), it follows that the tangential components of both \mathbf{E} and \mathbf{H} are continuous at the interface as [5]:

$$\mathbf{E}_{1t} = \mathbf{E}_{2t} \quad \text{and} \quad \mathbf{H}_{1t} = \mathbf{H}_{2t} \quad (1.36)$$

Similarly, by using equations (1.32) and (1.33) with Eq(1.7) and Eq (1.8), the normal components of the electric displacement and the magnetic inductance are continuous at the interface as in [5]:

$$\mathbf{D}_{1n} = \mathbf{D}_{2n} \quad \text{and} \quad \mathbf{B}_{1n} = \mathbf{B}_{2n} \quad (1.37)$$

The continuity conditions, given by Eq. (1.36) and (1.37), are very important in the analysis of the propagation of electromagnetic waves.

1.2.4. Poynting's Vector

Poynting's theorem states that the time rate of flow of the electromagnetic energy per unit area is given by the vector \mathbf{S} , called the Poynting vector which is defined as the cross product of the electric and magnetic fields as [4]:

$$\mathbf{S} = \mathbf{E} \times \mathbf{H} \quad (1.38)$$

Since \mathbf{S} has the physical meaning of energy flow, it must be real. Therefore, in Eq. (1.38), only the real parts of all three vectors \mathbf{E} , \mathbf{H} , and \mathbf{S} should be considered:

$$\mathbf{S} = \text{Re}(\mathbf{E} \times \mathbf{H}) \quad (1.39)$$

Here, we are interested only in the propagation of electromagnetic waves where both the electric and the magnetic fields oscillate as $e^{i\omega t}$. Therefore, it is more convenient to average the Poynting vector \mathbf{S} over one period in Eq. (1.22) of the oscillation of electric and magnetic fields. From the plane wave in Eq. (1.9) and Eq. (1.10), we get:

$$\mathbf{E}(t) = \text{Re}(\mathbf{E}_0 e^{i(\mathbf{k}\mathbf{r} - \omega t)}) = \frac{1}{2} \left[(\mathbf{E}_0 e^{i(\mathbf{k}\mathbf{r} - \omega t)}) + (\mathbf{E}_0^* e^{-i(\mathbf{k}\mathbf{r} - \omega t)}) \right] \quad (1.40)$$

$$\mathbf{H}(t) = \text{Re}(\mathbf{H}_0 e^{i(\mathbf{k}\mathbf{r} - \omega t)}) = \frac{1}{2} \left[(\mathbf{H}_0 e^{i(\mathbf{k}\mathbf{r} - \omega t)}) + (\mathbf{H}_0^* e^{-i(\mathbf{k}\mathbf{r} - \omega t)}) \right] \quad (1.41)$$

After substitution of these two expressions into the R.H.S of Eq. (1.39), we get:

$$\mathbf{S} = \frac{1}{4} \left[\left(\mathbf{E}_0 e^{i(\mathbf{k}\mathbf{r} - \omega t)} \right) + \left(\mathbf{E}_0^* e^{-i(\mathbf{k}\mathbf{r} - \omega t)} \right) \right] \times \left[\left(\mathbf{H}_0 e^{i(\mathbf{k}\mathbf{r} - \omega t)} \right) + \left(\mathbf{H}_0^* e^{-i(\mathbf{k}\mathbf{r} - \omega t)} \right) \right] \quad (1.42)$$

$$\mathbf{S} = \frac{1}{4} \left(\mathbf{E}_0 \times \mathbf{H}_0^* + \mathbf{E}_0^* \times \mathbf{H}_0 \right) \quad (1.43)$$

$$\mathbf{S} = \frac{1}{2} \text{Re} \left(\mathbf{E} \times \mathbf{H}^* \right) \quad (1.44)$$

where * is the complex conjugate of electric and magnetic wave. \mathbf{S} can be expressed in terms of the complex fields \mathbf{E} and \mathbf{H} in the form of Eq. (1.44). By using Eq. (1.11) and Eq. (1.12) into Eq (1.44), we can find the new two relations for poynting vector \mathbf{S} as

$$\mathbf{S} = \frac{1}{2} \frac{\mathbf{k}}{\mu\omega} |\mathbf{E}_0|^2 \hat{\mathbf{k}} \quad (1.45)$$

Also that

$$\mathbf{S} = \frac{1}{2} \frac{\mathbf{k}}{\epsilon\omega} |\mathbf{H}_0|^2 \hat{\mathbf{k}} \quad (1.46)$$

1.3. Polarization

Polarization of light has numerous applications, many of these applications can easily be seen through a polarizing film, which selectively passes light with a particular direction of the vector \mathbf{E} , and for any given direction of propagation there are two independent polarization vectors, which can be in any two mutually orthogonal directions normal to \mathbf{k} . The first case is that in which the vector of the electric field \mathbf{E} , of the incident wave is parallel to the boundary plane. This case is called transverse electric or TE polarization (we will use also the name s-wave). The second case is that in which the vector of the magnetic field \mathbf{H} , of the incident wave is parallel to the boundary plane. This is called transverse magnetic or TM polarization. This type also call the TM polarized wave the (p-wave).

1- S- polarized light

By definition, in the case of the TE polarization the electric intensity \mathbf{E} is parallel to the interface, there is no electric field in the direction of propagation. In the notation that vector \mathbf{E} has only one component,

$$\mathbf{E} = (0, E_y, 0) \quad (1.47)$$

and vector \mathbf{H} has two components only,

$$\mathbf{H} = (H_x, 0, H_z) \quad (1.48)$$

2- P- Polarized light

For the TM polarization, the magnetic field vector \mathbf{H} parallel to the interface and, there is no magnetic field in the direction of propagation. therefore, it has only one component.

$$\mathbf{H} = (0, H_y, 0) \quad (1.49)$$

The electric field vector \mathbf{E} has two components as

$$\mathbf{E} = (E_x, 0, E_z) \quad (1.50)$$

1.4. Optical Fiber

1.4.1. History and Definition of Optical Fiber

One of the most important types of waveguides are optical fibers. An optical fiber is basically a cylindrical dielectric waveguide with a circular cross section where a high-index wave guiding core is surrounded by a low-index cladding. Optical fibers are usually made of silica SiO_2 glass. The index step and profile are controlled by the concentration and distribution of dopants. Light propagates in an optical fiber by repeated total internal reflection at the core–cladding glass boundary. Optical fibers have a phenomenally large capacity to carry information and are able to deliver this information to extremely distant locations. They are therefore suitable for optical communications and most laser applications in this range of the spectrum. Optical fibers made of other materials are also developed for special applications.. In 1870 John Tyndall [2] demonstrated that light can travel within a curved jet stream of water from a hole made on the side of a water pail. Propagation was based on repeated total internal reflection at the air–water boundary. However. In 1936 Carson et al [7] have shown that a circular dielectric waveguide can support a hybrid dominant mode with no cutoff frequency, it was almost for 30 years until 1966, when Kao and Hockham [2] promoted the use of a glass fiber as the transmission medium, that the doors were opened for using the principle of total internal reflection as a viable means of communication. In 1970 the whole field of optical communication links through

optical fibers was awakened by the successful development of low-loss fibers (with losses less than 20 dB km) [7].

Fiber-optic communication systems possess such advantages as:

- 1- Low transmission loss.
- 2- Large capacity of information transmission.
- 3- No electromagnetic interference.
- 4 -Lighter weight than copper.
- 5- No sparks even when short-circuited.
- 6- Higher melting point than copper.
- 7- Practically inexhaustible raw material supply.

On the other hand, the disadvantages are:

- 1- Connections and taps are more difficult to make than for copper wire.
- 2- Fiber is not as flexible as a copper wire.

1.4.2. Types of Optical Fibers

1. Multimode Step-Index Fiber

In this type the core diameter is $50\ \mu\text{m}$, and the refractive index difference Δ is equal to 0.5–1.0%. The normalized radius V is 30, and the number of modes is on the order of hundreds. The advantage of this fiber is the ease of coupling to a source or connecting to another fiber because of the large core diameter and large numerical aperture (NA) value. But this fiber has a limited capacity for information transmission due to mode dispersion and is used primarily for short-distance communication. The capacity (bandwidth–length product) is about 65 Mb/s.km with $\text{NA} = 0.1$.

2-Single-Mode Fiber

The core diameter is reduced to 8–10 μm , and refractive index difference $\Delta = 0.3$ –0.5, so that the normalized radius V of the fiber is smaller than the cutoff $V = 2.4$ of the mode that is the next higher mode from the dominant mode. Coupling is difficult in the single mode fiber, but the information transmission capacity is significantly larger.

3- Dispersion-Shifted Fiber

The dispersion-shifted fiber is not only nominally free from dispersion, but also the wavelength of operation is at $1.55 \mu\text{m}$. The dispersion of the fiber is removed by choosing a refractive index distribution such that waveguide dispersion cancels material dispersion at wavelength $1.55 \mu\text{m}$. Transmission loss is about 0.2 dB/km and the practical limit on the capacity of information transmission is about a Tb/s.km. The refractive index distribution is either one large peak of $\Delta = 0.6\text{--}0.9$, or a concentric step modulation in the cladding layer.

4-Silica Core Fluorine-Added Cladding Fiber

The cladding glass is normally pure SiO_2 . Germanium dioxide (GeO_2) is usually used to raise the refractive index of the core glass with respect to that of the cladding glass. The inclusion of GeO_2 is an additional inhomogeneity in the core and increase the transmission loss of the fiber.

5-Plastic Fiber

This fiber is made out of low-transmission-loss plastic material. Being made of plastic, the diameter of the core can be as large as 1–2 mm and large NA value of 0.5. It is primarily used for short-distance communication. Plastic fiber whose core is made of poly methyl meth acrylate (PMMA) and whose cladding is made of fluorinated alkyl metha crylate copolymer is useful in the region of wave length $0.6\text{--}0.8 \mu\text{m}$ and the minimum transmission loss is 20 dB/km at $0.68 \mu\text{m}$.

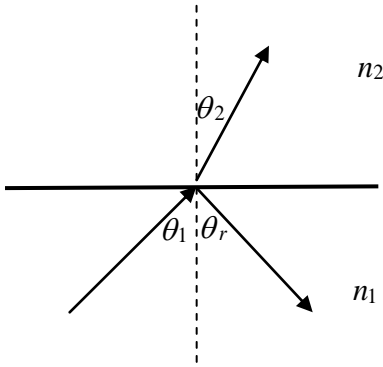
6- Holey Optical Fiber (HF)

Holey optical fiber (HF) is a single material fiber with a periodic array of circular or elliptical air holes running in the axial direction of the optical fiber. The effective refractive index difference can be achieved from a single material. This type of fiber is single mode over an exceptionally wide wave length range from 458 to 1550 nm, as determined by measuring the numerical aperture (NA). It was found that the value of NA almost linearly increases with wavelength. ($\text{NA} = 0.13$ at $\lambda = 458 \text{ nm}$, and $\text{NA} = 0.36$ at $\lambda = 1, 550 \text{ nm}$).

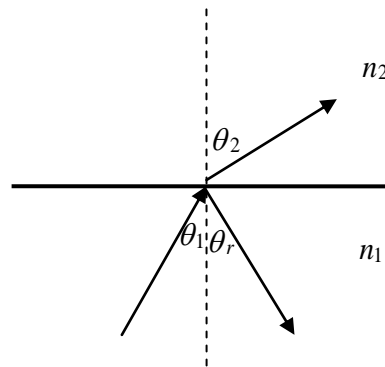
1.4.3. Total Internal Reflection (TIR)

At the heart of an optical communication system is the optical fiber which acts as the transmission channel carrying the light beam loaded with information. As mentioned earlier, the guidance of the light beam (through the optical fiber) takes place because of the phenomenon of total internal reflection (TIR). We first define the refractive index (n) of a medium in Eq (1.31). As you know, when a ray of light is incident at the interface of two media (like air and glass), the ray undergoes partial reflection and partial refraction as shown in Figure 1.2 (a,b,c) satisfying the condition:

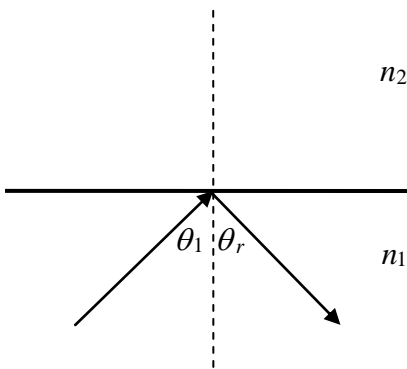
$$n_1 \sin \theta_1 = n_2 \sin \theta_2 \quad (1.51)$$



(a) $n_1 < n_2, \theta_1 > \theta_c$



(b) $n_1 > n_2, \theta_1 < \theta_c$



(c) $n_1 > n_2, \theta_1 \geq \theta_c$ (TIR)

Figure 1.2: Light reflection at different cases with a) $n_1 < n_2, \theta_1 > \theta_c$ and b) $n_1 > n_2, \theta_1 < \theta_c$ and c) $n_1 > n_2, \theta_1 \geq \theta_c$ (TIR).

The vertical dotted line represents the normal to the surface. The angles θ_1 is the incident angle, θ_2 is the refraction angle and, θ_r represents the reflection angle.

Further, the incident ray, reflected ray, and refracted ray lie in the same plane. In (Figure 1.2.a), since $n_1 < n_2$ we must have (from Snell's law) $\theta_1 > \theta_2$, i.e., the ray will bend toward the normal. On the other hand, if a ray is incident at the interface of a rarer medium ($n_1 > n_2$), the ray will bend away from the normal (see Figure 1.2.b).

The angle of incidence, for which the angle of refraction is 90° , is known as the critical angle θ_c and is denoted by [6]:

$$\theta_1 = \theta_c = \sin^{-1}\left(\frac{n_2}{n_1}\right) \quad (1.52)$$

$\theta_2 = 90^\circ$. When the angle of incidence exceeds the critical angle (i.e., when $\theta_1 \geq \theta_c$), there is no refracted ray and we have total internal reflection as in Figure 1.2.c

1.4.4. Structure of Optical Fiber

Light propagates in an optical fiber by repeated total internal reflection at the core-cladding cylindrical glass boundary. An optical fiber consists of a core and a cladding (cylindrical) and is axially symmetric. Since the refractive index of the core is slightly higher than that of the cladding, the optical field is largely confined to the core. The corresponding refractive index distribution (in the transverse direction) is given by:

$$\begin{aligned} n &= n_1 & \text{for } a \geq r > 0 \\ n &= n_2 & \text{for } r > a \end{aligned} \quad (1.53)$$

where n_1 represent the refractive index of core and n_2 refractive index of cladding and a represents the radius of the core. The relative index difference or relative profile height Δ , through the following equations as in [7]:

$$\Delta = \frac{n_1^2 - n_2^2}{2n_2^2} \quad (1.54)$$

When $\Delta \ll 1$ (as is indeed true for silica fibers where n_1 is very nearly equal to n_2) we may write as in [7]:

$$\Delta = \frac{(n_1 + n_2)(n_1 - n_2)}{2n_1^2} \approx \frac{(n_1 - n_2)}{n_1} \approx \frac{(n_1 - n_2)}{n_2} \quad (1.55)$$

Now, for a ray entering the fiber core at its end, if the angle of incidence θ_1 at the internal core-cladding interface is greater than the critical angle θ_c , the ray will undergo TIR at that interface. Further, because of the cylindrical symmetry in the fiber structure, this ray will suffer TIR at the interface also and therefore be guided through the core by repeated total internal reflections. Even for a bent fiber, light guidance can occur through multiple total internal reflections. For transmission of light from one place to another, the fiber must be supported. Supporting structures, however, may considerably distort the fiber, there by affecting the guidance of the light wave. This is avoided by choosing a sufficiently thick cladding. Further, in a fiber bundle, in the absence of the cladding, light can leak through from one fiber to another.

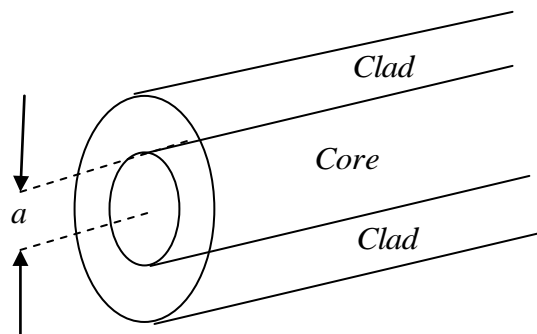


Figure 1.3: Fiber consists of a cylindrical central core clad by a material

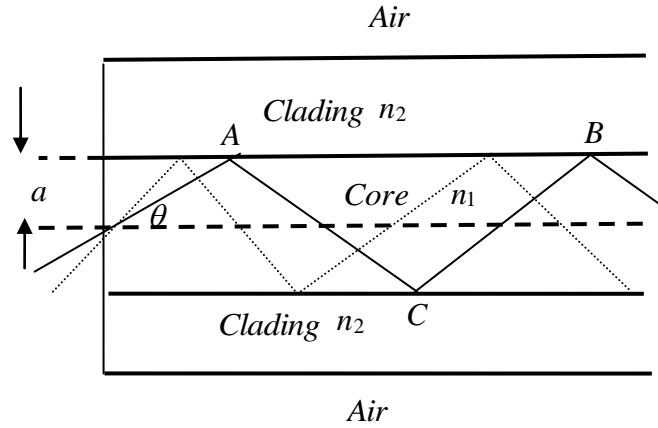


Figure 1.4: Light rays impinging on the core-cladding interface at an angle greater than the critical angle are trapped inside the core of the fiber

1.5. Left Handed Materials (LHM)

1.5.1. Introduction to LHM Materials

Veselago [8] was the first who theoretically predicted such media. He revealed that a material with simultaneously negative dielectric permittivity and magnetic permeability is equivalent to a negative refractive-index medium, and investigated the electromagnetic wave propagation through such media. Material can be divided according to the sign of magnetic permeability μ and electric permittivity ϵ into many groups as in figure 1.5, the first type have two positive sign values of magnetic permeability μ and electric permittivity ϵ be named right handed material (RHM). The second type has positive sign of magnetic permeability μ and negative sign of permittivity ϵ called metal. The third type has negative sign values of magnetic permeability μ and positive sign permittivity ϵ be called ferromagnetic material, and the last type material has two negative sign values of magnetic permeability μ and permittivity ϵ be called left handed material (LHM) or metamaterial. Also we know that the refractive index depends of the magnetic permeability μ and permittivity ϵ where $n = \pm\sqrt{\epsilon\mu}$ as [9]. Metmaterials (MTMs) are broadly defined as artificial effectively homogeneous electromagnetic structures with unusual properties not readily available in nature. An effectively homogeneous structure is a structure whose structural average cell size p is much smaller than the guided wavelength

λ_g . Therefore, this average cell size should be at least smaller than a quarter of wave length, $p < \lambda_g/4$. We will refer to the condition $p = \lambda_g/4$ as the effective homogeneity limit or effective-homogeneity condition 1, to ensure that refractive phenomena will dominate over scattering/diffraction phenomena when a wave propagates inside the MTM medium. If the condition of effective-homogeneity is satisfied, the structure behaves as a real material in the sense that electromagnetic waves are essentially myopic to the lattice and only probe the average, or effective, macroscopic and well-defined constitutive parameters, which depend on the nature of the unit cell, the structure is thus electromagnetically uniform along the direction of propagation. The constitutive parameters are the permittivity ε and the permeability μ , which are related to the refractive index n by $n = \pm\sqrt{\varepsilon_r\mu_r}$, where ε_r and μ_r are the relative permittivity and permeability related to the free space permittivity and permeability by $\varepsilon_0 = \varepsilon/\varepsilon_r = 8.854 \times 10^{-12}$ and $\mu_0 = \mu/\mu_r = 4\pi \times 10^{-7}$, respectively. In the sign \pm for the double valued square root function has been a priority admitted for generality. LH materials, as a consequence of their double negative parameters, are characterized by antiparallel phase and group velocities, or negative refractive index (NRI). LH structures are clearly MTMs, according to the definition given above, since they are artificial, effectively homogeneous ($p < \lambda_g/4$), and exhibit highly unusual properties ($\varepsilon_r, \mu_r < 0$). It should be noted that, although the term MTM has been used most often in reference to LH structures in the literature, However, LH structures have been by far the most popular of the MTMs, due to their exceptional property of negative refractive index .

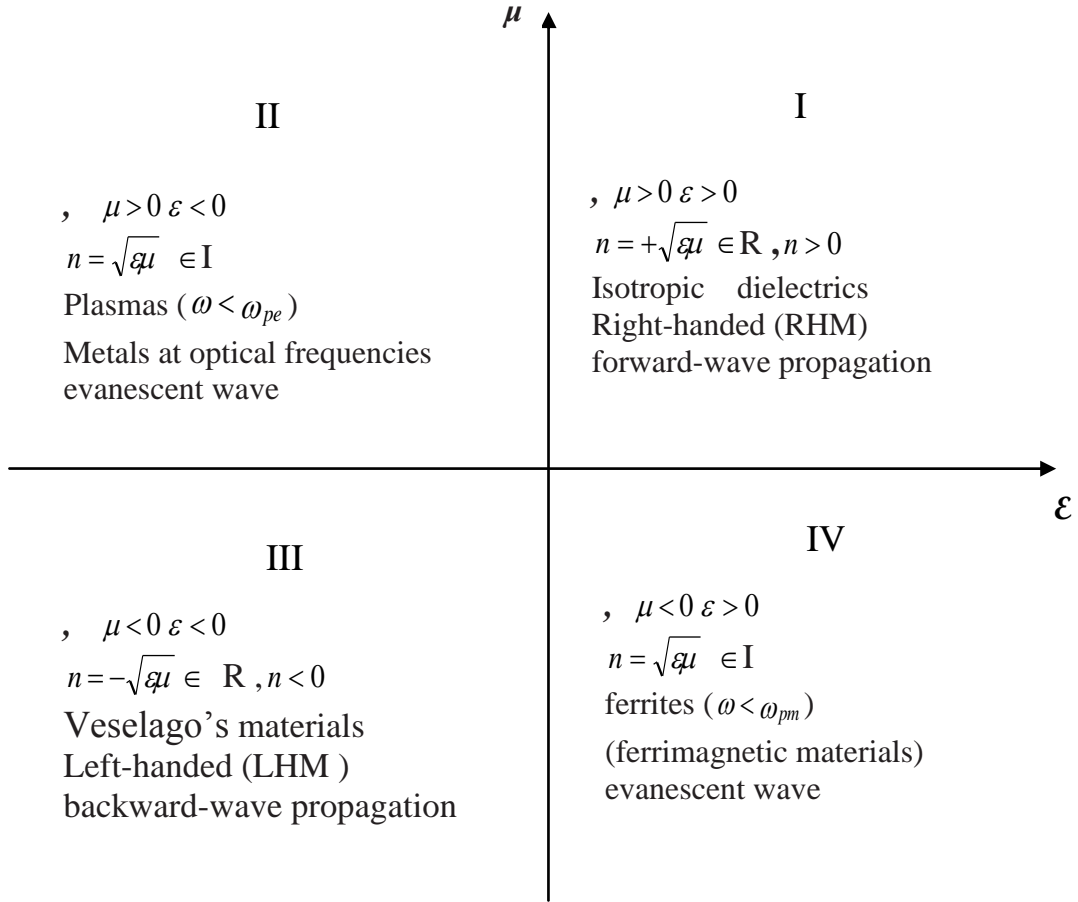


Figure. 1.5: Permittivity-permeability ($\varepsilon - \mu$) and refractive index (n) diagram for all materials.

1.5.2. Electromagnetic Properties of Left-Handed Materials

A-Wave Equation

The wave equation for an electromagnetic wave in a medium with ε and μ is given by [10]:

$$\left(k^2 - \varepsilon\mu \frac{\omega^2}{c^2} \right) \mathbf{E} = 0 \quad (1.56)$$

from which it follows that the plane wave in Eq (1.9) can propagate in the medium if the product $\varepsilon\mu$ is positive. This is possible if either both ε and μ are positive, or both parameters are negative. Thus we conclude that propagation of electromagnetic waves is possible in a left-handed medium .

B- Left-Handed Rule

The electric field vector \mathbf{E} , magnetic field vector \mathbf{H} and wave vector \mathbf{k} follow the right handed triplet of vectors, and the Poynting vector \mathbf{S} parallel to \mathbf{k} . However, if both ε and μ are negative, we obtain from Maxwell's equations that [9]:

$$\mathbf{k} \times \mathbf{E} = -|\mu| \omega \mathbf{H} \quad (1.57)$$

$$\mathbf{k} \times \mathbf{H} = +|\varepsilon| \omega \mathbf{E} \quad (1.58)$$

It is clear that the vectors \mathbf{E} , \mathbf{H} , and \mathbf{k} follow now the left-handed triplet of vectors, and vectors \mathbf{k} and \mathbf{S} have opposite orientation as shown in figure 1.6.

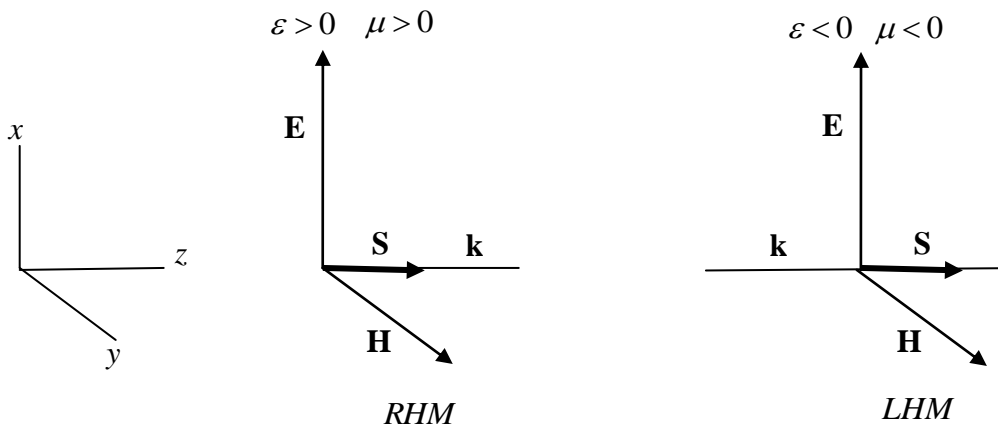


Figure 1.6: Orientation of the electric and magnetic vectors of the intensity of electromagnetic fields \mathbf{E} and \mathbf{H} with respect to the wave vector \mathbf{k} and Poynting vector \mathbf{S} for LHM and RHM.

Note that the direction of the propagation of the electromagnetic wave is determined by the orientation of the Poynting vector \mathbf{S} , and not by the orientation of the wave vector \mathbf{k} . The opposite sign of \mathbf{k} only means that the phase velocity of the wave inside the left handed medium is negative.

C- Dispersion

The energy of the electromagnetic field U may be written [10] as:

$$U = \frac{1}{8\pi} \left(\frac{\partial(\epsilon\omega)}{\partial\omega} E^2 + \frac{\partial(\mu\omega)}{\partial\omega} H^2 \right) \quad (1.59)$$

We immediately see that both permittivity ϵ and permeability μ must depend on the frequency. Otherwise, the energy U reduces to the relation $U = (\epsilon \mathbf{E}^2 + \mu \mathbf{H}^2)/8\pi$ which would be negative for both ϵ and μ are negative. On the other hand, the energy U is always positive this mean that equation satisfy as [9]:

$$\frac{\partial\omega\epsilon(\omega)}{\partial\omega} > 0 \quad \text{and} \quad \frac{\partial\omega\mu(\omega)}{\partial\omega} > 0 \quad (1.60)$$

The frequency dependence of ϵ and μ means, due to the Kramers-Kronig relations, that both the permittivity and permeability must be complex. The nonzero imaginary parts of the permittivity and permeability lead unavoidably to absorption losses of the electromagnetic wave propagating through the left-handed material. The dielectric permittivity and magnetic permeability in some material of LHM become simultaneously negative in the frequency range from 4 to 6 GHz.

CHAPTER TWO

GUIDED MODES IN NEGATIVE REFRACTIVE INDEX FIBERS

In this chapter we need to analyze the previous studies represented by A.V. Novitsky and L.M. Barkovsy in [25], which including electromagnetic wave propagate along the fiber consist of LHM core and dielectric material in the clad, solution of wave equation and Maxwell's equations to the optical fiber in cylindrical coordinate are obtained in sections 2.2 and 2.3, the component of electric and magnetic fields with (r, θ) are proved in section 2.4, solution of electric and magnetic fields at z- direction in the core and clad regions are described in section 2.5, the expressions value to the electric and magnetic fields components in terms of Bessel function for the core and clad regions are summarized in section 2.6, dispersion equations for the fast and slow mode are defined in section 2.7, dispersion relation for TE, TM, HE, and EH modes in the fiber are included in section 2.8. Finally the electromagnetic properties in the fiber are studied where the dispersion curves for all modes are plotted in section 2.9.

2.1. Structure Analysis

A.V. Novitsky and L.M. Barkovsy [11] have studied the properties of electromagnetic wave propagating in optical fiber with radius a at the z- direction. The considered optical fiber consist of LHM in the core in the region $a \geq r > 0$ which characterized by an electric relative permittivity ϵ_{co} and magnetic relative permeability μ_{co} as [12]:

$$\epsilon_{co}(\omega) = 1 - \frac{\omega_p^2}{\omega^2} \quad (2.1)$$

$$\mu_{co}(\omega) = 1 - \frac{F \omega^2}{\omega^2 - \omega_0^2} \quad (2.2)$$

where ω_p is the plasma frequency in the LHM, ω_0 is the resonant frequency and F is the fractional area of the unit cell. The clad region is filled with dielectric material which have an electric relative permittivity ϵ_{cl} and magnetic relative permeability μ_{cl} given by [12]:

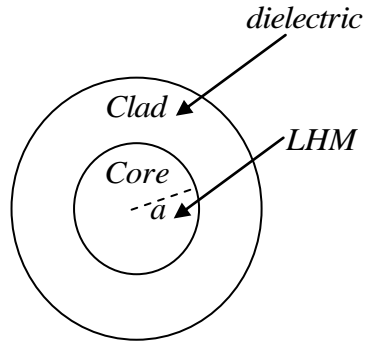


Figure 2.1: Structure of the optical fiber with LHM core and dielectric clad.

2.2. Solution of Wave Equations in the Cylindrical Coordinate

Consider an optical fiber cylindrical coordinate with core radius a and refractive index core is n_{co} bounded by cladding layer with radius b , the assumption of $b = \infty$ is made. The clad refractive index is n_{cl} as shown in Figure 2.2.

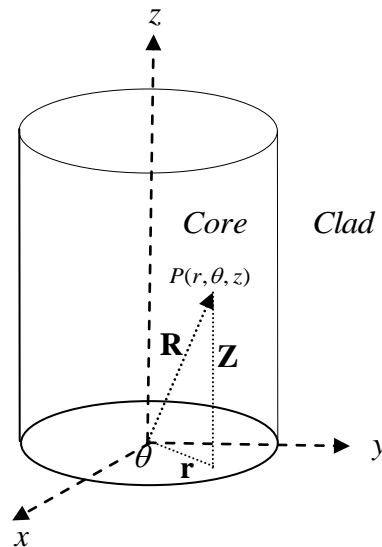


Figure 2.2: Optical fiber in a cylindrical coordinate system (r, θ, z)

The electric field \mathbf{E} and magnetic field \mathbf{H} in cylindrical coordinates are written as[2]:

$$\mathbf{E} = E_r \hat{\mathbf{r}} + E_\theta \hat{\boldsymbol{\theta}} + E_z \hat{\mathbf{z}} \quad (2.3)$$

$$\mathbf{H} = H_r \hat{\mathbf{r}} + H_\theta \hat{\boldsymbol{\theta}} + H_z \hat{\mathbf{z}} \quad (2.4)$$

To solve the wave equation in Eq. (1.26), in the cylindrical coordinates must use the identity as in [13]:

$$\nabla^2 \mathbf{A} = \left(\nabla^2 A_r - \frac{2}{r^2} \frac{\partial A_\theta}{\partial \theta} - \frac{A_r}{r^2} \right) \hat{\mathbf{r}} + \left(\nabla^2 A_\theta + \frac{2}{r^2} \frac{\partial A_r}{\partial \theta} - \frac{A_\theta}{r^2} \right) \hat{\boldsymbol{\theta}} + \nabla^2 A_z \hat{\mathbf{z}} \quad (2.5)$$

Using Eq. (2.5) and substituting into Eq. (1.26) to find the components of the electric field \mathbf{E} in the cylindrical coordinates to get:

$$\begin{aligned} \nabla^2 E + (nk)^2 E = & \left(\nabla^2 E_r - \frac{2}{r^2} \frac{\partial E_\theta}{\partial \theta} - \frac{E_r}{r^2} + (nk)^2 E_r \right) \hat{\mathbf{r}} + \\ & \left(\nabla^2 E_\theta + \frac{2}{r^2} \frac{\partial E_r}{\partial \theta} - \frac{E_\theta}{r^2} + (nk)^2 E_\theta \right) \hat{\boldsymbol{\theta}} + (\nabla^2 E_z + (nk)^2 E_z) \hat{\mathbf{z}} = 0 \end{aligned} \quad (2.6)$$

Similarly to solve the wave equation in the magnetic field Eq. (1.30), using the same way to find the components of the magnetic field \mathbf{H} in the cylindrical coordinates, where that the value of ∇^2 in the cylindrical coordinate given by [2]:

$$\nabla^2 = \frac{1}{r} \frac{\partial}{\partial r} \left(r \frac{\partial}{\partial r} \right) + \frac{1}{r^2} \frac{\partial^2}{\partial \theta^2} + \frac{\partial^2}{\partial z^2} \quad (2.7)$$

Note that in Eq. (2.6), the $\hat{\mathbf{r}}$ component contains both E_r and E_θ likewise with the $\hat{\boldsymbol{\theta}}$ component, but the $\hat{\mathbf{z}}$ component contains only E_z . Because of this fact, the z component is first solved and then the other components E_r and E_θ will be obtained directly from Maxwell's equation as we want to explain later in this chapter.

2.3. Solution of Maxwells Equations in Cylindrical Coordinate

Consider that an electromagnetic wave propagating along the z -direction as in [1]:

$$E(r, \theta) = E_0 e^{j(\alpha t - \beta z)} \quad \text{and} \quad H(r, \theta) = H_0 e^{j(\alpha t - \beta z)} \quad (2.8)$$

where β is the propagation constant.

Using Eq. (2.8) and Eq. (1.8) then substituting into Maxwell equation, Eq. (1.1) become

$$\nabla \times \mathbf{E} = -j\mu\omega\mathbf{H} \quad (2.9)$$

Eq. (2.9) can be rewritten as in [13]:

$$\nabla \times \mathbf{E} = \frac{1}{r} \begin{vmatrix} \hat{\mathbf{r}} & r\hat{\boldsymbol{\theta}} & \hat{\mathbf{z}} \\ \partial/\partial r & \partial/\partial\theta & \partial/\partial z \\ E_r & rE_\theta & E_z \end{vmatrix} = -j\mu\omega\mathbf{H} \quad (2.10)$$

The expanded for Eq. (2.10) gives that

$$\frac{1}{r} \frac{\partial}{\partial\theta} E_z - \frac{\partial}{\partial z} E_\theta = -j\mu\omega H_r \quad (2.11)$$

$$\frac{\partial}{\partial z} E_r - \frac{\partial}{\partial r} E_z = -j\mu\omega H_\theta \quad (2.12)$$

$$\frac{1}{r} \frac{\partial}{\partial r} (r E_\theta) - \frac{1}{r} \frac{\partial}{\partial\theta} E_r = -j\mu\omega H_z \quad (2.13)$$

From Eq. (2.8) we find that:

$$\frac{\partial}{\partial z} = -\beta j \quad (2.14)$$

Using Eq. (2.14) and substituting into Eqs. (2.12) and (2.13) we get:

$$\frac{1}{r} \frac{\partial}{\partial\theta} E_z + j\beta E_\theta = -j\mu\omega H_r \quad (2.15)$$

$$-j\beta E_r - \frac{\partial}{\partial r} E_z = -j\mu\omega H_\theta \quad (2.16)$$

Eqs. (2.15), Eq. (2.16) and Eq. (2.13) are the solutions of Maxwell equation give Eq. (1.1) in cylindrical coordinates.

Similarly use the same way to solve Eq. (1.2) with no currents ($\mathbf{J}=0$), using Eq. (2.8) and Eq. (1.7) then substituting into Maxwell equation, Eq. (1.2) as in [13]:

$$\nabla \times \mathbf{H} = j\varepsilon\omega\mathbf{E} \quad (2.17)$$

$$\nabla \times \mathbf{H} = \frac{1}{r} \begin{vmatrix} \hat{\mathbf{r}} & r\hat{\boldsymbol{\theta}} & \hat{\mathbf{z}} \\ \partial/\partial r & \partial/\partial \theta & \partial/\partial z \\ H_r & rH_\theta & H_z \end{vmatrix} = j\omega \mathbf{E} \quad (2.18)$$

The expanded form Eq (2.18) gives

$$\frac{1}{r} \frac{\partial}{\partial \theta} H_z - \frac{\partial}{\partial z} H_\theta = j\omega E_r \quad (2.19)$$

$$\frac{\partial}{\partial z} H_r - \frac{\partial}{\partial r} H_z = j\omega E_\theta \quad (2.20)$$

$$\frac{1}{r} \frac{\partial}{\partial r} (rH_\theta) - \frac{1}{r} \frac{\partial}{\partial \theta} H_r = j\omega E_z \quad (2.21)$$

Using Eq. (2.14) and substituting into Eqs. (2.19) and (2.20) in order to get:

$$\frac{1}{r} \frac{\partial}{\partial \theta} H_z + j\beta H_\theta = j\omega E_r \quad (2.22)$$

$$-j\beta H_r - \frac{\partial}{\partial r} H_z = j\omega E_\theta \quad (2.23)$$

Eqs. (2.22), Eq. (2.23) and Eq. (2.21) are the solution of Maxwell equation give Eq. (1.5) in cylindrical coordinates.

2.4. Expressions For $E_r, H_r, E_\theta, H_\theta$ Components

After solving Maxwell equations it is easy to find the components of electric and magnetic fields E_r, H_r, E_θ and H_θ . Using Eq. (2.16) and substituting into Eq. (2.22), getting:

$$E_r = -\frac{j}{(\epsilon\mu\omega^2 - \beta^2)} \left(\frac{\mu\omega}{r} \frac{\partial H_z}{\partial \theta} + \beta \frac{\partial E_z}{\partial r} \right) \quad (2.24)$$

Eq. (2.24) represents the value of E_r .

Using Eq. (2.15) and substituting into Eq. (2.23) we get:

$$E_{\theta} = -\frac{j}{(\epsilon\mu\omega^2 - \beta^2)} \left(\frac{\beta}{r} \frac{\partial E_z}{\partial \theta} - \mu\omega \frac{\partial H_z}{\partial r} \right) \quad (2.25)$$

Eq. (2.25) represents the value of E_{θ} .

Using Eq. (2.22) and substituting into Eq. (2.16) we get:

$$H_{\theta} = \frac{-j}{(\epsilon\mu\omega^2 - \beta^2)} \left(\frac{\beta}{r} \frac{\partial H_z}{\partial \theta} + \epsilon\omega \frac{\partial E_z}{\partial r} \right) \quad (2.26)$$

Eq. (2.26) represents the value of H_{θ} .

Use Eq. (2.23) and substituting into Eq. (2.15) getting that:

$$H_r = -\frac{j}{(\epsilon\mu\omega^2 - \beta^2)} \left(\beta \frac{\partial H_z}{\partial r} - \frac{\epsilon\omega}{r} \frac{\partial E_z}{\partial \theta} \right) \quad (2.27)$$

Eq. (2.27) represents the value of H_r .

2.5. Expressions of E_z and H_z Components

Equation (2.6) being a vector equation, each component has to vanish individually in order for the vector sum of the components to be zero. Using Eq. (2.7), the z component of Eq. (2.6) is expressed as in [2,3]:

$$\nabla^2 E_z + (nk)^2 E_z = 0 \quad (2.28)$$

$$\frac{1}{r} \frac{\partial}{\partial r} \left(r \frac{\partial E_z}{\partial r} \right) + \frac{1}{r^2} \frac{\partial^2 E_z}{\partial \theta^2} + \frac{\partial^2 E_z}{\partial z^2} + (nk)^2 E_z = 0 \quad (2.29)$$

The differential equation, Eq. (2.29), is solved by the method of separation of variables. as a product of three functions, each r, θ, z letting that as [2]:

$$E_z = F_r \theta_{\theta} Z_z \quad (2.30)$$

Inserting Eq. (2.30) into Eq. (2.29) then use the separation of variables method we get::

$$Z_z'' + \beta^2 Z_z = 0 \quad (2.31)$$

$$\theta_\theta'' + m^2 \theta_\theta = 0 \quad (2.32)$$

$$\left(F_r'' + \frac{F_r'}{r} + (n^2 k^2 - \beta^2) \right) F_r - \frac{m^2}{r^2} F_r = 0 \quad (2.33)$$

2.5.1. Solutions In The Core Region $a \geq r > 0$

First, the considered solutions of Eq. (2.31) inside the core region is given in [2]:

$$Z_z = a e^{j\beta z} + b e^{-j\beta z} \quad (2.34)$$

also, the solution of the Eq. (2.32) is given by [2]:

$$\theta_\theta = c \cos m\theta + d \sin m\theta \quad (2.35)$$

also, the solution of the Eq. (2.33) in terms of Bessel function given by [2]:

$$F_r = e J_m(Kr) + f N_m(Kr) \quad (2.36)$$

where a, b, c, d, e and f is constant, m is the order of Bessel function, $J_m(Kr)$ is Bessel function of the first kind, $N_m(Kr)$ is Bessel function of the second kind with $n = n_1$. Since the variation rather than exponential in r is inside the core, a positive value as [1,2]:

$$K^2 = (\varepsilon_1 \mu_1 \omega^2 - \beta^2) = (n_{co}^2 k^2 - \beta^2) \quad (2.37)$$

where K is the wave number in the core .

Equation (2.32) consists of forward and backward waves. For the most part, fibers are reciprocal. There do exist some nonreciprocal effects that are employed in certain fiber sensors, but these are unusual. Reciprocity means that, coupling conditions being

equal, it does not matter which end of the fiber is connected to the source. It is sufficient to choose one term from the right-hand side of Eq. (2.65) in this case

$$Z_z = a e^{j\beta z} \quad (2.38)$$

Equation (2.33) represents two skew rays that are rotating in opposite senses. Mode patterns are standing waves generated by oppositely winding skew rays and both terms in Eq. (2.66) are needed. The location of θ and $\theta + 2\pi$ are the same. From Eq. (2.33) with m^{th} order Bessel function The curves of $N_m(x)$ are shown in Figure 2.3, $N_m(Kr)$ becomes negative infinity at $r = 0$ and physically cannot be accepted, and f in Eq. (2.33) has to be zero and the solution of Eq. (2.33) become

$$F_r = e J_m(Kr) \quad (2.39)$$

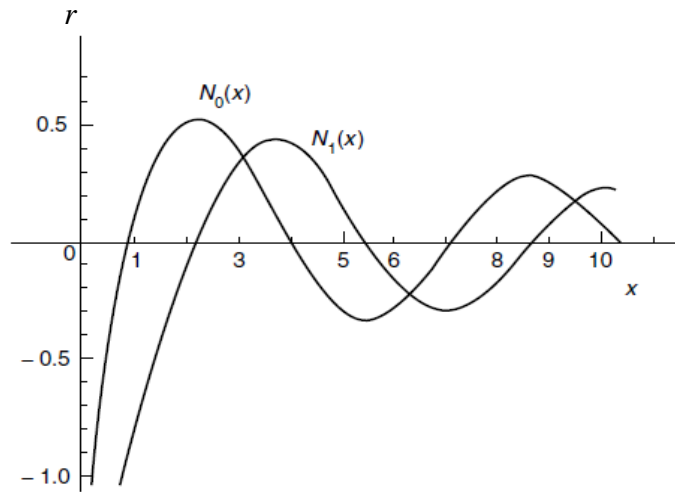


Figure 2.3: Zero- and first-order Bessel functions of the second kind with $m = 0, 1$.

In the core region $a \geq r > 0$, E_z and H_z are given as in [2]:

$$E_z = A J_m(Kr) \cos(m\theta) e^{j\beta z} \quad (2.40)$$

$$H_z = C J_m(Kr) \sin(m\theta) e^{j\beta z} \quad (2.41)$$

2.5.2. Solutions In The Clad Region $r > a$

The type of solution in the cladding region is one where the value of the function rapidly decreases with an increase in r . As mentioned earlier, the solution of Eq. (2.33) becomes a decaying function if the value of the square bracket is negative with $n = n_2$, where γ is the wave number in the clad as in [1,2]:

$$\gamma^2 = (\beta^2 - \epsilon_2 \mu_2 \omega^2) = (\beta^2 - n_{cl}^2 k^2) \quad (2.42)$$

The solution for F_r is then

$$F_r = e I_m(\gamma r) + f K_m(\gamma r) \quad (2.43)$$

where the functions $I_m(\gamma r)$ are called the modified Bessel functions of the first kind and $K_m(\gamma r)$ are modified Bessel functions of the second kind of the order m . The value of $I_m(x)$ increases with an increase in x but that of $K_m(x)$ decreases with an increase in x , as shown in Figure. 2.4. Since $I_m(x)$ becomes indefinitely large with an increase in r , it is rejected on physical grounds, and in Eq. (2.43) should be zero.

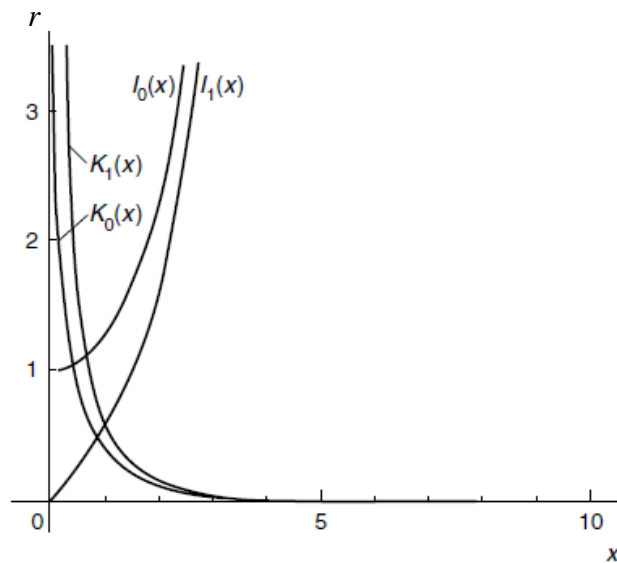


Figure 2.4: Modified Bessel functions of first $I_m(x)$ and the second $K_m(x)$ kinds with $m = 0,1$.

Then the expressions for E_z and H_z in the cladding region, $r > a$ are

$$E_z = B K_m(\gamma r) \cos(m\theta) e^{j\beta z} \quad (2.44)$$

$$H_z = D K_m(\gamma r) \sin(m\theta) e^{j\beta z} \quad (2.45)$$

2.6. Expressions for E_z and H_z Components in Terms of Bessel Function

From the boundary condition that the tangential field components (E_z and H_z) should be continuous at the core - cladding interface ($r = a$), we obtain the two following expiration conditions to find the E_z and H_z components in term of Bessel function.

Then we have defined two parameter U and W , where U is the normalized transverse wave number in the core is given as in [2]:

$$K^2 = \frac{U^2}{a^2} = (n_{co}^2 k^2 - \beta^2) \quad (2.46)$$

Also, γ is the wave number in the clad is given by

$$\gamma^2 = \frac{W^2}{a^2} = (\beta^2 - n_{cl}^2 k^2) \quad (2.47)$$

where W is the normalized transverse wave number in the clad.

From Eq. (2.46), we find $K = U/a$ and from Eq. (2.47) we find $\gamma = W/a$ then using the first boundary condition $E_{z1} = E_{z2}$ at ($r = a$) to get:

$$B = A \frac{J_m(U)}{K_m(W)} \quad (2.48)$$

where the function $J_m(Ur/a)$ describes the longitudinal component of the electric and magnetic field in the core, and the function $K_m(Wr/a)$ describes the longitudinal component of the electric and magnetic field in the clad.

Using the second boundary condition at $r = a$ that $H_{z1} = H_{z2}$ as in [1,2] we get:

$$D = C \frac{J_m(U)}{K_m(W)} \quad (2.49)$$

Using Eq. (2.48) and Eq. (2.49) where $e^{j\beta z}$ was suppressed, then Eqs. (2.40), (2.41), (2.44) and (2.45) can be rewritten to find E_z and H_z in the core and clad.

First the electric field in the core and the clad E_z become as in [14]:

$$E_z = \begin{cases} A J_m\left(\frac{U}{a}r\right) \cos(m\theta) & a \geq r > 0 \\ A \frac{J_m(U)}{K_m(W)} K_m\left(\frac{W}{a}r\right) \cos(m\theta) & r > a \end{cases} \quad (2.50)$$

Also, the magnetic field in the core and the clad H_z becomes as in [14]:

$$H_z = \begin{cases} C J_m\left(\frac{U}{a}r\right) \sin(m\theta) & a \geq r > 0 \\ C \frac{J_m(U)}{K_m(W)} K_m\left(\frac{W}{a}r\right) \sin(m\theta) & r > a \end{cases} \quad (2.51)$$

2.6.1. Expressions for $E_r, H_r, E_\theta, H_\theta$ In The Core Region $a \geq r > 0$

By using the Eqs. (2.46), (2.50) and Eq. (2.51) for $a \geq r > 0$ and substituting into Eqs. (2.24), (2.25), (2.26) and Eq. (2.27), we have:

$$E_r = -\frac{j a^2}{U^2} \left(\frac{U A \beta}{a} J_m'\left(\frac{U r}{a}\right) + \frac{C \omega m \mu_1}{r} J_m\left(\frac{U r}{a}\right) \right) \cos(m\theta) \quad (2.52)$$

$$E_\theta = -\frac{j a^2}{U^2} \left(\frac{-m A \beta}{r} J_m\left(\frac{U r}{a}\right) - C \omega \mu_1 \frac{U}{a} J_m'\left(\frac{U r}{a}\right) \right) \sin(m\theta) \quad (2.53)$$

$$H_r = -\frac{j a^2}{U^2} \left(A \omega \epsilon_1 \frac{m}{r} J_m\left(\frac{U r}{a}\right) + C \beta \frac{U}{a} J_m'\left(\frac{U r}{a}\right) \right) \sin(m\theta) \quad (2.54)$$

$$H_{\theta} = -\frac{j a^2}{U^2} \left(A \omega \varepsilon_1 \frac{U}{a} J_m' \left(\frac{Ur}{a} \right) + C \beta \frac{m}{r} J_m \left(\frac{Ur}{a} \right) \right) \cos(m\theta) \quad (2.55)$$

2.6.2. Expressions for the $E_r, H_r, E_{\theta}, H_{\theta}$ in the clad region $r > a$

Similarly using Eqs. (2.47), (2.50) and Eq. (2.51) for $r > a$ and Substituting into Eqs. (2.24), (2.25), (2.26) and Eq. (2.27) to get:

$$E_r = \frac{j a^2}{W^2} \left(A \beta \frac{W}{a} K_m' \left(\frac{Wr}{a} \right) + C \omega \mu_2 \frac{m}{r} K_m \left(\frac{Wr}{a} \right) \right) \frac{J_m(U)}{K_m(W)} \cos(m\theta) \quad (2.56)$$

$$E_{\theta} = \frac{j a^2}{W^2} \left(-A \beta \frac{m}{r} K_m \left(\frac{Wr}{a} \right) - C \omega \mu_2 \frac{W}{a} K_m' \left(\frac{Wr}{a} \right) \right) \frac{J_m(U)}{K_m(W)} \sin(m\theta) \quad (2.57)$$

$$H_r = \frac{j a^2}{W^2} \left(A \omega \varepsilon_2 \frac{m}{r} K_m \left(\frac{Wr}{a} \right) + C \beta \frac{W}{a} K_m' \left(\frac{Wr}{a} \right) \right) \frac{J_m(U)}{K_m(W)} \sin(m\theta) \quad (2.58)$$

$$H_{\theta} = \frac{j a^2}{W^2} \left(A \omega \varepsilon_2 \frac{W}{a} K_m' \left(\frac{Wr}{a} \right) + C \beta \frac{m}{r} K_m \left(\frac{Wr}{a} \right) \right) \frac{J_m(U)}{K_m(W)} \cos(m\theta) \quad (2.59)$$

2.7. Dispersion Equation of an Optical Fiber

Boundary conditions are applied at the interfase. The tangential components of \mathbf{E} and \mathbf{H} have to be continuous at $r = a$. The tangential components of \mathbf{E} are E_z and E_{θ} and those of \mathbf{H} are H_z and H_{θ} . At the first starting with the initial boundary condition as [1,2]:

$$E_{\theta 1} = E_{\theta 2} \quad \text{at} \quad r = a \quad (2.60)$$

Using Eq. (2.53) and Eq. (2.57) and substituting into Eq. (2.60) we get:

$$m A \beta \left(\frac{1}{U^2} + \frac{1}{W^2} \right) = -C \omega \left(\frac{\mu_1}{U} \frac{J_m'(U)}{J_m(U)} + \frac{\mu_2}{W} \frac{K_m'(W)}{K_m(W)} \right) \quad (2.61)$$

Using the second boundary condition at $r = a$ as in [1,2], we get:

$$H_{\theta 1} = H_{\theta 2} \quad \text{at} \quad r = a \quad (2.62)$$

Using Eq. (2.55) and Eq. (2.59) then substituting into Eq. (2.62) we get:

$$C\beta m \left(\frac{1}{U^2} + \frac{1}{W^2} \right) = -A\omega \left(\frac{\varepsilon_1 J'_m(U)}{U J_m(U)} + \frac{\varepsilon_2 K'_m(W)}{W K_m(W)} \right) \quad (2.63)$$

Using the relations as in [1]

$$\mu = \mu_0 \mu_r \quad (2.64)$$

$$\varepsilon = \varepsilon_0 \varepsilon_r \quad (2.65)$$

Using Eq. (2.64) and Eq. (2.65), and multiplying both Eq. (2.61) and Eq. (2.63) to each other, we obtain that:

$$\frac{m^2 \beta^2}{\omega^2 \mu_0 \varepsilon_0} \left(\frac{1}{U^2} + \frac{1}{W^2} \right)^2 = \left(\frac{\mu_{co} J'_m(U)}{U J_m(U)} + \frac{\mu_{cl} K'_m(W)}{W K_m(W)} \right) \left(\frac{\varepsilon_{co} J'_m(U)}{U J_m(U)} + \frac{\varepsilon_{cl} K'_m(W)}{W K_m(W)} \right) \quad (2.66)$$

We get the relations as in [6]:

$$k^2 = \frac{\omega^2}{c^2} = \omega^2 \varepsilon_0 \mu_0 \quad \text{and} \quad c = \frac{1}{\sqrt{\varepsilon_0 \mu_0}} \quad (2.67)$$

Using Eq. (2.67) then substituting into Eq. (2.66) we get:

$$\frac{m^2 \beta^2}{k^2} \left(\frac{1}{U^2} + \frac{1}{W^2} \right)^2 = \left(\frac{\mu_{co} J'_m(U)}{U J_m(U)} + \frac{\mu_{cl} K'_m(W)}{W K_m(W)} \right) \left(\frac{\varepsilon_{co} J'_m(U)}{U J_m(U)} + \frac{\varepsilon_{cl} K'_m(W)}{W K_m(W)} \right) \quad (2.68)$$

The LHS of Eq. (2.68) can be rewritten as:

$$\frac{\beta^2}{k^2} \left(\frac{1}{U^2} + \frac{1}{W^2} \right) = \frac{\beta^2}{k^2 U^2} + \frac{\beta^2}{k^2 W^2} \quad (2.69)$$

From Eq. (2.46) and Eq. (2.47) we get:

$$\frac{\beta^2}{U^2} = \frac{k^2 n_{co}^2}{U^2} - \frac{1}{a^2} \quad (2.70)$$

$$\frac{\beta^2}{W^2} = \frac{k^2 n_{cl}^2}{W^2} + \frac{1}{a^2} \quad (2.71)$$

Using Eq. (2.70) and Eq. (2.62) then substituting into Eq. (2.69), getting that:

$$\frac{\beta^2}{k^2} \left(\frac{1}{U^2} + \frac{1}{W^2} \right) = \frac{n_{co}^2}{U^2} + \frac{n_{cl}^2}{W^2} \quad (2.72)$$

Using Eq (2.63) then Eq. (2.68) rewritten as

$$\left(\frac{n_{co}^2}{U^2} + \frac{n_{cl}^2}{W^2} \right) \left(\frac{1}{U^2} + \frac{1}{W^2} \right) m^2 = \left(\frac{\mu_{co}}{U} \frac{J'_m(U)}{J_m(U)} + \frac{\mu_{cl}}{W} \frac{K'_m(W)}{K_m(W)} \right) \left(\frac{\varepsilon_{co}}{U} \frac{J'_m(U)}{J_m(U)} + \frac{\varepsilon_{cl}}{W} \frac{K'_m(W)}{K_m(W)} \right) \quad (2.73)$$

Dividing both side of Eq. (2.73) by $\varepsilon_{co} \mu_{co}$ and using the relation $n_{co}^2 = \varepsilon_{co} \mu_{co}$ we get:

$$\left(\frac{\mu_{co}}{U} \frac{J'_m(U)}{J_m(U)} + \frac{\mu_{cl}}{W} \frac{K'_m(W)}{K_m(W)} \right) \left(\frac{1}{\mu_{co} U} \frac{J'_m(U)}{J_m(U)} + \frac{\varepsilon_{cl}}{\varepsilon_{co} \mu_{co} W} \frac{K'_m(W)}{K_m(W)} \right) = \left(\frac{1}{U^2} + \frac{\frac{n_{cl}^2}{n_{co}^2}}{W^2} \right) \left(\frac{1}{U^2} + \frac{1}{W^2} \right) m^2 \quad (2.74)$$

Taking the L.H.S of Eq. (2.74) to be simplify

$$L H S = \frac{1}{U^2} \left(\frac{J'_m(U)}{J_m(U)} \right)^2 + \left(\frac{\varepsilon_{cl}}{\varepsilon_{co}} + \frac{\mu_{cl}}{\mu_{co}} \right) \frac{1}{UW} \frac{J'_m(U)}{J_m(U)} \frac{K'_m(W)}{K_m(W)} + \frac{\mu_{cl} \varepsilon_{cl}}{\mu_{co} \varepsilon_{co}} \frac{1}{W^2} \left(\frac{K'_m(W)}{K_m(W)} \right)^2 \quad (2.75)$$

Rearranging Eq. (2.75) we get:

$$L H S = \left(\frac{1}{U} \frac{J'_m(U)}{J_m(U)} + \frac{\mu_{cl}}{\mu_{co}} \frac{1}{W} \frac{K'_m(W)}{K_m(W)} \right) \left(\frac{1}{U} \frac{J'_m(U)}{J_m(U)} + \frac{\varepsilon_{cl}}{\varepsilon_{co}} \frac{1}{W} \frac{K'_m(W)}{K_m(W)} \right) \quad (2.76)$$

Now taking the R.H.S of Eq. (2.74) to be simplify we get:

$$RHS = \left(\frac{U^2 W^2 n_{co}^2 + U^4 n_{cl}^2 + W^4 n_{co}^2 + U^2 W^2 n_{cl}^2}{U^4 W^4 n_{co}^2} \right) m^2 \quad (2.77)$$

Now taking the numerator from the Eq. (2.77) R.H.S to simplify, using the Eq. (2.46) and Eq. (2.47) the first term becomes:

$$1-U^2 W^2 n_{co}^2 = \left(\beta^2 k^2 n_{co}^4 - k^4 n_{co}^4 n_{cl}^2 - \beta^4 n_{co}^2 + \beta^2 k^2 n_{co}^2 n_{cl}^2 \right) a^4 \quad (2.78)$$

For Eq. (2.77) the second term of the R.H.S written as:

$$2-U^2 W^2 n_{cl}^2 = \left(\beta^2 k^2 n_{cl}^4 - k^4 n_{co}^4 n_{cl}^2 - \beta^4 n_{cl}^2 + \beta^2 k^2 n_{co}^2 n_{cl}^2 \right) a^4 \quad (2.79)$$

By adding the two Eq (2.78) and Eq (2.79) to get:

$$U^2 W^2 n_{co}^2 + U^2 W^2 n_{cl}^2 = \left[\beta^2 k^2 (n_{co}^4 + n_{cl}^4) + 2 \beta^2 k^2 n_{co}^2 n_{cl}^2 - \beta^4 (n_{co}^2 + n_{cl}^2) - k^4 (n_{co}^4 n_{cl}^2 + n_{cl}^4 n_{co}^2) \right] a^4 \quad (2.80)$$

For Eq. (2.77) the third term of the R.H.S becomes:

$$3-U^4 n_{cl}^2 = a^4 \left(k^4 n_{co}^4 n_{cl}^2 + \beta^4 n_{cl}^2 - 2k^2 \beta^2 n_{co}^2 n_{cl}^2 \right) \quad (2.81)$$

From Eq. (2.77), the last term of the R.H.S becomes:

$$4-W^4 n_{co}^2 = a^4 \left(k^4 n_{cl}^4 n_{co}^2 + \beta^4 n_{co}^2 - 2k^2 \beta^2 n_{cl}^2 n_{co}^2 \right) \quad (2.82)$$

By adding the two Eq. (2.81) and Eq. (2.82), we get:

$$U^4 n_{cl}^2 + W^4 n_{co}^2 = \left[\beta^4 (n_{co}^2 + n_{cl}^2) + \beta^4 (n_{co}^2 + n_{cl}^2) - k^4 (n_{co}^4 n_{cl}^2 + n_{cl}^4 n_{co}^2) - 4 \beta^2 k^2 n_{co}^2 n_{cl}^2 \right] a^4 \quad (2.83)$$

Then adding Eq. (2.80) and Eq. (2.83) to get:

$$U^2 W^2 n_{co}^2 + U^2 W^2 n_{cl}^2 + U^4 n_{cl}^2 + W^4 n_{co}^2 = \beta^2 k^2 (\epsilon_{co} \mu_{co} - \epsilon_{cl} \mu_{cl})^2 a^4 \quad (2.84)$$

Using Eq. (2.84) and substituting into Eq. (2.77), now R.H.S read as:

$$RHS = \frac{\beta^2 k^2 (\varepsilon_{co} \mu_{co} - \varepsilon_{cl} \mu_{cl})^2 a^4}{W^4 U^4 \varepsilon_{co} \mu_{co}} m^2 \quad (2.85)$$

Using Eq. (2.76) and Eq. (2.85) and substituting into Eq. (2.74) to get:

$$\left(\frac{1}{U} \frac{J'_m(U)}{J_m(U)} + \frac{\mu_{cl}}{\mu_{co}} \frac{1}{W} \frac{K'_m(W)}{K_m(W)} \right) \left(\frac{1}{U} \frac{J'_m(U)}{J_m(U)} + \frac{\varepsilon_{cl}}{\varepsilon_{co}} \frac{1}{W} \frac{K'_m(W)}{K_m(W)} \right) = \frac{\beta^2 k^2 a^4 m^2 (\varepsilon_{co} \mu_{co} - \varepsilon_{cl} \mu_{cl})^2}{W^4 U^4 \varepsilon_{co} \mu_{co}} \quad (2.86)$$

Eq. (2.105) called the dispersion relation which satisfy the condition $U^2 > 0$ this mean that the product of $\varepsilon_{co} \mu_{co} > \varepsilon_{cl} \mu_{cl}$ in fast mode. But when the product $\varepsilon_{co} \mu_{co} \leq \varepsilon_{cl} \mu_{cl}$ then $U^2 < 0$ it has an imaginary value, so leading in this case $U = iU_1$ to be $U_1^2 > 0$. Substituting $U = iU_1$ into Eq. (2.86) and using the relations as [12,15]:

$$J_m(x) = i^m I_m(-ix) \quad (2.87)$$

$$J'_m(U) = i^{m+1} I'_m(-iU) = -i^{m+1} I'_m(-U_1) \quad (2.88)$$

$$J'_m(U) = i^{m+1} I'_m(-iU) = -i^{m+1} I'_m(U_1) \quad (2.89)$$

Using Eqs. (2.87) – Eq. (2.89) then substituting into Eq. (2.86) we get:

$$\left(\frac{-i^{m+1} I'_m(U_1)}{iU_1 i^m I_m(U_1)} + \frac{\mu_{cl}}{\mu_{co}} \frac{1}{W} \frac{K'_m(W)}{K_m(W)} \right) \left(\frac{-i^{m+1} I'_m(U_1)}{iU_1 i^m I_m(U_1)} + \frac{\varepsilon_{cl}}{\varepsilon_{co}} \frac{1}{W} \frac{K'_m(W)}{K_m(W)} \right) = \frac{\beta^2 k^2 a^4 m^2 (\varepsilon_{co} \mu_{co} - \varepsilon_{cl} \mu_{cl})^2}{W^4 (iU_1)^4 \varepsilon_{co} \mu_{co}} \quad (2.90)$$

After some calculation, Eq. (2.90) becomes:

$$\left(\frac{1}{U_1} \frac{I'_m(U_1)}{I_m(U_1)} - \frac{\mu_{cl}}{\mu_{co}} \frac{1}{W} \frac{K'_m(W)}{K_m(W)} \right) \left(\frac{1}{U_1} \frac{I'_m(U_1)}{I_m(U_1)} - \frac{\varepsilon_{cl}}{\varepsilon_{co}} \frac{1}{W} \frac{K'_m(W)}{K_m(W)} \right) = \frac{\beta^2 k^2 a^4 m^2 (\varepsilon_{co} \mu_{co} - \varepsilon_{cl} \mu_{cl})^2}{W^4 U_1^4 \varepsilon_{co} \mu_{co}} \quad (2.91)$$

Eq.(2.91) described the dispersion relation to the surface mode for the fiberin slow mode with $m \geq 0$.

2.8. Modes in Optical Fibers

Eq. (2.86) is a combination of Bessel functions. The solutions of the characteristic equation depend of the order m , whether $m = 0$ or $m \neq 0$. Hence, they will be treated in two separate subsections.

2.8.1. Meridional Modes $m = 0$

The characteristic equation is significantly simplified with $m = 0$ the order of the Bessel function reduces, and the right-hand side of Eq. (2.86) becomes zero so that Eq. (2.86) reduces to the two modes TE and TM mode. Use the relations for the Bessel functions as [13,15]:

$$J'_m(x) = -J_{m+1}(x) \quad (2.92)$$

$$K'_m(x) = -K_{m+1}(x) \quad (2.93)$$

From Eq. (2.92) and Eq. (2.93) then the L.H.S of Eq. (2.91) becomes as [12,13]:

$$\frac{1}{U} \frac{J_1(U)}{J_0(U)} + \frac{\mu_{cl}}{\mu_{co}} \frac{1}{W} \frac{K_1(W)}{K_0(W)} = 0 \quad \text{TE mode} \quad (2.94)$$

$$\frac{1}{U} \frac{J_1(U)}{J_0(U)} + \frac{\varepsilon_{cl}}{\varepsilon_{co}} \frac{1}{W} \frac{K_1(W)}{K_0(W)} = 0 \quad \text{TM mode} \quad (2.95)$$

2.8.2. Skew Modes: $m \neq 0$

When $m \neq 0$, the right-hand side of Eq. (2.86) is not zero and the procedure for obtaining the solution of the characteristic equation is much more complicated. This means that the solution of the Eq. (2.86) one of them have '+' sign and another have '-' sign to give two hybrid mode HE and EH modes so there is two solution of Eq. (2.86) and letting that:

$$J = \frac{1}{U} \frac{J'_m(U)}{J_m(U)} + \frac{1}{W} \frac{K'_m(W)}{K_m(W)} \quad (2.96)$$

$$L = \frac{1}{U} \frac{J'_m(U)}{J_m(U)} + \frac{1}{W} \frac{K'_m(W)}{K_m(W)} \quad (2.97)$$

By using Eqs.(2.96) and (2.97), Eq. (2.86) become:

$$J^2 + \frac{\varepsilon_{cl}\mu_{cl}}{\varepsilon_{co}\mu_{co}} L^2 + \left(\frac{\varepsilon_{cl}}{\varepsilon_{co}} + \frac{\mu_{cl}}{\mu_{co}} \right) JL = \frac{\beta^2 k^2 a^4 m^2 (\varepsilon_{co}\mu_{co} - \varepsilon_{cl}\mu_{cl})^2}{W^4 U^4 \varepsilon_{co}\mu_{co}} \quad (2.98)$$

Multiply both side with $\frac{4\varepsilon_{co}^2\mu_{co}^2}{\varepsilon_{cl}^2\mu_{cl}^2}$ to find

$$\begin{aligned} \frac{4\varepsilon_{co}^2\mu_{co}^2}{\varepsilon_{cl}^2\mu_{cl}^2} J^2 + \frac{4\varepsilon_{co}\mu_{co}}{\varepsilon_{cl}\mu_{cl}} \left(\frac{\varepsilon_{co}\mu_{co}}{\varepsilon_{cl}\mu_{cl}} \frac{\varepsilon_{cl}}{\varepsilon_{co}} + \frac{\varepsilon_{co}\mu_{co}}{\varepsilon_{cl}\mu_{cl}} \frac{\mu_{cl}}{\mu_{co}} \right) JL = \\ \frac{4\varepsilon_{co}^2\mu_{co}^2}{\varepsilon_{cl}^2\mu_{cl}^2} \left(\frac{\beta^2 k^2 a^4 m^2 (\varepsilon_{co}\mu_{co} - \varepsilon_{cl}\mu_{cl})^2}{W^4 U^4 \varepsilon_{co}\mu_{co}} \right) - \frac{4\varepsilon_{co}\mu_{co}}{\varepsilon_{cl}\mu_{cl}} L^2 \end{aligned} \quad (2.99)$$

Adding to the both side of Eq. (2.99) $\left(\frac{\varepsilon_{co}}{\varepsilon_{cl}} + \frac{\mu_{co}}{\mu_{cl}} \right)^2 L^2$ find

$$\begin{aligned} \frac{4\varepsilon_{co}^2\mu_{co}^2}{\varepsilon_{cl}^2\mu_{cl}^2} J^2 + \left(\frac{\varepsilon_{co}}{\varepsilon_{cl}} + \frac{\mu_{co}}{\mu_{cl}} \right)^2 L^2 + \frac{4\varepsilon_{co}\mu_{co}}{\varepsilon_{cl}\mu_{cl}} JL = \\ \frac{4\varepsilon_{co}^2\mu_{co}^2}{\varepsilon_{cl}^2\mu_{cl}^2} \left(\frac{\beta^2 k^2 a^4 m^2 (\varepsilon_{co}\mu_{co} - \varepsilon_{cl}\mu_{cl})^2}{W^4 U^4 \varepsilon_{co}\mu_{co}} \right) - \frac{4\varepsilon_{co}\mu_{co}}{\varepsilon_{cl}\mu_{cl}} L^2 + \left(\frac{\varepsilon_{co}}{\varepsilon_{cl}} + \frac{\mu_{co}}{\mu_{cl}} \right)^2 L^2 \end{aligned} \quad (2.100)$$

After some mathmatical calculation Eq. (2.100) rewritten as:

$$\left(\left(\frac{2\varepsilon_{co}\mu_{co}}{\varepsilon_{cl}\mu_{cl}} \right) J + \left(\frac{\varepsilon_{co} + \mu_{co}}{\varepsilon_{cl} \mu_{cl}} \right) L \right)^2 = 4\varepsilon_{co}\mu_{co} \left(\frac{\beta^2 k^2 a^4 m^2 (\varepsilon_{co}\mu_{co} - \varepsilon_{cl}\mu_{cl})^2}{W^4 U^4 \varepsilon_{cl}^2 \mu_{cl}^2} \right) + \left(\frac{\varepsilon_{co} - \mu_{co}}{\varepsilon_{cl} \mu_{cl}} \right)^2 L^2 \quad (2.101)$$

Taking the square root to the booth side in the equation (2.101), we get:

$$\left(\frac{2\varepsilon_{co}\mu_{co}}{\varepsilon_{cl}\mu_{cl}} \right) J + \left(\frac{\varepsilon_{co} + \mu_{co}}{\varepsilon_{cl} \mu_{cl}} \right) L = \pm \sqrt{4\varepsilon_{co}\mu_{co} \left(\frac{\beta^2 k^2 a^4 m^2 (\varepsilon_{co}\mu_{co} - \varepsilon_{cl}\mu_{cl})^2}{W^4 U^4 \varepsilon_{cl}^2 \mu_{cl}^2} \right) + \left(\frac{\varepsilon_{co} - \mu_{co}}{\varepsilon_{cl} \mu_{cl}} \right)^2 L^2} \quad (2.102)$$

Eq. (2.102) have two solutions named hybrid mode, one '+' sign EH mode and the '-' sign HE mode as in [12,14]:

$$\left(\frac{2\varepsilon_{co}\mu_{co}}{\varepsilon_{cl}\mu_{cl}} \right) J + \left(\frac{\varepsilon_{co} + \mu_{co}}{\varepsilon_{cl} \mu_{cl}} \right) L = + \sqrt{4\varepsilon_{co}\mu_{co} \left(\frac{\beta^2 k^2 a^4 m^2 (\varepsilon_{co}\mu_{co} - \varepsilon_{cl}\mu_{cl})^2}{W^4 U^4 \varepsilon_{cl}^2 \mu_{cl}^2} \right) + \left(\frac{\varepsilon_{co} - \mu_{co}}{\varepsilon_{cl} \mu_{cl}} \right)^2 L^2} \quad \text{EH mode} \quad (2.103)$$

$$\left(\frac{2\varepsilon_{co}\mu_{co}}{\varepsilon_{cl}\mu_{cl}} \right) J + \left(\frac{\varepsilon_{co} + \mu_{co}}{\varepsilon_{cl} \mu_{cl}} \right) L = - \sqrt{4\varepsilon_{co}\mu_{co} \left(\frac{\beta^2 k^2 a^4 m^2 (\varepsilon_{co}\mu_{co} - \varepsilon_{cl}\mu_{cl})^2}{W^4 U^4 \varepsilon_{cl}^2 \mu_{cl}^2} \right) + \left(\frac{\varepsilon_{co} - \mu_{co}}{\varepsilon_{cl} \mu_{cl}} \right)^2 L^2} \quad \text{HE mode} \quad (2.104)$$

2.9. Numerical Results

In the analysis below, Novitsky and Barkovsy [11] considered the propagation of electromagnetic wave along circular fiber with core LHM have radius a bounded by a dielectric material in the clad as shown in figure 2.1. The electric permittivity ε_{co} and magnetic permeability μ_{co} in the core are given by Eq. (2.1) and Eq. (2.2). The clad has dielectric material with electric permittivity ε_{cl} and magnetic permeability μ_{cl} . Novitsky and Barkovsy in [11] studied the fast and slow guided modes in the fiber.

They also studied the mode properties dependence on the fiber parameters. The fiber parameter in [11], plasma frequency $\omega_p/2\pi = 10$ GHz, resonant frequency $\omega_0/2\pi = 4$ GHz, fractional area unit cell $F = 0.56$, core radius $a = 1\text{cm}$, dielectric permittivity $\epsilon_{cl} = 2.5$ and magnetic permeability $\mu_{cl} = 1$. In Figure 2.5, there are the three regions of mode existence in a dispersive fibre. In region (I) the conditions $U^2 > 0$, $\epsilon_{co}\mu_{co} > \epsilon_{cl}\mu_{cl}$ hold true and fast guided modes arise, the fast modes correspond to two types of dispersion curves. One of them is in region (I) completely (curve AB), and the other lies in both regions (I) and (II) (curve CF). Point D divides the fast mode from the slow one and satisfies the condition $U = 0$. Therefore, the dispersion curve segment CD describes a fast mode and DF a slow one. From figure 2.6, The dispersion curve of AB-type cannot be a fundamental guided mode and at the same time the mode polarizations are arranged in the following way: at $m = 0$ the TE mode alternates with the TM one, starting with TE; at $m \geq 1$ the hybrid EH mode alternates with the HE one, starting with EH. From Figure 2.7. The high-order fast modes exist at lower frequencies close to the resonant one. However, fast fundamental guided modes in a circular left-handed fibre are possible. They appear at $m = 0$ and correspond to the dispersion curves of CD-type. There are two fast fundamental modes, the first is TE and the second is TM polarized. Region (II) in figure 2.5 is characterized by $U^2 < 0$, $\epsilon_{co}\mu_{co} < \epsilon_{cl}\mu_{cl}$ and includes only slow modes. Dispersion curve DF at $m > 0$ corresponds to the HE polarized wave, the TE mode determines the asymptotic of lowfrequency curves of DF-type (at $m = 1$ the dispersion curve intersects the TE-mode curve, for $m > 1$ dispersion curves appear at higher frequencies than the TE-mode curve), TM mode determines the asymptotic of high-order curves of PLtype (all these dispersion curves are higher than the TM mode). The dispersion curve PL always corresponds to a slow mode. It can lie in regions (II) and (III) in figure 2.5 $U^2 < 0$, $\epsilon_{co}\mu_{co} < \epsilon_{cl}\mu_{cl}$. The curve GK in region (II) is characterized by EH polarization. The dispersion curve -PL in region (III) is HE polarized.

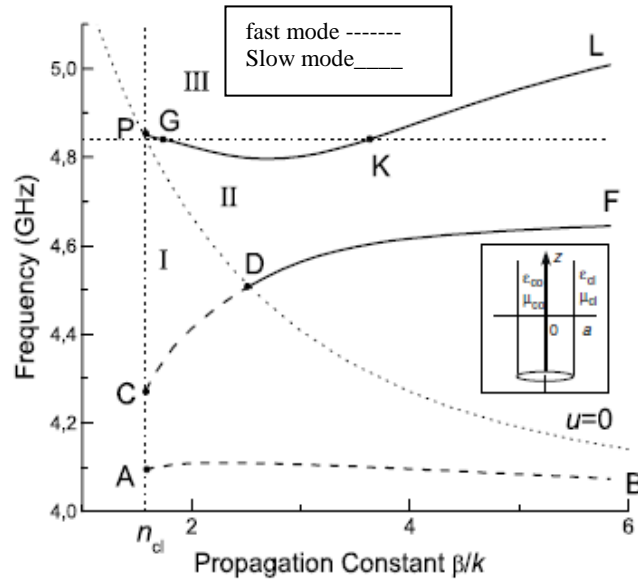


Figure 2.5 : Dispersion curves describing the fast modes (AB curve), fast- slow mode (CF curve) and slow mode (PL curve). Fiber parameters: cladding ($\epsilon_{cl} = 2.5$, $\mu_{cl} = 1$) with $n_{cl} = \sqrt{\epsilon_{cl}\mu_{cl}}$, and fiber radius $a = 1cm$ as [11].

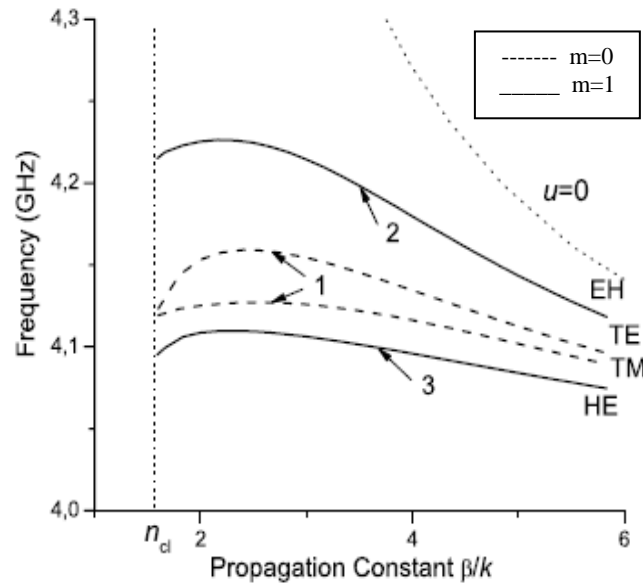


Figure 2.6: Fast guided modes with curve AB- type at $m = 0,1$. Fiber parameters : $\epsilon_{cl} = 2.5$, $\mu_{cl} = 1$, and fiber radius $a = 1cm$ as [11].

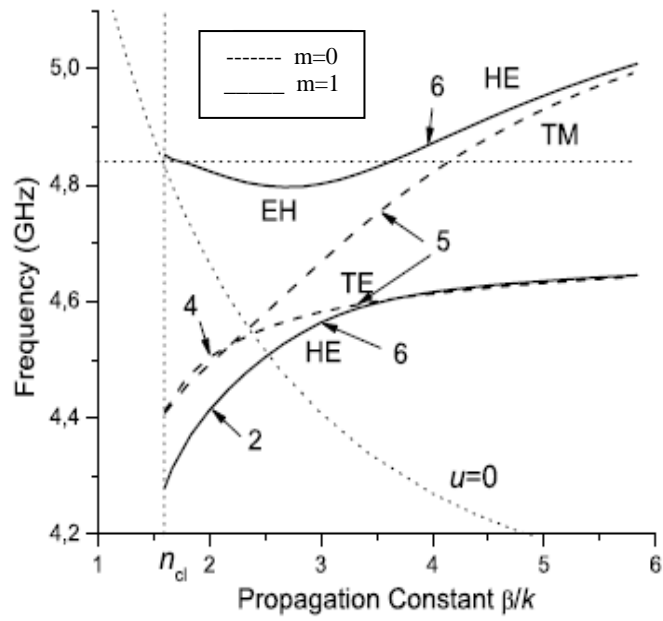


Figure 2.7: The fast-slow and slow low-order guided modes $m = 0,1$. Fiber parameters : $\epsilon_{cl} = 2.5$, $\mu_{cl} = 1$, and fiber radius $a = 1cm$ as [11].

CHAPTER THREE

MODES IN OPTICAL FIBERS WITH SEMICONDUCTOR CLADDING AND LHM CORE

In this chapter, the wave propagation characteristics in optical fiber consisting of LHM core bonded by a semiconductor are investigated theoretically. The basic concepts and equations, optical and electromagnetic properties for the semiconductor are presented in section 3.2. Solution of Maxwell's equations in the semiconductor clad will be derived in section 3.4. The electromagnetic field components in the semiconductor clad are obtained in section 3.5. The dispersion equations for TE, TM, HE and EH modes are proved in section 3.6. Finally, the total power in cases of TE and TM mode is explained in section 3.6.

3.1. Introduction to Semiconductors

Optoelectronics brings together optics and electronics within a single device. Metals are excellent electrical conductors, but do not allow light to travel inside. Glass and related dielectric materials can accommodate and guide light waves, like in optical fibers, but they are electrical insulators. Semiconductors are in between these two material types, as they can carry electrical current as well as light waves. Semiconductors can be designed to allow for the transformation of light into current and vice versa. The conduction of electrical current is based on the flow of electrons. Most electrons are attached to single atoms and are not able to move freely. Only some loosely bound electrons are released and become conduction electrons. The same number of positively charged atoms (ions) is left behind; the net charge is zero. The positive charges can also move, as valence electrons jump from atom to atom. Thus, both valence electrons (holes) and conduction electrons are able to carry electrical current. Both the carriers are separated by an energy gap; i.e., valence electrons need to receive at least the gap energy E_g to become conduction electrons. In semiconductors, the gap energy is on the order of 1 eV. The energy can be provided, e.g., by light having a wavelength of less than the gap wavelength. In the wave picture, light is represented by periodic electromagnetic fields with the wavelength. In the particle

picture, light is represented by a term of energy packets (photons) with the energy is E_{ph} in [16]

$$E_{ph} = \frac{hc}{\lambda} = h\nu = \hbar\omega \quad (3.1)$$

where $\omega = 2\pi\nu$, $\hbar = h/2\pi$ with h is Planck constant.

The photon energy must be at least as large as the band gap E_g to generate electron-hole pair. Vice versa, conduction electrons can also release energy in the form of light and become valence electrons. This energy exchange between electrons and photons is the key physical mechanism in optoelectronic devices. From an atomic point of view, valence electrons belong to the outermost electron shell of the atom, which is fully occupied in the case of semiconductors; i.e., no more electrons with the same energy are allowed. As these atoms are joined together in a semiconductor crystal, the electrons start to interact and the valence energy levels separate slightly, forming a valence energy band. Electrons within this band can exchange places but no charge flow is possible unless there is a hole. To generate holes, some electrons must be excited into the next higher energy band, the conduction band, which is initially empty. The concentration N of electrons in the conduction band and the concentration P of holes in the valence band control the electrical conductivity σ of semiconductors as [16]:

$$\sigma = qN\mu_n + qP\mu_p \quad (3.2)$$

with q is the elementary charge and the mobility μ_n and μ_p are the mobility of the hole and electrons respectively.

3.2. Optical Properties of Semiconductor

3.2.1. Electromagnetic Energy

The flow of electromagnetic energy is given by the Pointing vector as in Eq. (1.42) whose time average gives the intensity W/cm^2 of the optical wave I_{opt} as [16]:

$$I_{opt} = \sqrt{\frac{\epsilon_{opt} \epsilon_0}{4\mu_0}} |E_0|^2 \quad (3.3)$$

The photon flux density ϕ_{ph} is given as [17]:

$$\phi_{ph} = I_{opt} / \hbar\omega \quad (3.4)$$

The time-averaged local optical energy density W_{opt} is given as [17]:

$$W_{opt} = \varepsilon_{opt} \varepsilon_0 |E_0|^2 \quad (3.5)$$

3.2.2. Maxwell's Equations

Maxwell's equations are the fundamental basis for the classical treatment of electrical and magnetic fields. For high-frequency optical waves and semiconductor waveguides, several simplifications are possible as discussed in the following. The charge density acts as source of the electrostatic field vector \mathbf{F} and it can be neglected in the case of high-frequency electric fields vector \mathbf{E} . Magnetic field variations in time $\partial\mathbf{H}/\partial t$ generate curls $\nabla \times \mathbf{E}$ of the electrical field. Vice versa, electrical field variations in time $\partial\mathbf{E}/\partial t$ as well as generate the current curls $\nabla \times \mathbf{H}$ of the magnetic field. The steady-state or low-frequency current density $\mathbf{J} = \sigma\mathbf{F}$ can be excluded here (conductivity at low frequencies). The remaining "optical" current density $\mathbf{J} = \sigma_{opt}\mathbf{E}$ depends on the semiconductor conductivity σ_{opt} at high frequencies. This means that at high frequencies we get [17]:

$$\mathbf{J} = \sigma\mathbf{F} = 0 \quad (3.6)$$

$$\mathbf{J} = \sigma_{opt}\mathbf{E} \quad (3.7)$$

And for non-magnetic semiconductor $\mu=1$. Using Eq. (1.7) and Eq. (1.8) and substituting into Eq. (1.1) to Eq. (1.4) for $\rho=0$ and $\mathbf{J}=0$ we get as [18]:

$$\nabla \times \mathbf{E} = -i\omega \mu_0 \mathbf{H} \quad (3.8)$$

$$\nabla \times \mathbf{H} = (\sigma_{opt} + i\omega \varepsilon_{opt} \varepsilon_0) \mathbf{E} \quad (3.9)$$

$$\nabla \cdot \varepsilon_{opt} \varepsilon_0 \mathbf{E} = 0 \quad (3.10)$$

$$\nabla \cdot \mu_0 \mathbf{H} = 0 \quad (3.11)$$

3.3. Structure Analysis

We consider an electromagnetic wave propagating in the optical fiber along z-direction. The structure consisting of LHM in the core with radius a which is characterized by an electric relative permittivity ϵ_{co} as in Eq. (2.1) and amagnetic relative permeability μ_{co} as in Eq. (2.2) bounded by semiconductor material in the clad that is characterized by an electric relative permittivity ϵ_{cl} and amagnetic relative permeability $\mu_{cl}=1$. The semiconductor permittivity tensor can be written as [18,19]:

$$\epsilon(\omega) = \begin{bmatrix} \epsilon_{xx} & \epsilon_{xz} & 0 \\ -\epsilon_{xz} & \epsilon_{yy} & 0 \\ 0 & 0 & \epsilon_{zz} \end{bmatrix} \quad (3.12)$$

where ϵ_{xx} , ϵ_{zz} , ϵ_{yy} , ϵ_{xz} and ϵ_{zx} can be written as [19,20]:

$$\epsilon_{xx} = \epsilon_{zz} = \epsilon_0 \left(1 - \frac{\omega_p^2 (\omega + i\nu)}{\omega \left((\omega + i\nu)^2 - \omega_c^2 \right)} \right) \quad (3.13)$$

$$\epsilon_{xz} = -\epsilon_{zx} = -i \epsilon_0 \frac{\omega_p^2 \omega_c}{\omega \left((\omega + i\nu)^2 - \omega_c^2 \right)} \quad (3.14)$$

$$\epsilon_{yy} = \epsilon_0 \left(1 - \frac{\omega_p^2}{\omega(\omega + i\nu)} \right) \quad (3.15)$$

where ω_p the plasma frequency, ω_c is the cyclotron frequency, ν is the collection frequency and the magnetic relative permeability tensor $\mu_{ii}=1$. This structure is shown in figure 3.1 .

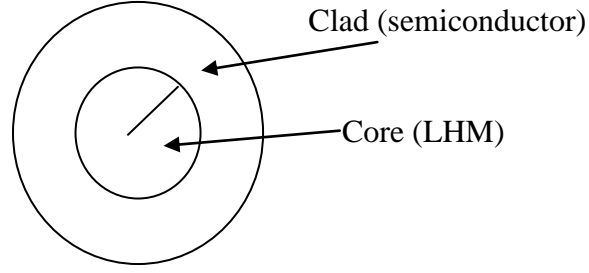


Figure 3.1: Schematic for an optical fiber with LHM core layer and semiconductor clad.

3.4. Solutions of Maxwell's Equations in Clad Region (Semiconductor)

Maxwell Eq. (1.5) can be solved with tensor electric relative permittivity ϵ_{cl} by using Eq. (3.12) and substituting into Eq. (2.17), we get:

$$\nabla \times \mathbf{H} = \frac{1}{r} \begin{vmatrix} \hat{\mathbf{r}} & r\hat{\boldsymbol{\theta}} & \hat{\mathbf{z}} \\ \partial/\partial r & \partial/\partial \theta & \partial/\partial z \\ H_r & rH_\theta & H_z \end{vmatrix} = j\omega \begin{bmatrix} \epsilon_{xx} & \epsilon_{xz} & 0 \\ -\epsilon_{xz} & \epsilon_{yy} & 0 \\ 0 & 0 & \epsilon_{zz} \end{bmatrix} \begin{bmatrix} E_r \\ E_\theta \\ E_z \end{bmatrix} \quad (3.16)$$

Taking the expansion of Eq. (3.16), we get:

$$\frac{1}{r} \frac{\partial}{\partial \theta} H_z - \frac{\partial}{\partial z} H_\theta = j\omega(\epsilon_{xx} E_r + \epsilon_{xz} E_\theta) \quad (3.17)$$

$$\frac{\partial}{\partial z} H_r - \frac{\partial}{\partial r} H_z = j\omega(-\epsilon_{xz} E_r + \epsilon_{yy} E_\theta) \quad (3.18)$$

$$\frac{1}{r} \frac{\partial}{\partial r} (rH_\theta) - \frac{1}{r} \frac{\partial}{\partial \theta} H_r = j\omega \epsilon_{zz} E_z \quad (3.19)$$

Using Eq. (2.14). and substituting into Eqs. (3.17 – 3.18), we get:

$$\frac{1}{r} \frac{\partial}{\partial \theta} H_z + j\beta H_\theta = j\omega(\epsilon_{xx} E_r + \epsilon_{xz} E_\theta) \quad (3.20)$$

$$-j\beta H_r - \frac{\partial}{\partial r} H_z = j\omega(-\epsilon_{xz} E_r + \epsilon_{yy} E_\theta) \quad (3.21)$$

Eqs. (3.19 – 3.21) are the solution of Maxwell equation Eq. (1.5) in cylindrical coordinates for semiconductor.

3.5. Expressions for $E_r, H_r, E_\theta, H_\theta$ in the Semiconductor Clad

After solving the Maxwell's equation for semiconductor in the clad region as show in the previous section we can find Expressions for $E_r, H_r, E_\theta, H_\theta$ starting with E_r . Using Eq. (2.13) for $\mu_{cl}=1$ and substituting into Eq. (3.20), the electric filed E_r can be written as:

$$E_r = \frac{-j}{\left(\omega^2 \mu_0 \varepsilon_{xx} - \beta^2\right)} \left(\frac{\mu_0 \omega}{r} \frac{\partial H_z}{\partial \theta} + \beta \frac{\partial E_z}{\partial r} + j \omega^2 \mu_0 \varepsilon_{xz} E_\theta \right) \quad (3.22)$$

Eq. (3.22) represents the value of E_r .

Using Eq. (2.15) for $\mu_{cl}=1$ and substituting into Eq. (3.21), we get:

$$E_\theta = \frac{-j}{\left(\omega^2 \mu_0 \varepsilon_{yy} - \beta^2\right)} \left(\frac{\beta}{r} \frac{\partial E_z}{\partial \theta} - \mu_0 \omega \frac{\partial H_z}{\partial r} + j \omega^2 \mu_0 \varepsilon_{yy} E_r \right) \quad (3.23)$$

Eq. (3.23) represents the value of E_θ .

Using Eq. (2.16) for $\mu_{cl}=1$ and substituting into Eq. (3.20), we get:

$$H_\theta = \frac{-j}{\left(\varepsilon_{xx} \mu_0 \omega^2 - \beta^2\right)} \left(\frac{\beta}{r} \frac{\partial}{\partial \theta} H_z + \omega \varepsilon_{xx} \frac{\partial}{\partial r} E_z - j \beta \omega \varepsilon_{xz} E_\theta \right) \quad (3.24)$$

Eq. (3.24) represents the value of H_θ .

Using Eq. (2.15) for $\mu_{cl}=1$ and substituting into Eq. (3.21) we get:

$$H_r = \frac{-j}{\left(\varepsilon_{yy} \mu_0 \omega^2 - \beta^2\right)} \left(\beta \frac{\partial}{\partial r} H_z + \frac{\omega \varepsilon_{yy}}{r} \frac{\partial}{\partial \theta} E_z - j \beta \omega \varepsilon_{xz} E_r \right) \quad (3.25)$$

Eq. (3.25) represents the value of H_r .

3.6. Dispersion Relations

3.6.1. TE Mode

From the cylindrical waveguide in case of TE polarized, we have $\partial/\partial\theta=0$ and the electric field parallel to the interface core- cladding along θ - direction to give only on component this mean there is no electric field in the direction of propagation, but the magnetic field perpendicular to interface. This physical meaning become $E_z=0$, E_r and H_θ to be not found, so we have a set of equations as [1]:

$$E_z = E_r = H_\theta = 0 \quad (3.26)$$

Here we want to explain the another components of electric and magnetic fields that be found in the core and clad region for TE mode

1- In the core region $a \geq r > 0$

using Eq. (3.26) and substituting into Eq.(2.25) and Eq. (2.27) we get:

$$E_\theta = \frac{-j}{(\omega^2 \mu_1 \varepsilon_1 - \beta^2)} \left(-\mu_1 \omega \frac{\partial H_z}{\partial r} \right) \quad (3.27)$$

$$H_r = \frac{-j}{(\varepsilon_1 \mu_1 \omega^2 - \beta^2)} \left(\beta \frac{\partial}{\partial r} H_z \right) \quad (3.28)$$

2- In the clad region $r > a$

Using Eq. (3.26) then Eqs. (3.23) , (3.25) can be rewritten as:

$$E_\theta = \frac{-j}{(\omega^2 \mu_0 \varepsilon_{yy} - \beta^2)} \left(-\mu_0 \omega \frac{\partial H_z}{\partial r} \right) \quad (3.29)$$

$$H_r = \frac{-j}{(\varepsilon_{yy} \mu_0 \omega^2 - \beta^2)} \left(\beta \frac{\partial}{\partial r} H_z \right) \quad (3.30)$$

But to find H_z the wave equation in TE mode can be rewritten as [1]:

$$\frac{\partial^2 H_z}{\partial r^2} + \frac{1}{r} \left(\frac{\partial H_z}{\partial r} \right) + (\mu \varepsilon \omega^2 - \beta^2) H_z = 0 \quad (3.31)$$

Where the magnetic field in the core and cladding expressed as:

$$H_z = \begin{cases} g(r) \cos(m\theta) & a \geq r > 0 \\ h(r) \cos(m\theta) & r > a \end{cases} \quad (3.32)$$

where $g(r)$ is the arbitrary function describe the longitudinal magnetic field in the core region along the z-direction and $h(r)$ is the arbitrary function describe the longitudinal magnetic field in the clad region along the z-direction.

The wave equation in Eq. (3.31) for the core field $H_z = g(r)$ can be written as in [1]:

$$\frac{\partial^2 g(r)}{\partial r^2} + \frac{1}{r} \left(\frac{\partial g(r)}{\partial r} \right) + K^2 g(r) = 0 \quad a \geq r > 0 \quad (3.33)$$

where K^2 is defined in Eq. (2.46).

The wave equation in in Eq. (3.31) for the clad field $H_z = h(r)$ can be written as [1]:

$$\frac{\partial^2 h(r)}{\partial r^2} + \frac{1}{r} \left(\frac{\partial h(r)}{\partial r} \right) - \eta^2 h(r) = 0 \quad r > a \quad (3.34)$$

$$\eta^2 = (\beta^2 - \mu_0 \varepsilon_{yy} \omega^2) \quad (3.35)$$

where η the wave number in the clad semiconductor along the transversal y- direction.

- The solutions of Eq. (3.33) for are $J_0(Kr)$ and $N_0(Kr)$ for m^{th} order Bessel function with $m=0$, but $N_0(Kr)$ negative infinity at at $r=0$ as shown in figure 2.3. This means that the solution in the core is $J_0(Kr)$ only.
- The solutions of Eq. (3.34) for $m=0$ are $K_0(\eta r)$ and $I_0(\eta r)$ but $I_0(\eta r)$ becomes indefinitely large at $r=\infty$ as shown in figure 2.4. This means that the solution in the clad is $K_0(\eta r)$,

Then Eq. (3.32) can be written as:

$$H_z = \begin{cases} C J_0(Kr) & a \geq r > 0 \\ D K_0(\eta r) & r > a \end{cases} \quad (3.36)$$

$$\text{where } K = \frac{U}{a} \quad \text{and} \quad \eta = \frac{W_1}{a} \quad (3.37)$$

with W_1 is the normalized transverse wave number in the clad semiconductor at y- direction.

Using Eq. (3.37) then Eq. (3.36) can be written as

$$H_z = \begin{cases} C J_0\left(\frac{U}{a}r\right) & a \geq r > 0 \\ D K_0\left(\frac{W_1}{a}r\right) & r > a \end{cases} \quad (3.38)$$

From the first boundary condition, the tangential component H_z should be continuous at core- cladding interface $r = a$ where C and D are constants given as in [1]:

$$H_{z1} = H_{z2} \quad (3.39)$$

$$D = \frac{C J_0(U)}{K_0(W_1)} \quad (3.40)$$

Then Eq. (3.55) can be written as:

$$H_z = \begin{cases} C J_0\left(\frac{U}{a}r\right) & 0 > r \geq a \\ C \frac{J_0(U)}{K_0(W_1)} K_0\left(\frac{W_1}{a}r\right) & r > a \end{cases} \quad (3.41)$$

Using Eq. (2.92) for $m=0$, Eq. (3.41) and substituting into Eq.(3.27) and Eq. (3.28) the electromagnetic fields for TE mode in the core region $a \geq r > 0$ are obtained:

$$E_\theta = \left(-j\omega C \mu_1 \frac{a}{U} J_1\left(\frac{Ur}{a}\right) \right) \quad (3.42)$$

$$H_r = \left(j\beta C \frac{a}{U} J_1\left(\frac{Ur}{a}\right) \right) \quad (3.43)$$

$$H_z = C J_0\left(\frac{U}{a}r\right) \quad (3.44)$$

Using Eq. (2.93) for $m=0$, Eq. (3.41) and substituting into Eq.(3.29) and Eq. (3.30) the electromagnetic fields for TE mode in the clad region $r > a$ are obtained:

$$E_\theta = \left(j\omega C \mu_0 \frac{a}{W_1} \right) \frac{J_0(U)}{K_0(W_1)} K_1\left(\frac{W_1}{a}r\right) \quad (3.45)$$

$$H_r = \left(-j\beta C \frac{a}{W_1} \right) \frac{J_0(U)}{K_0(W_1)} K_1\left(\frac{W_1}{a}r\right) \quad (3.46)$$

$$H_z = C \frac{J_0(U)}{K_0(W_1)} K_0\left(\frac{W_1}{a}r\right) \quad (3.47)$$

To find the dispersion equation for TE mode, we use the second boundary condition. The tangential component E_θ should be continuous at core-cladding interface $r = a$ as:

$$E_{\theta 1} = E_{\theta 2} \quad (3.48)$$

Using Eq. (2.64), Eq. (3.42) and Eq. (3.45) then substituting into Eq. (3.48) we get:

$$\left(\frac{1}{U} \frac{J'_m(U)}{J(U)} + \frac{1}{\mu_{co}} \frac{1}{W_1} \frac{K'_m(W_1)}{K_m(W_1)} \right) = 0 \quad (3.49)$$

Eq. (3.49) called the dispersion equation which describe the surface wave and the waveguide in TE polarized.

3.6.2. TM Mode

In TM mode, we have $H_z = 0$, $\partial/\partial\theta = 0$, H_r and E_θ have to be not found, this mean that magnetic field parallel to the interface core-cladding along θ - direction and the electric field perpendicular to interface along $r = a$, so we have set of equations as [1]:

$$H_z = H_r = E_\theta = 0 \quad (3.50)$$

The components of electric and magnetic fields that be found in the core and clad regions for TM mode become

1- In the core region $a \geq r > 0$

Using Eq. (3.50) then Eq. (2.24), Eq. (2.26) can be written as:

$$E_r = \frac{-j}{(\omega^2 \mu_0 \epsilon_{xx} - \beta^2)} \left(\beta \frac{\partial E_z}{\partial r} \right) \quad (3.51)$$

$$H_\theta = \frac{-j}{(\epsilon_{xx} \mu_0 \omega^2 - \beta^2)} \left(\omega \epsilon_1 \frac{\partial}{\partial r} E_z \right) \quad (3.52)$$

2- In the clad region $r > a$

Using Eq. (3.50) then Eq. (3.22) and Eq. (2.24) can be written as:

$$E_r = \frac{-j}{(\omega^2 \mu_1 \epsilon_1 - \beta^2)} \left(\beta \frac{\partial E_z}{\partial r} \right) \quad (3.53)$$

$$H_\theta = \frac{-j}{(\epsilon_1 \mu_1 \omega^2 - \beta^2)} \left(\omega \epsilon_{xx} \frac{\partial}{\partial r} E_z \right) \quad (3.54)$$

To find E_z , the wave equation in TM mode can be written as [1]:

$$\frac{\partial^2 E_z}{\partial r^2} + \frac{1}{r} \left(\frac{\partial E_z}{\partial r} \right) + (\mu \epsilon \omega^2 - \beta^2) E_z = 0 \quad (3.55)$$

magnetic field in the core and cladding expressed as:

$$E_z = \begin{cases} f(r) \cos(m\theta) & a \geq r > 0 \\ s(r) \cos(m\theta) & r > a \end{cases} \quad (3.56)$$

where $f(r)$ is the arbitrary function describe the longitudinal electric field in the core region along the z-direction and $s(r)$ is the arbitrary function describe the longitudinal electric field in the clad region along the z-direction.

The wave equation in Eq. (3.31) for the core field $E_z = f(r)$ can be written as in [1]:

$$\frac{\partial^2 f(r)}{\partial r^2} + \frac{1}{r} \left(\frac{\partial f(r)}{\partial r} \right) + K^2 f(r) = 0 \quad a \geq r > 0 \quad (3.57)$$

where K^2 are defined in Eq. (2.46).

The wave equation in in Eq. (3.31) for the clad field $E_z = s(r)$ can be written as [1]:

$$\frac{\partial^2 s(r)}{\partial r^2} + \frac{1}{r} \left(\frac{\partial s(r)}{\partial r} \right) - \xi^2 s(r) = 0 \quad r > a \quad (3.58)$$

With

$$\xi^2 = (\beta^2 - \mu_0 \epsilon_{xx} \omega^2) \quad (3.59)$$

where ξ is the wave number in the clad semiconductor along the transversal x- direction.

Eq. (3.58) have two solutions, the first $I_0(\xi r)$ and the second $K_0(\xi r)$. As shown in figure 2.4 $I_0(\xi r)$ becomes indefinitely large at $r = \infty$, this mean the solutions in the clad $K_0(\xi r)$ in this case.

Then Eq. (3.56) can be written as:

$$E_z = \begin{cases} A J_0(Kr) & a \geq r > 0 \\ B K_0(\xi r) & r > a \end{cases} \quad (3.60)$$

where $\xi = \frac{W_2}{a}$ (3.61)

with W_2 is the normalized transverse wave number in the clad semiconductor at x- direction.

Using Eq. (2.46) and Eq. (3.61) then Eq. (3.60) can be written as:

$$E_z = \begin{cases} A J_0\left(\frac{U}{a}r\right) & a \geq r > 0 \\ B K_0\left(\frac{W_2}{a}r\right) & r > a \end{cases} \quad (3.62)$$

From the first boundary condition, the tangential component E_z should be continuous at core-cladding interface $r = a$ where A and B are constants as in [1]:

$$E_{1z} = E_{2z} \quad (3.63)$$

$$B = \frac{A J_0(U)}{K_0(W_2)} \quad (3.64)$$

Using Eq. (3.64) then Eq. (3.62) can be rewritten as:

$$E_z = \begin{cases} A J_0\left(\frac{U}{a}r\right) & a \geq r > 0 \\ A \frac{J_0(U)}{K_0(W_1)} K_0\left(\frac{W_2}{a}r\right) & r > a \end{cases} \quad (3.65)$$

Using Eq. (2.93) for $m=0$, Eq. (3.65) and substituting into Eq.(3.51) and Eq. (3.52) the electromagnetic fields for TM mode in the core region $a \geq r > 0$ are obtained:

$$E_r = \left(j\beta A \frac{a}{U} J_1\left(\frac{Ur}{a}\right) \right) \quad (3.66)$$

$$H_\theta = \left(j\omega \varepsilon_1 A \frac{a}{U} J_1\left(\frac{Ur}{a}\right) \right) \quad (3.67)$$

$$E_z = A J_0\left(\frac{U}{a}r\right) \quad (3.68)$$

Using Eq. (2.93) for $m=0$, and Eq. (3.65) then substituting into Eq. (3.53) and Eq. (3.54) the electromagnetic fields for TM mode in the clad region $r > a$ are obtained:

$$E_r = \left(-j\beta A \frac{a}{W_2} \right) \frac{J_0(U)}{K_0(W_2)} K_1\left(\frac{W_2}{a}r\right) \quad (3.69)$$

$$H_{\theta} = \left(-j\omega \varepsilon_{xx} A \frac{a}{W_2} \right) \frac{J_0(U)}{K_0(W_2)} K_1\left(\frac{W_2}{a} r\right) \quad (3.70)$$

$$E_z = A \frac{J_0(U)}{K_0(W_2)} K_0\left(\frac{W_2}{a} r\right) \quad (3.71)$$

To find the dispersion equation for TM mode, we use the second boundary condition. The tangential component H_{θ} should be continuous at core-cladding interface

$r = a$ as

$$H_{\theta 1} = H_{\theta 2} \quad (3.72)$$

using Eq. (2.65), Eq. (3.67), and Eq. (3.61) then substituting into Eq. (3.72) we get:

$$\left(\frac{1}{U} \frac{J_m'(U)}{J_m(U)} + \frac{\varepsilon_{xx}^{cl}}{\varepsilon_{co}} \frac{1}{W_2} \frac{K_m'(W_2)}{K_m(W_2)} \right) = 0 \quad (3.73)$$

Eq. (3.73) describe dispersion relation in TM polarized.

3.6.3. Hybrid Mode

In hybrid mode, the electromagnetic field components E_z and H_z should not be zero. The wave equation for this type for H_z is given by Eq. (3.31), and the wave equation for E_z is given by Eq. (3.55). The solutions for Eqs. (3.31) and (3.55) are given by the product of m^{th} order Bessel functions and $\cos(m\theta)$ or $\sin(m\theta)$. E_z and H_z should be continuous at $r = a$. Where the solution for Eq. (3.31) is given by Eq. (2.51), and the solution for Eq. (3.55) is given by Eq. (2.50). Also it is known that $\partial E_z / \partial r$ and $\partial H_z / \partial \theta$ (or $\partial E_z / \partial \theta$ and $\partial H_z / \partial r$) have the same θ dependencies. Then the component of electromagnetic field in the core region are expressed by Eqs. (2.52-2.55).

To find the components of electromagnetic field in semiconductor clad. Using Eq. (2.50) and Eq. (2.51) then substituting from Eq. (3.22) to Eq. (3.25), we get

$$E_r = \frac{j a^2}{W_2^2} \left(\frac{C \omega \mu_0}{r} K_m \left(\frac{W_2 r}{a} \right) + \frac{A \beta W_2}{a} K_m' \left(\frac{W_2 r}{a} \right) + \frac{j \mu_2 \omega^2 \varepsilon_{xz}}{\cos(m\theta)} \frac{K_m(W_2)}{J_m(U)} E_\theta \right) \frac{J_m(U)}{K_m(W_2)} \cos(m\theta) \quad (3.74)$$

$$E_\theta = \frac{j a^2}{W_1^2} \left(-C \omega \mu_2 \frac{W_1}{a} K_m' \left(\frac{W_1 r}{a} \right) - \frac{A \beta m}{r} K_m \left(\frac{W_1 r}{a} \right) - \frac{j \mu_2 \omega^2 \varepsilon_{xz}}{\sin(m\theta)} \frac{K_m(W_1)}{J_m(U)} E_r \right) \frac{J_m(U)}{K_m(W_1)} \sin(m\theta) \quad (3.75)$$

$$H_r = \frac{j a^2}{W_1^2} \left(C \beta \frac{W_1}{a} K_m' \left(\frac{W_1 r}{a} \right) + A \omega \varepsilon_{yy} \frac{m}{r} K_m \left(\frac{W_1 r}{a} \right) - \frac{j \omega \beta \varepsilon_{xz}}{\sin(m\theta)} \frac{K_m(W_1)}{J_m(U)} E_r \right) \frac{J_m(U)}{K_m(W_1)} \sin(m\theta) \quad (3.75)$$

$$H_\theta = \frac{j a^2}{W_2^2} \left(A \omega \varepsilon_{xx} \frac{W_2}{a} K_m' \left(\frac{W_2 r}{a} \right) + c \beta \frac{m}{r} K_m \left(\frac{W_2 r}{a} \right) - \frac{j \omega \beta \varepsilon_{xz}}{\cos(m\theta)} \frac{K_m(W_2)}{J_m(U)} E_\theta \right) \frac{J_m(U)}{K_m(W_2)} \cos(m\theta) \quad (3.77)$$

To find the dispersion relation, we use the first boundary condition. Using Eq. (2.53) and Eq. (3.75) then substituting into Eq. (3.48) we get:

$$A \beta m \left(\frac{1}{U^2} + \frac{1}{W_1^2} \right) = -C \omega \left(\frac{\mu_1 J_m'(U)}{U J_m(U)} + \frac{\mu_2 K_m'(W_1)}{W_1 K_m(W_1)} + j \frac{\mu_2 \varepsilon_{xz} \omega^2}{a W_1^2} \frac{1}{J_m(U) \sin(m\theta)} E_r \right) \quad (3.78)$$

Applying the second boundary condition at $r = a$, Using Eq. (2.55) and Eq. (3.77) then substituting into Eq. (3.72) we get:

$$C \beta m \left(\frac{1}{U^2} + \frac{1}{W_2^2} \right) = -A \omega \left(\frac{\varepsilon_1 J_m'(U)}{U J_m(U)} + \frac{\varepsilon_{xx} K_m'(W_2)}{W_2 K_m(W_2)} + j \frac{\beta \varepsilon_{xz}}{W_2^2} \frac{1}{a J_m(U) \cos(m\theta)} E_\theta \right) \quad (3.79)$$

Multiplying Eq. (3.78) with Eq. (3.79), we get:

$$\omega^2 \left(\frac{\mu_1 J'_m(U)}{U J_m(U)} + \frac{\mu_2 K'_m(W_1)}{W_1 K_m(W_1)} + j \frac{\mu_2 \varepsilon_{xz}}{aC W_1^2} \frac{1}{J_m(U) \sin(m\theta)} E_r \right) \left(\frac{\varepsilon_1 J'_m(U)}{U J_m(U)} + \frac{\varepsilon_{xx} K'_m(W_2)}{W_2 K_m(W_2)} + j \frac{\beta \varepsilon_{xz}}{W_2^2 aA J_m(U) \cos(m\theta)} \frac{E_\theta}{\cos(m\theta)} \right) = \beta^2 m^2 \left(\frac{1}{U^2} + \frac{1}{W_1^2} \right) \left(\frac{1}{U^2} + \frac{1}{W_2^2} \right) \quad (3.80)$$

From Eq. (2.65) we get

$$\varepsilon_{xx} = \varepsilon_0 \varepsilon_{xx}^{cl} \quad (3.81)$$

$$\varepsilon_{xz} = \varepsilon_0 \varepsilon_{xz}^{cl} \quad (3.82)$$

where ε_{xx}^{cl} is the clad relative permittivity in x- direction, and ε_{xz}^{cl} is the clad relative permittivity in xz- direction.

Using Eq. (2.67), Eq. (3.81) and Eq. (3.82), then substituting into Eq. (3.80) we get:

$$\left(\frac{\mu_{co} J'_m(U)}{U J_m(U)} + \frac{1}{W_1} \frac{K'_m(W_1)}{K_m(W_1)} + j \frac{\varepsilon_0 \varepsilon_{xz}^{cl}}{aC W_1^2} \frac{1}{J_m(U) \sin(m\theta)} E_r \right) \left(\frac{\varepsilon_{co} J'_m(U)}{U J_m(U)} + \frac{\varepsilon_{xx}^{cl} K'_m(W_2)}{W_2 K_m(W_2)} + j \frac{\beta \varepsilon_{xz}^{cl}}{W_2^2 aA J_m(U) \cos(m\theta)} \frac{E_\theta}{\cos(m\theta)} \right) = \frac{m^2 \beta^2}{k^2} \left(\frac{1}{U^2} + \frac{1}{W_1^2} \right) \left(\frac{1}{U^2} + \frac{1}{W_2^2} \right) \quad (3.83)$$

Using Eq. (3.59) and Eq. (3.61), we get:

$$\frac{\beta^2}{W_2^2} = \frac{k^2 \varepsilon_{xx}^{cl}}{W_2^2} + \frac{1}{a^2} \quad (3.84)$$

Using Eq. (2.70) and Eq. (3.84), we get:

$$\frac{\beta^2}{k^2} \left(\frac{1}{U^2} + \frac{1}{W_2^2} \right) = \frac{n_{co}^2}{U^2} + \frac{\varepsilon_{xx}^{cl}}{W_2^2} \quad (3.85)$$

Using Eq. (3.85) and dividing Eq. (3.83) by $\varepsilon_{co} \mu_{co}$ where $n_{co}^2 = \varepsilon_{co} \mu_{co}$ we get:

$$\frac{1}{\varepsilon_{co}\mu_{co}} \left(\frac{\mu_{co} J'_m(U)}{U J_m(U)} + \frac{1}{W_1} \frac{K'_m(W_1)}{K_m(W_1)} + j \frac{\varepsilon_0 \varepsilon_{xz}^{cl}}{a C W_1^2} \frac{1}{J_m(U) \sin(m\theta)} E_r \right) \\ \left(\frac{\varepsilon_{co} J'_m(U)}{U J_m(U)} + \frac{\varepsilon_{xx}^{cl}}{W_2} \frac{K'_m(W_2)}{K_m(W_2)} + j \frac{\beta \varepsilon_{xz}^{cl}}{W_2^2} \frac{1}{a A J_m(U)} \frac{E_\theta}{\cos(m\theta)} \right) = m^2 \left(\frac{1}{U^2} + \frac{\varepsilon_{xx}^{cl}}{n_{co}^2} \left(\frac{1}{W_2^2} \right) \right) \left(\frac{1}{U^2} + \frac{1}{W_1^2} \right) \quad (3.86)$$

The R.H.S of Eq. (3.84) can be rewritten as:

$$R.H.S = \frac{\beta^2 k^2 (\varepsilon_{co}\mu_{co} - \varepsilon_{xx}^{cl})^2 a^4}{W_1^2 W_2^2 U^4 \varepsilon_{co}\mu_{co}} m^2 \quad (3.87)$$

Where non-magnetic semiconductor clad $\mu_{cl}=1$.

Then the dispersion relation for hybrid mode can be written as

$$\left(\frac{1}{U} \frac{J'_m(U)}{J_m(U)} + \frac{1}{\mu_{co}} \frac{1}{W_1} \frac{K'_m(W_1)}{K_m(W_1)} + j \frac{\varepsilon_0 \varepsilon_{xz}^{cl}}{a \mu_{co} C W_1^2} \frac{1}{J_m(U) \sin(m\theta)} E_r \right) \\ \left(\frac{1}{U} \frac{J'_m(U)}{J_m(U)} + \frac{\varepsilon_{xx}^{cl}}{\varepsilon_{co}} \frac{1}{W_2} \frac{K'_m(W_2)}{K_m(W_2)} + j \frac{\beta \varepsilon_{xz}^{cl}}{\varepsilon_{co} W_2^2} \frac{1}{a A J_m(U)} \frac{E_\theta}{\cos(m\theta)} \right) = \frac{\beta^2 k^2 (\varepsilon_{co}\mu_{co} - \varepsilon_{xx}^{cl})^2 a^4}{W_1^2 W_2^2 U^4 \varepsilon_{co}\mu_{co}} m^2 \quad (3.88)$$

Eq. (3.88) is the general dispersion equation for each $m \geq 1$ in hybrid mode with $\varepsilon_{co}\mu_{co} > \varepsilon_{cl}$ to be fast mode. The Eq. (3.113) describes the dispersion relation for the fast mode which satisfies the value of product $\varepsilon_{co}\mu_{co} > \varepsilon_{cl}$, this means that $U^2 > 0$. But when the product $\varepsilon_{co}\mu_{co} \leq \varepsilon_{cl}$ this means $U^2 < 0$ so it has an imaginary value. In this case, we must let $U = jU_1$ to give $U_1^2 > 0$. By using Eqs. (2.87 – 2.89) and substituting into Eq. (3.88) with $U = jU_1$ to find the new dispersion relation for the slow mode, we get:

$$\left(\frac{1}{U_1} \frac{I'_m(U_1)}{I_m(U_1)} - \frac{1}{\mu_{co}} \frac{1}{W_1} \frac{K'_m(W_1)}{K_m(W_1)} - j^{1-m} \frac{\epsilon_0 \epsilon_{xz}^{cl}}{a \mu_{co} C W_1^2} \frac{1}{I_m(U_1) \sin(m\theta)} E_r \right) \\ \left(\frac{1}{U_1} \frac{I'_m(U_1)}{I_m(U_1)} - \frac{\epsilon_{xx}^{cl}}{\epsilon_{co}} \frac{1}{W_2} \frac{K'_m(W_2)}{K_m(W_2)} - j^{1-m} \frac{\beta \epsilon_{xz}^{cl}}{\epsilon_{co} W_2^2} \frac{1}{a A I_m(U_1)_m \cos(m\theta)} E_\theta \right) = \frac{\beta^2 k^2 (\epsilon_{co} \mu_{co} - \epsilon_{xx}^{cl})^2 a^4}{W_1^2 W_2^2 U_1^4 \epsilon_{co} \mu_{co}} m^2 \quad (3.89)$$

Eq. (3.89) is the general dispersion equation for each $m \geq 0$ in the slow mode with $\epsilon_{co} \mu_{co} \leq \epsilon_{cl}$.

3.7. Optical Power for TE and TM Modes

The averaged pointing vector component along z- axis per unit area is expressed by Eq. (1.38) as in [1,18]:

$$S_z = \frac{1}{2} (\mathbf{E} \times \mathbf{H}^*) \cdot \mathbf{e}_z = \frac{1}{2} (E_r H_\theta^* - E_\theta H_r^*) \quad (3.90)$$

where \mathbf{e}_z is the unit vector in z-direction. The power P carried by the optical fiber is given by using the relation as in [1,21]:

$$P = \int_0^{2\pi} \int_0^\infty S_z r dr d\theta \quad (3.91)$$

Using Eq. (3.90) and substituting into Eq. (3.91), we find that as [22,23]:

$$P = \frac{1}{2} \int_0^{2\pi} \int_0^\infty (E_r H_\theta^* - E_\theta H_r^*) r dr d\theta \quad (3.92)$$

The analytical expressions for transmission power in each mode are described in the following:

3.7.1. TE mode

A-In the LHM core region $a \geq r > 0$

The power in the core for TE mode, from Eq. (3.26) we have $E_r = 0$ then substituting into Eq. (3.92), we get:

$$P_{TE1} = -\frac{1}{2} \int_0^{2\pi} \int_0^a E_\theta H_r^* r dr d\theta \quad (3.93)$$

where P_{TE1} is the power in the core for TE mode. Using Eq. (3.43) we find out:

$$H_r^* = -\frac{jC^* \beta a}{U} J_1\left(\frac{Ur}{a}\right) \quad (3.94)$$

Where the integral formula can be written as in [1,15]:

$$\int_0^a J_m^2\left(\frac{Ur}{a}\right) r dr = \begin{cases} \frac{a^2}{2} (J_0^2(U) + J_1^2(U)) & m = 0 \\ \frac{a^2}{2} (J_m^2(U) - J_{m-1}(U) J_{m+1}(U)) & m \geq 1 \end{cases} \quad (3.95)$$

Using Eq. (3.42) and Eq. (3.94) then substituting into Eq. (3.93) we find:

$$P_{TE1} = \frac{1}{2} \frac{|C|^2 a^2 \beta \mu_1 \omega}{U^2} \left((2\pi) \int_0^a J_1^2\left(\frac{Ur}{a}\right) r dr \right) \quad (3.96)$$

Using and Eq. (3.95) for $m \geq 0$ and substituting into Eq. (3.96), we get:

$$P_{TE1} = \frac{\pi |C|^2 a^4 \beta \mu_1 \omega}{2 U^2} (J_1^2(U) - J_0(U) J_2(U)) \quad (3.97)$$

Using Eq. (2.2) and Eq. (2.64) then substituting into Eq. (3.97), we find the power in the core in TE mode are:

$$P_{TE1} = \frac{\pi}{2} \beta \omega |C|^2 \frac{a^4}{U^2} \mu_0 \left(1 - \frac{F \omega^2}{\omega^2 - \omega_0^2} \right) \left(J_1^2(U) - J_0(U) J_2(U) \right) \quad (3.98)$$

where P_{TE1} is the power in the core region for TE mode.

B- In the semiconductor clad region $r > a$

To find the power in the clad region for TE mode, must using Eq. (3.26) for $E_r = 0$, and substituting into Eq. (3.92), we get:

$$P_{TE2} = -\frac{1}{2} \int_0^{2\pi} \int_a^\infty E_\theta H_r^* r dr d\theta \quad (3.99)$$

from Eq. (3.46) we find that:

$$H_r^* = j\beta C^* \frac{a}{W_1} \frac{J_0(U)}{K_0(W_1)} K_1\left(\frac{W_1}{a} r\right) \quad (3.100)$$

Using Eq. (3.46) and Eq. (3.100) then substituting into Eq. (3.92), we get:

$$P_{TE2} = \frac{1}{2} \frac{|C|^2 a^2 \beta \mu_0 \omega}{W_1^2} \frac{J_0^2(U)}{K_0^2(W_1)} \left((2\pi - 0) \int_a^\infty K_1^2\left(\frac{W_1 r}{a}\right) r dr \right) \quad (3.101)$$

By using the integral formula as [1,15]:

$$\int_a^\infty K_m^2\left(\frac{W}{a} r\right) r dr = \begin{cases} \frac{a^2}{2} (K_1^2(W) - K_0^2(W)) & m = 0 \\ \frac{a^2}{2} (K_{m-1}(W) K_{m+1}(W) - K_m^2(W)) & m \geq 1 \end{cases} \quad (3.102)$$

Using Eq. (3.102) for $m \geq 0$ and substituting into Eq. (3.101), we get:

$$P_{TE2} = \frac{\pi}{2} \frac{|C|^2 a^4 \beta \mu_0 \omega}{W_1^2} \frac{J_0^2(U)}{K_0^2(W_1)} \left(K_0(W_1) K_2(W_1) - K_1^2(W_1) \right) \quad (3.103)$$

Using Eq. (2.2) and Eq. (2.64) then substituting into Eq. (3.103), to find the power in the clad region for TE mode, we get:

$$P_{TE2} = \frac{\pi}{2} \beta \omega |C|^2 \mu_0 \frac{a^4}{W_1^2} \frac{J_0^2(U)}{K_0^2(W_1)} \left(K_0(W_1) K_2(W_1) - K_1^2(W_1) \right) \quad (3.104)$$

where P_{TE2} is the power in the clad region for TE mode.

To find the total power in TE mode, using Eq. (3.98) and Eq. (3.104) as [21,22]:

$$P_{TE} = P_{TE1} + P_{TE2} \quad (3.105)$$

where P_{TE} is the total power in the case of TE mode.

3.7.2. TM mode

A-In the LHM core region $a \geq r > 0$

To calculate the power flow in the core region for TM mode P_{TM1} we have $E_\theta = 0$ from Eq. (3.50), substituting into Eq. (3.92), we get:

$$P_{TM1} = \frac{1}{2} \int_0^{2\pi} \int_0^a \left(E_r H_\theta^* - 0 \right) r dr d\theta \quad (3.106)$$

Using Eq. (3.67) we find:

$$H_\theta^* = -j \varepsilon_1 \omega A^* \frac{a}{U} J_1\left(\frac{Ur}{a}\right) \quad (3.107)$$

Using Eq. (3.69) and Eq. (3.107), then substituting into Eq. (3.106), we get:

$$P_{TM1} = \frac{1}{2} \frac{|A|^2}{U^2} \frac{a^2 \beta \varepsilon_1 \omega}{U^2} \left((2\pi - 0) \int_0^a J_1^2\left(\frac{Ur}{a}\right) r dr \right) \quad (3.108)$$

Using Eq. (3.95) for $m \geq 1$ and substituting into Eq. (3.108) we get:

$$P_{TM1} = \frac{\pi |A|^2 a^4 \beta \varepsilon_1 \omega}{2 U^2} \left(J_1^2(U) - J_0(U) J_2(U) \right) \quad (3.109)$$

Using Eq. (2.1) and Eq. (2.65) and substituting into Eq. (3.109), we get:

$$P_{TM1} = \frac{\pi \beta \omega |A|^2 a^4}{2 U^2} \varepsilon_0 \left(1 - \frac{\omega_p^2}{\omega^2} \right) \left(J_1^2(U) - J_0(U) J_2(U) \right) \quad (3.110)$$

B- In the semiconductor clad region $r > a$

In TM ode we have $E_\theta = 0$, The power flow in the clad region for TM mode P_{TM2} can be found for using Eq. (3.50) then substituting into Eq. (3.92) we get:

$$P_{TM2} = \frac{1}{2} \int_0^{2\pi} \int_a^\infty \left(E_r H_\theta^* - 0 \right) r dr d\theta \quad (3.111)$$

.Using Eq. (3.70) we find:

$$H_\theta^* = j \varepsilon_{xx} \omega A^* \frac{a}{W_2} \frac{J_0(U)}{K_0(W_2)} K_1\left(\frac{W_2 r}{a}\right) \quad (3.112)$$

Using Eq. (3.69) and Eq. (3.112), then substituting into Eq. (3.111) we get::

$$P_{TM2} = \frac{1}{2} \frac{|A|^2 a^2 \beta \varepsilon_{xx} \omega}{W_2^2} \frac{J_0^2(U)}{K_0^2(W_2)} \left((2\pi) \int_a^\infty K_1^2\left(\frac{W_2 r}{a}\right) r dr \right) \quad (3.113)$$

Using Eq. (3.102) with $m \geq 1$ and substituting into Eq. (3.113), we get:

$$P_{TM2} = \frac{\pi |A|^2 a^4 \beta \varepsilon_{xx} \omega}{2 W_2^2} \frac{J_0^2(U)}{K_0^2(W_2)} \left(K_0(W_2) K_2(W_2) - K_1^2(W_2) \right) \quad (3.114)$$

Using Eq. (2.65) with $\varepsilon_{xx} = \varepsilon_0 \varepsilon_{xx}^{cl}$ and Eq. (3.13), then substituting into Eq. (3.114), we get

$$P_{TM2} = \frac{\pi}{2} \beta \omega |A|^2 \frac{a^4}{W_2^2} \epsilon_0 \left(1 - \frac{\omega_p^2 (\omega + i\nu)}{\omega \left((\omega + i\nu)^2 - \omega_c^2 \right)} \right) \frac{J_0^2(U)}{K_0^2(W_2)} \left(K_0(W_2) K_2(W_2) - K_1^2(W_2) \right) \quad (3.115)$$

But the total power flow for TM mode can be calculated by using Eq. (3.110) and Eq. (3.115) as [21,22]

$$P_{TM} = P_{TM1} + P_{TM2} \quad (3.116)$$

CHAPTER FOUR

MODES IN OPTICAL FIBER WITH LHM CORE AND SEMICNDUCTOR CLAD: GENERAL CASE

In this chapter, the propagation properties of waves in optical fiber consisting of LHM core and semiconductor clad will be studied. The dispersion relations of TE, TM, HE and EH mode polarization for the proposed fiber will be investigated in section 4.2. The total power transported within the core and clad in case of TE and TM modes will be calculated in section 4.3. The dispersion curves and the total power flow will be studied for different parameters in section 4.4.

4.1. Structure Analysis

We consider the electromagnetic wave propagating along the symmetric fiber for cylindrical waveguide with LHM as core layer occupying the region $a \geq r > 0$ which characterize by electric relative permittivity ϵ_{co} given by Eq. (2.1) and magnetic relative permeability μ_{co} given by Eq. (2.2). The core layer is bounded by the a semiconductor material which occupies the region $r > a$ as shown in figure (3.1). The clad semiconductor layer is characterized by the electric relative permittivity in the three dimensions (ϵ_{xx}^{cl} , ϵ_{yy}^{cl} and ϵ_{zz}^{cl}) and magnetic relative permeability $\mu_{cl} = 1$, using Eq. (2.65) and substituting into Eq. (3.13) and Eq. (3.14) we get:

$$\epsilon_{cl}^{xx} = \frac{\epsilon_{xx}}{\epsilon_0} = \left(1 - \frac{\omega_p^2(\omega + i\nu)}{\omega((\omega + i\nu)^2 - \omega_c^2)} \right) \quad (4.1)$$

$$\epsilon_{cl}^{yy} = \frac{\epsilon_{yy}}{\epsilon_0} \left(1 - \frac{\omega_p^2}{\omega(\omega + i\nu)} \right) \quad (4.2)$$

$$\varepsilon_{cl}^{zz} = \frac{\varepsilon_{zz}}{\varepsilon_0} = \left(1 - \frac{\omega_p^2(\omega + i\nu)}{\omega((\omega + i\nu)^2 - \omega_c^2)} \right) \quad (4.3)$$

where ε_{xx}^{cl} is the electric permittivity in the clad at x- direction, ε_{yy}^{cl} the electric permittivity in the clad at y- direction and ε_{zz}^{cl} the electric permittivity in the clad at z- direction.

In this, case semiconductor permittivity tensor is expressed as:

$$\varepsilon_{cl}(\omega) = \frac{1}{\varepsilon_0} \begin{bmatrix} \varepsilon_{xx} & 0 & 0 \\ 0 & \varepsilon_{yy} & 0 \\ 0 & 0 & \varepsilon_{zz} \end{bmatrix} = \begin{bmatrix} \varepsilon_{xx}^{cl} & 0 & 0 \\ 0 & \varepsilon_{yy}^{cl} & 0 \\ 0 & 0 & \varepsilon_{zz}^{cl} \end{bmatrix} \quad (4.4)$$

where

$$\varepsilon_{xz} = \varepsilon_{zx} = 0 \quad (4.5)$$

4.2. The Dispersion Relations

For TE mode, the dispersion equation is given by Eq. (3.49). Also for TM mode the dispersion equation is given by Eq. (3.73). To obtain the dispersion equation in the hybrid mode in this case, using Eq. (4.5) and subsisting into Eq. (3.88), we get:

$$\left(\frac{1}{U} \frac{J'_m(U)}{J(U)} + \frac{1}{\mu_{co}} \frac{1}{W} \frac{K'_m(W_1)}{K_m(W_1)} \right) \left(\frac{1}{U} \frac{J'_m(U)}{J_m(U)} + \frac{\varepsilon_{xx}^{cl}}{\varepsilon_{co}} \frac{1}{W_2} \frac{K'_m(W_2)}{K_m(W_2)} \right) = \frac{\beta^2 k^2 (\varepsilon_{co} \mu_{co} - \varepsilon_{xx}^{cl})^2 a^4}{W_1^2 W_2^2 U^4 \varepsilon_{co} \mu_{co}} m^2 \quad (4.6)$$

where W_1 are defined in Eq. (3.37) and W_2 in Eq. (3.61).

Eq. (4.6) is the dispersion equation of the hybrid mode that has two solutions, one of them (+) EH mode and the another is (-) HE mode as:

$$+ \sqrt{\left(\frac{1}{U} \frac{J'_m(U)}{J(U)} + \frac{1}{\mu_{co}} \frac{1}{W} \frac{K'_m(W_1)}{K_m(W_1)} \right) \left(\frac{1}{U} \frac{J'_m(U)}{J_m(U)} + \frac{\varepsilon_{xx}^{cl}}{\varepsilon_{co}} \frac{1}{W_2} \frac{K'_m(W_2)}{K_m(W_2)} \right)} = \frac{\beta k (\varepsilon_{co} \mu_{co} - \varepsilon_{xx}^{cl}) a^2}{W_1 W_2 U^2 \sqrt{\varepsilon_{co} \mu_{co}}} m \quad \text{EH mode} \quad (4.7)$$

$$-\sqrt{\left(\frac{1}{U} \frac{J'_m(U)}{J(U)} + \frac{1}{\mu_{co}} \frac{1}{W} \frac{K'_m(W_1)}{K_m(W_1)}\right) \left(\frac{1}{U} \frac{J'_m(U)}{J_m(U)} + \frac{\epsilon_{xx}^{cl}}{\epsilon_{co}} \frac{1}{W_2} \frac{K'_m(W_2)}{K_m(W_2)}\right)} = \frac{\beta k (\epsilon_{co} \mu_{co} - \epsilon_{xx}^{cl}) a^2}{W_1 W_2 U^2 \sqrt{\epsilon_{co} \mu_{co}}} m \quad \text{HE mode} \quad (4.8)$$

4.3. Power Consideration

4.3.1. For TE Mode

The total power transported with the core and the clad can be calculated in this case by using Eq. (3.98) and Eq. (3.104) then substituting into Eq. (3.105), we get:

$$P_{TE} = \frac{\pi}{2} \beta \omega |C|^2 a^4 \mu_0 \left(\left(1 - \frac{F \omega^2}{\omega^2 - \omega_0^2}\right) \frac{1}{U^2} (J_1^2(U) - J_0(U) J_2(U)) + \frac{1}{W_1^2} \frac{J_0^2(U)}{K_0^2(W_1)} (K_0(W_1) K_2(W_1) - K_1^2(W_1)) \right) \quad (4.9)$$

4.3.2. For TM Mode

In case of TM mode the total power transported between the core and the clad by the waveguide can be calculated, using Eq. (3.110) and Eq. (3.115) then substituting into Eq. (3.116) to get:

$$P_{TM} = \frac{\pi}{2} \beta \omega |A|^2 a^4 \epsilon_0 \left(\left(1 - \frac{\omega_p^2}{\omega^2}\right) \frac{1}{U^2} (J_1^2(U) - J_0(U) J_2(U)) + \frac{1}{W_2^2} \left(1 - \frac{\omega_p^2 (\omega + i\nu)}{\omega ((\omega + i\nu)^2 - \omega_c^2)}\right) \frac{J_0^2(U)}{K_0^2(W_2)} (K_0(W_2) K_2(W_2) - K_1^2(W_2)) \right) \quad (4.10)$$

4.4. Numerical Results

In the below analysis, we have assumed that the electromagnetic wave propagating along the fiber with radius $a = 30\mu m$, the core to be LHM with range frequency from 4 to 6 GHz, plasma frequency $\omega_p/2\pi = 10$ GHz, the resonant frequency $\omega_0/2\pi = 4$ GHz, and fractional area of the unit cell $F = 0.56$. The cladding layer to be a semiconductor material with plasma frequency $\omega_p/2\pi = 10$ GHz, collision frequency $\nu = 3/2\pi$ GHz, the cyclotron frequency $\omega_c = 7/2\pi$ GHz and $\mu_{cl} = 1$. Eq. (3.69) and Eq. (3.94) are solved numerically to describe the dispersion relations for TE and TM mode curves with different value of fractional area F and core radius a . In Figure 4.1, the dispersion curves for TM polarization are plotted and shows the variation of the propagation constant β/k with given frequency and different value of F . As shown in the figure 4.1, the frequency decreases from largest to smallest value with increasing the propagation constant β/k because the dispersion equation for TM mode in Eq. (3.73) directly generated with electric relative permittivity $\varepsilon(\omega)$ for the guided layer that increases as the frequency increases. The effect of fractional area F clarify the different behaviors of TM dispersion curves and the propagation constant β/k increase as the fractional area F increase, this mean, the largest β/k released at largest value of F . Figure 4.2 shows the relation between the propagation constant β/k with given frequency and different value of core radius a , as shown in figure 4.2 the propagation constant increases when the frequency decreases and the effect of the core radius a has no change in the behaviors of dispersion curves. This means that, that the dispersion curves have the same behaviors with different value of core radius a in case TM polarization.

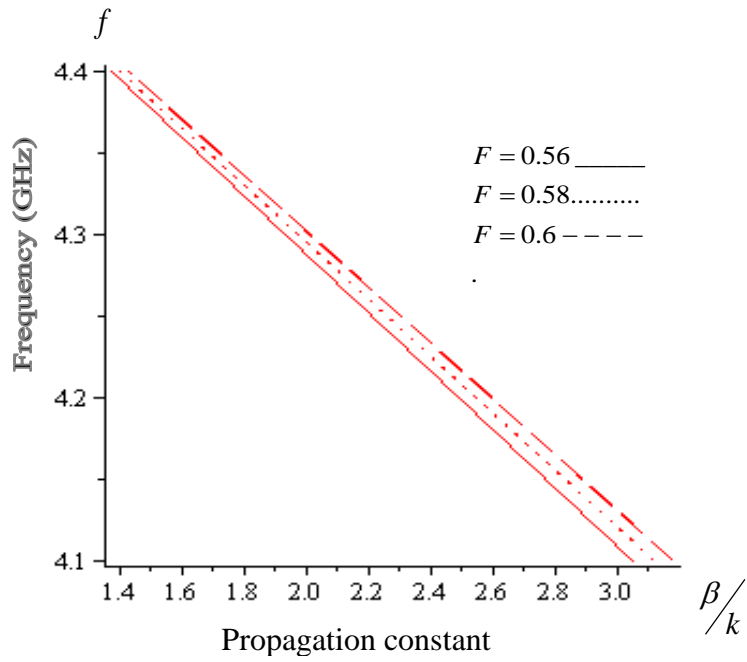


Figure 4.1: Dispersion relation for TM mode with different fractional area F . Fiber parameter $m = 0$, $\mu_{cl} = 1$, $a = 30\mu m$, $\omega_p/2\pi = 10GHz$, $v/2\pi = 3GHz$ and $\omega_c/2\pi = 7GHz$.

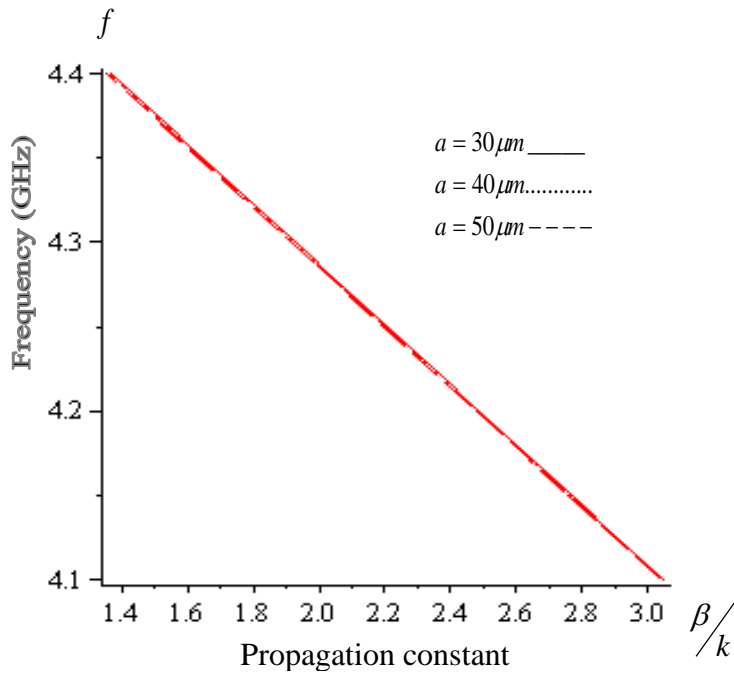


Figure 4.2: Dispersion relation for TM mode with different core fiber radius a . Fiber parameter $m = 0$, $\mu_{cl} = 1$, $F = 0.56$, $\omega_p/2\pi = 10GHz$, $v/2\pi = 3GHz$ and $\omega_c/2\pi = 7GHz$.

Figure 4.3 presents to study the relation of the propagation constant β/k with frequency for different value of F for TE polarization. As shown in figure 4.3, the propagation constant β/k decreases as the F increases and the propagation constant β/k increases with increasing the frequency also, so there is cut of frequency at largest value of β/k and smallest value of F and the physical meaning where the dispersion equation for TE mode Eq. (3.49) direct generated with magnetic relative permeability $\mu(\omega)$ which decreases as the frequency increases. Figure 4.4 describes the relation between propagation constant β/k with given frequency as change in the core radius a . As shown in figure 4.4, the effect of the core radius a dose not appear in the dispersion curves i.e the dispersion curves have the same behaviors for different value of core radius a in the case TE polarization.

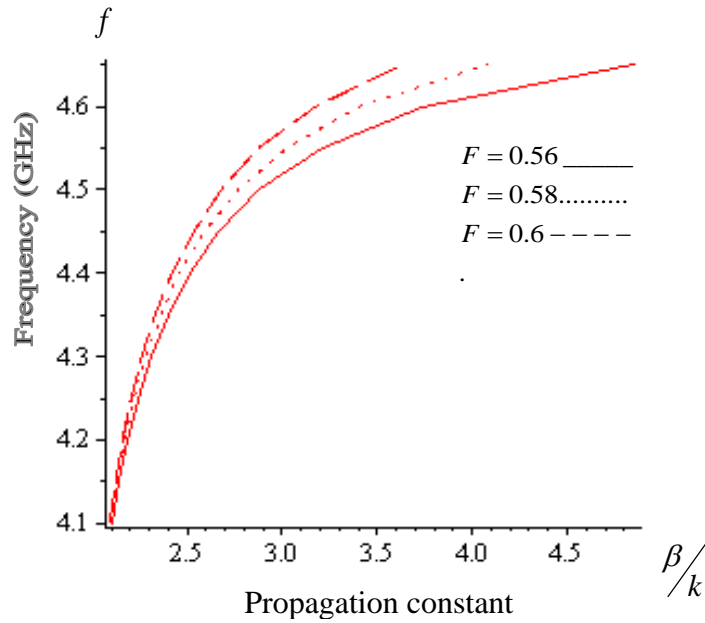


Figure 4.3: Dispersion relation for TE mode with different fractional area F . Fiber parameter $m = 0$, $\mu_{cl} = 1$, $a = 30\mu m$, $\omega_p / 2\pi = 10GHz$, $v / 2\pi = 3GHz$ and $\omega_c / 2\pi = 7GHz$.

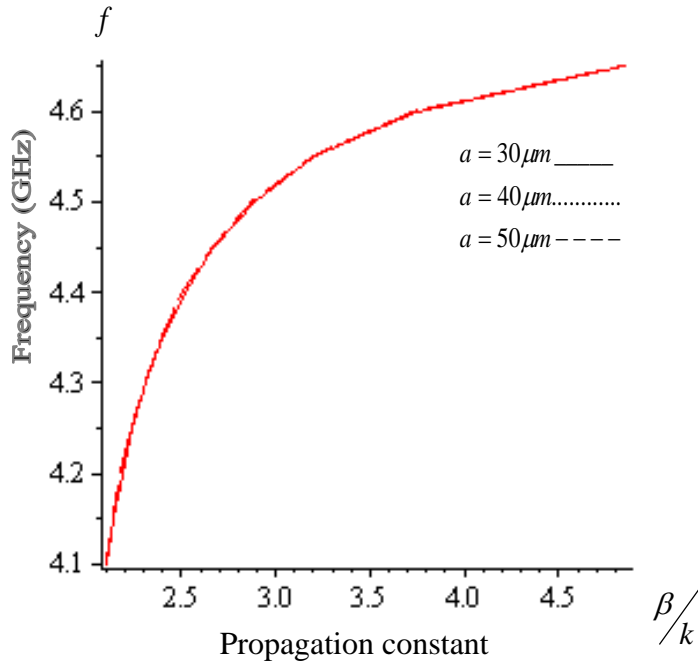


Figure 4.4: Dispersion relation for TE mode with different core fiber radius a . Fiber parameter $m = 0$, $\mu_{cl} = 1$, $F = 0.56$, $\omega_p / 2\pi = 10\text{GHz}$, $\nu / 2\pi = 3\text{GHz}$ and $\omega_c / 2\pi = 7\text{GHz}$.

Eq. (4.7) and Eq. (4.8) are solved numerically to clarify the dispersion relations for HE and EH mode curves respectively for different values of F and core radius a . Figure 4.5 and figure 4.7 show the variation of the propagation constant β/k with frequency for different values of F for HE and EH polarization, respectively. As shown in figure 4.5 and figure 4.7, the dispersion curves for HE and EH modes are plotted where the propagation constant β/k increases as the frequency decreases, the largest β/k appears at largest value of F and the dispersion curves have different behaviors with different F . This mean, the dispersion curves for HE and EH modes behave the same dispersion curves for TM mode. Figure 4.6 and figure 4.8 show the variation of the propagation constant β/k with frequency and different values of core radius a for HE and EH polarization respectively. As shows in figure 4.6 and figure 4.8, the dispersion curves has the same behaviors with different value of core radius a in HE and EH polarization that behave as TE and TM modes.

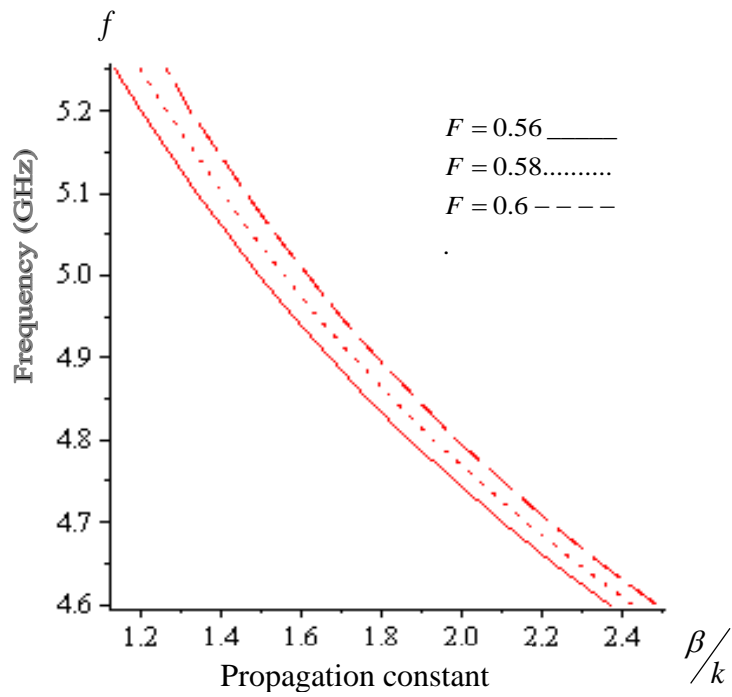


Figure 4.5: Dispersion relation for HE mode with different values of fractional area F . Fiber parameters: $m = 1, \mu_{cl} = 1, a = 30 \mu m, \omega_p / 2\pi = 10 GHz, \nu / 2\pi = 3 GHz$ and $\omega_c / 2\pi = 7 GHz$.

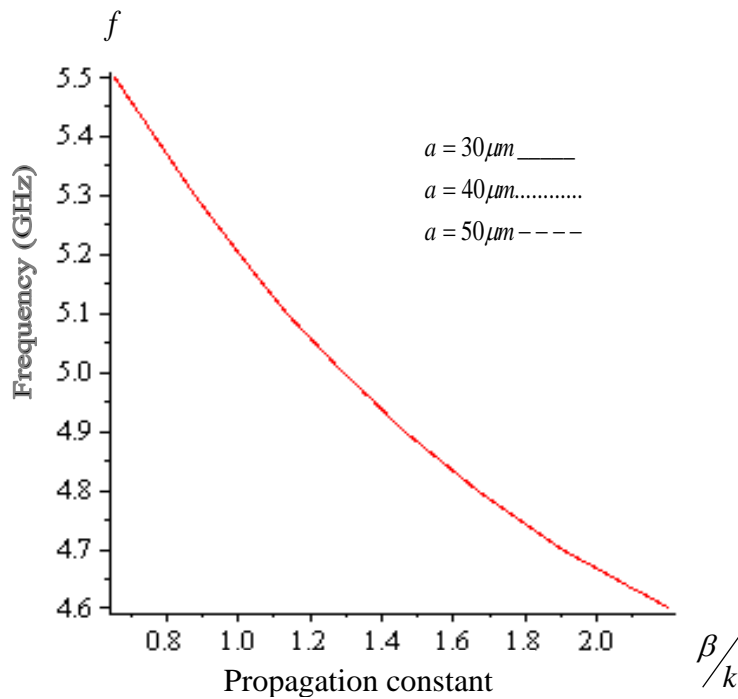


Figure 4.6: Dispersion relation for HE mode with different core fiber radius a . Fiber parameters: $m = 1, \mu_{cl} = 1, F = 0.56, \omega_p / 2\pi = 10 GHz, \nu / 2\pi = 3 GHz$ and $\omega_c / 2\pi = 7 GHz$.

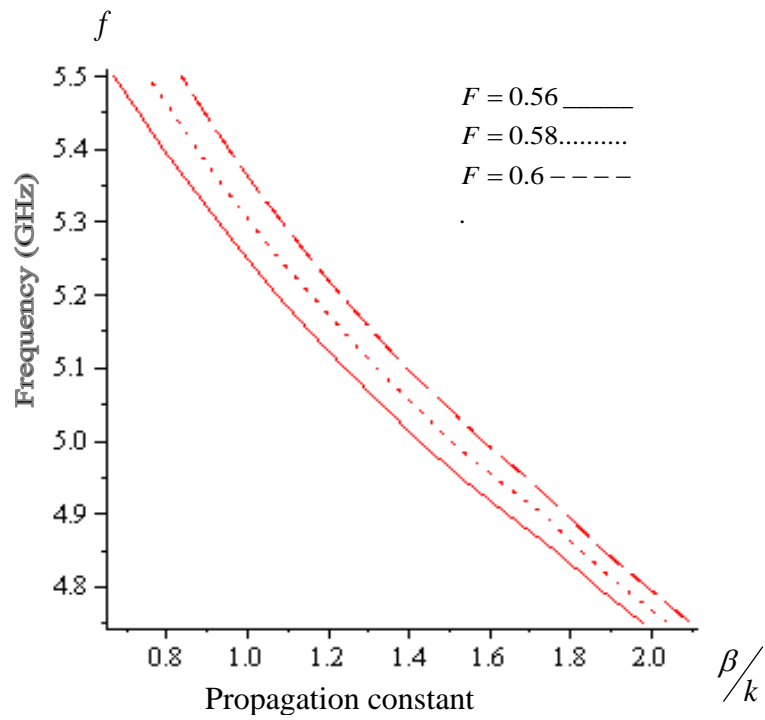


Figure 4.7: Dispersion relation for EH mode with different fractional area F . Fiber parameter $m = 1, \mu_{cl} = 1, a = 30\mu m, \omega_p / 2\pi = 10GHz, \nu / 2\pi = 3GHz$ and $\omega_c / 2\pi = 7GHz$.

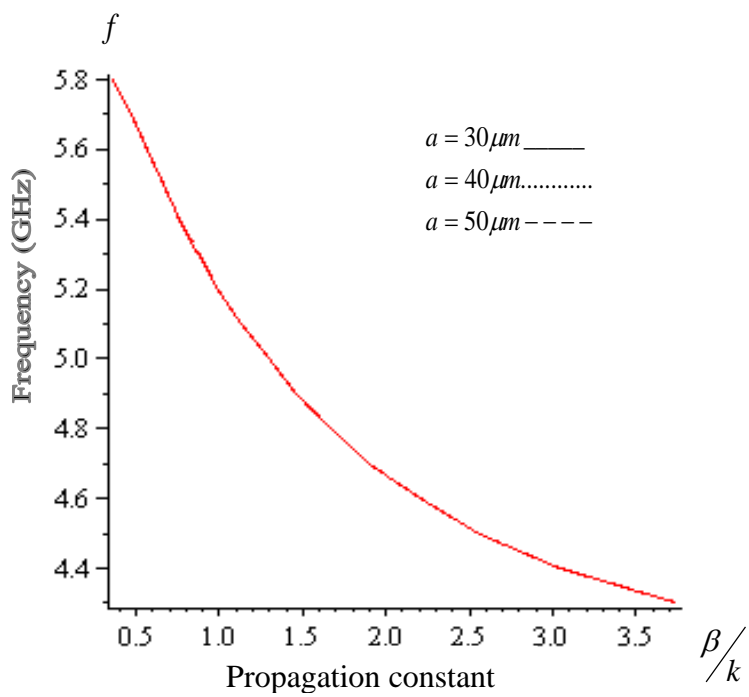


Figure 4.8: Dispersion relation for EH mode with different core fiber radius a . Fiber parameter $m = 1, \mu_{cl} = 1, F = 0.56, \omega_p / 2\pi = 10GHz, \nu / 2\pi = 3GHz$ and $\omega_c / 2\pi = 7GHz$.

Eq. (4.9) has been solved numerically to calculate the real part of the total power $\text{Re}(P)$ and total imaginary part of the total power $\text{Im}(P)$ transported within the core and clad layers in case of TE polarization. Figure 4.9 and figure 4.10 show the variation of the total real $\text{Re}(P)$ and total imaginary $\text{Im}(P)$ power with frequency for different value core radius a . As shown in figure 4.9 and figure 4.10 the total real power $\text{Re}(P)$ and total imaginary power $\text{Im}(P)$ have positive value. The total real power $\text{Re}(P)$ and total imaginary power $\text{Im}(P)$ increase when the frequency decreases to lower value. The effect of the core radius appears when the total real power $\text{Re}(P)$ and total imaginary power $\text{Im}(P)$ take different behaviors with different values core radius a and the total $\text{Re}(P)$ power, and the total $\text{Im}(P)$ power increases as the core radius a increases.

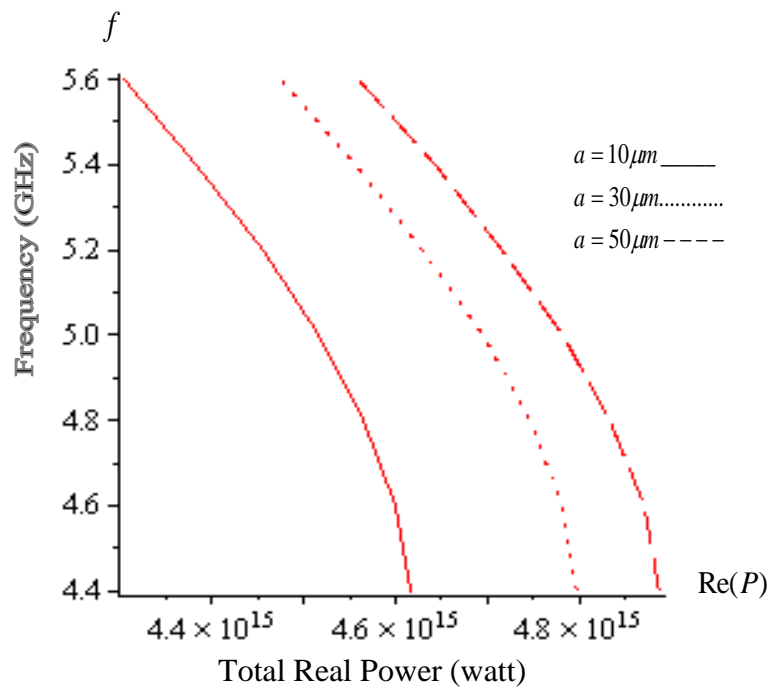


Figure 4.9: The total real part of the power flowing through the structure in TE mode versus the frequency with different values of core radius a . Fiber parameter $F = 0.56$, $\mu_{cl} = 1$, $C = 1$, $\omega_p/2\pi = 10\text{GHz}$, $\nu/2\pi = 3\text{GHz}$ and $\omega_c/2\pi = 7\text{GHz}$

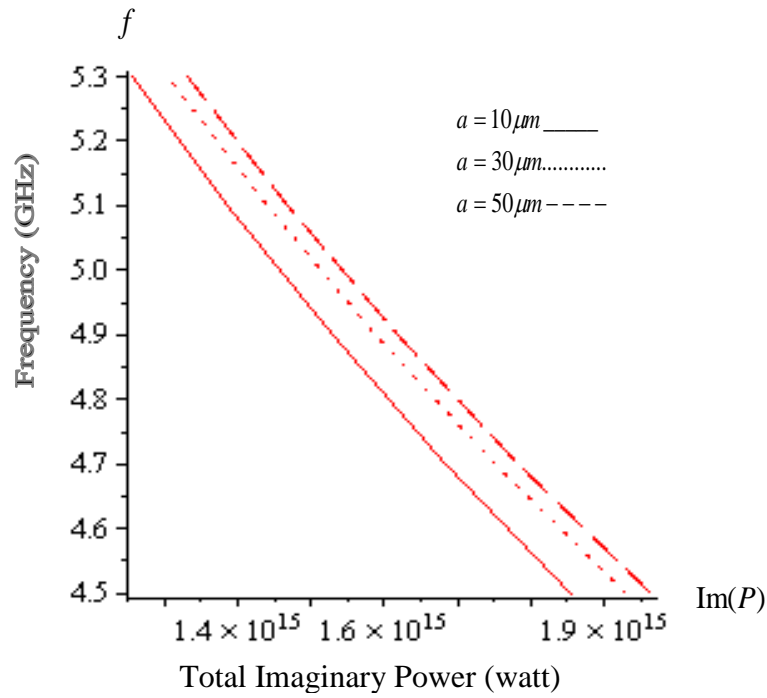


Figure 4.10: The total imaginary part of the power flowing through the structure in TE mode versus the frequency with different values of core radius a . Fiber parameter $F = 0.56, \mu_{cl} = 1, C = 1, \omega_p/2\pi = 10\text{GHz}, \omega_c/2\pi = 7\text{GHz}$ and $\nu/2\pi = 3\text{GHz}$.

Figure 4.11 and figure 4.12 show respectively the total Re (P) and total Im (P) for different values F with given frequency in case of TE polarization. As shown in figure 4.11 and figure 4.12, the Re (P) and Im (P) have positive values increases as the frequency decreases. The effect of F dose not appear in the curves and the total Re (P), Im (P) exhibit the same behaviors with different values of F .

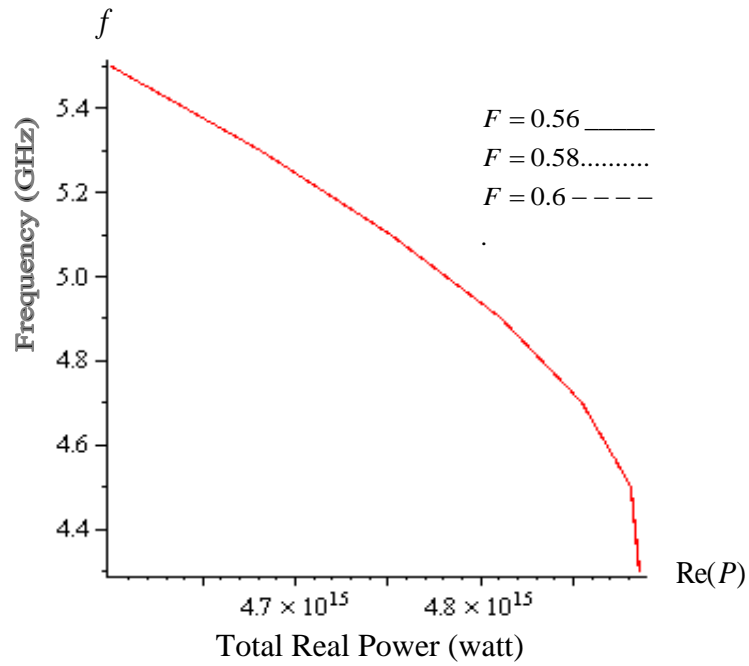


Figure 4.11: The total real part of the power flowing through the structure in TE mode versus the frequency with different values of F. Fiber parameter, $\mu_{cl}=1$, $C=1$, $\omega_p/2\pi = 10GHz$, $\omega_c/2\pi = 7GHz$, $\nu/2\pi = 3GHz$ and $a = 30\mu m$.

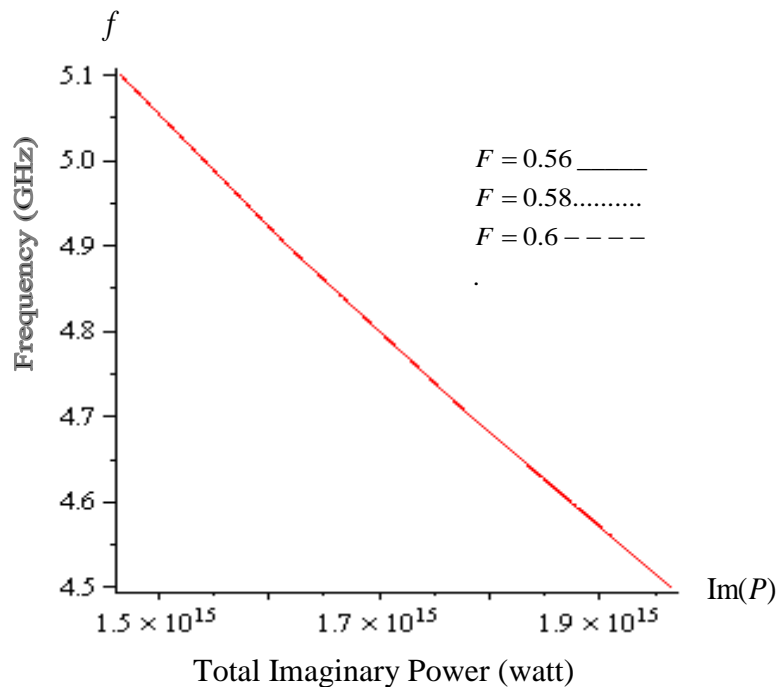
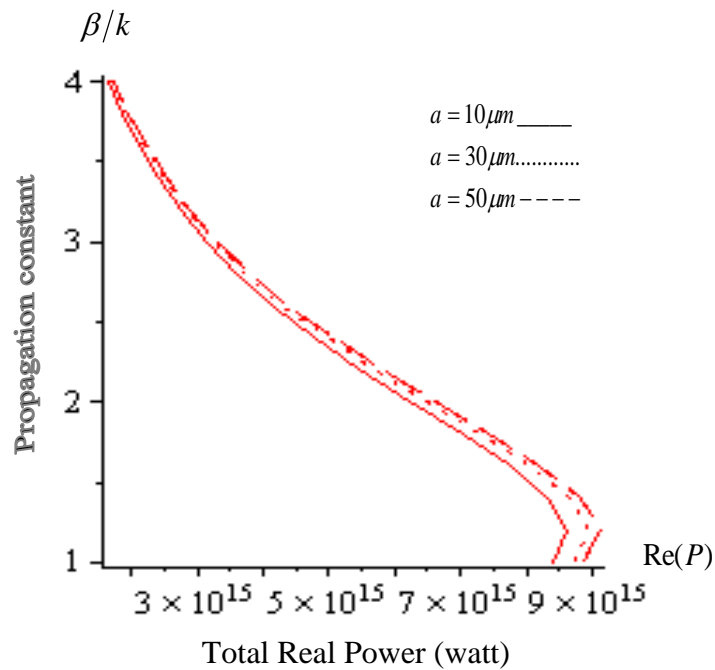


Figure 4.12: The total imaginary part of the power flowing through the structure in TE mode versus the frequency with different values of F. Fiber parameter, $\mu_{cl}=1$, $C=1$, $\omega_p/2\pi = 10GHz$, $\omega_c/2\pi = 7GHz$, $\nu/2\pi = 3GHz$ and $a = 30\mu m$.

In figure 4.13 and figure 4.14, the total $\text{Re}(P)$ and $\text{Im}(P)$, respectively, are plotted versus the propagation constant for different value of core radius a , in the case of TE polarization. As shown in the two figures, the $\text{Re}(P)$ and $\text{Im}(P)$ positive that increases as β/k decreases. The effect of core radius a appears in the curves where the largest total $\text{Re}(P)$ and $\text{Im}(P)$ released at the largest core radius and the total powers exhibit the different behaviors with different value core radius a .



.1

Figure 4.13: The total real part of the power flowing through the structure in TE mode versus the propagation constant with different values of core radius a . Fiber parameter $F = 0.56$, $\mu_{cl} = 1$, $C = 1$, $\omega_p/2\pi = 10\text{GHz}$, $\omega_c/2\pi = 7\text{GHz}$ and $\nu/2\pi = 3\text{GHz}$.

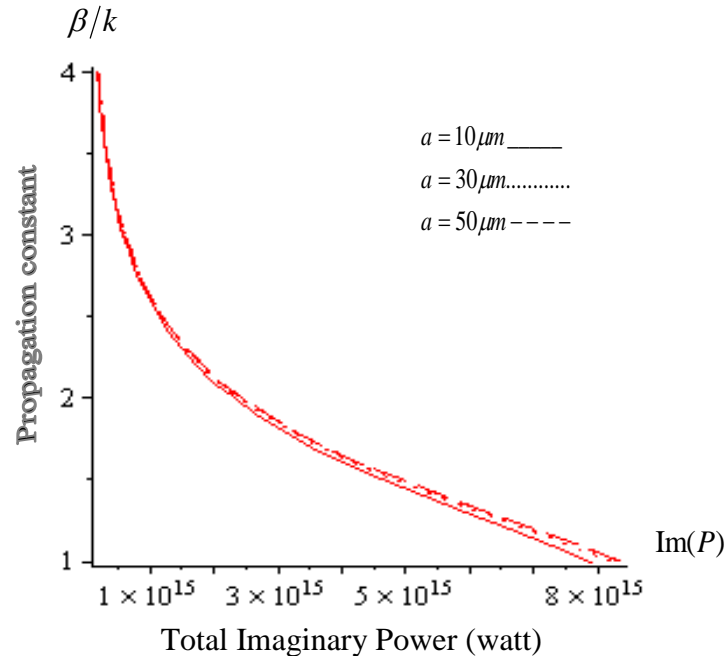


Figure 4.14: The total imaginary power flowing through the structure in TE mode versus the propagation constant with different values of core radius a . Fiber parameter $F = 0.56$, $\mu_{cl} = 1$, $C = 1$, $\omega_p / 2\pi = 10\text{GHz}$, $\omega_c / 2\pi = 7\text{GHz}$ and $v / 2\pi = 3\text{GHz}$

The total power flow are calculated using Eq. (4.10) in case of TM polarization. Figure 4.15 and figure 4.16 clarify the total $\text{Re}(P)$ and $\text{Im}(P)$ with the frequency and core radius a . As we can see from figure 4.15, the total $\text{Re}(P)$ is negative because the poyntings vector \mathbf{S} has the from left-handed triple with the vectors \mathbf{E} and \mathbf{H} , \mathbf{S} and wave vector \mathbf{k} are in opposite directions. So the $\text{Re}(P)$ decreases as the frequency decreases, total $\text{Re}(P)$ decreases with increasing a and the curves have different behaviors with different core radius a . As shown in figure 4.16, total $\text{Im}(P)$ is positive, the power increases as the core radius increases and the frequency decays towards lower values for high values of $\text{Im}(P)$ due to the high fields confinement.

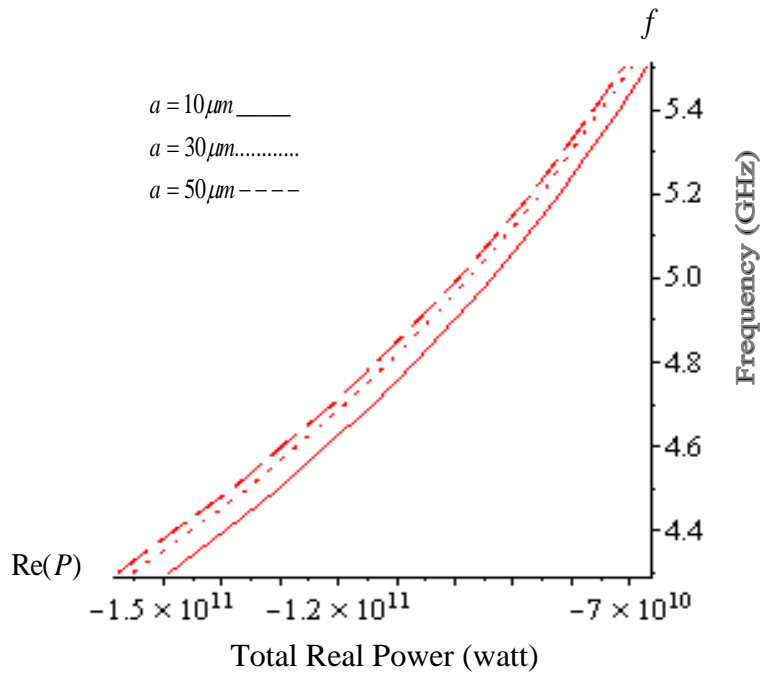


Figure 4.15: The total real part of the power flowing through the structure in TM mode versus the frequency with different values of core radius a . Fiber parameter $F = 0.56$, $\mu_{cl} = 1$, $C = 1$, $\omega_p/2\pi = 10\text{GHz}$, $\nu/2\pi = 3\text{GHz}$ and $\omega_c/2\pi = 7\text{GHz}$.

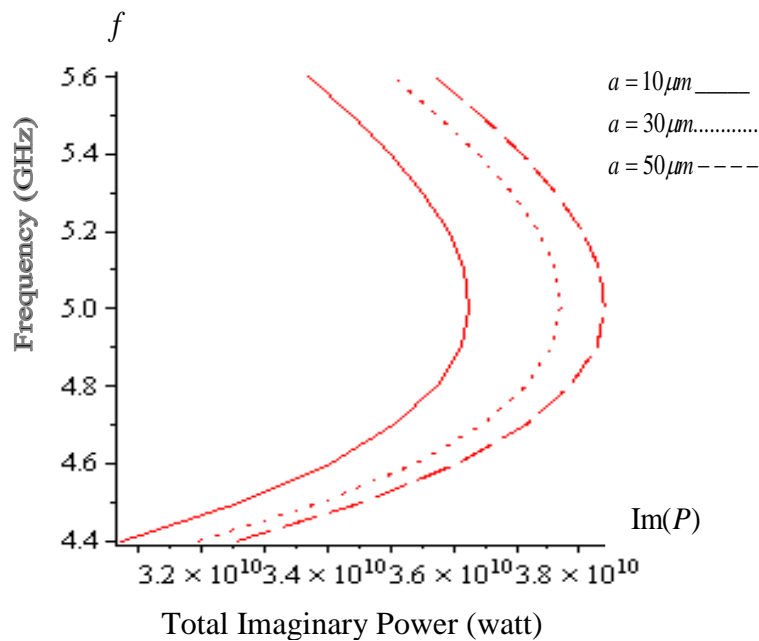


Figure 4.16: The total imaginary part of the power flowing through the structure in TM mode versus the frequency with different values of core radius a . Fiber parameter $F = 0.56$, $\mu_{cl} = 1$, $C = 1$, $\omega_p/2\pi = 10\text{GHz}$, $\omega_c/2\pi = 7\text{GHz}$ and $\nu/2\pi = 3\text{GHz}$.

Figure 4.17 and figure 4.18 are illustrated the relation between the total real power $\text{Re}(P)$ and imaginary $\text{Im}(P)$ flow with frequency and change in fractional area unit cell F in case TM polarization. As shown in figure 4.17, the total $\text{Re}(P)$ is negative as we obtained the physical meaning from figure 4.15, the curves behave as the same in figure 4.15 but the power curves have the same behaviors for different F . As can see from figure 4.18, the total $\text{Im}(P)$ curves have the same as in figure 4.16 but the change of fractional area does not effect in the behaviors that exhibit the same for different values of F .

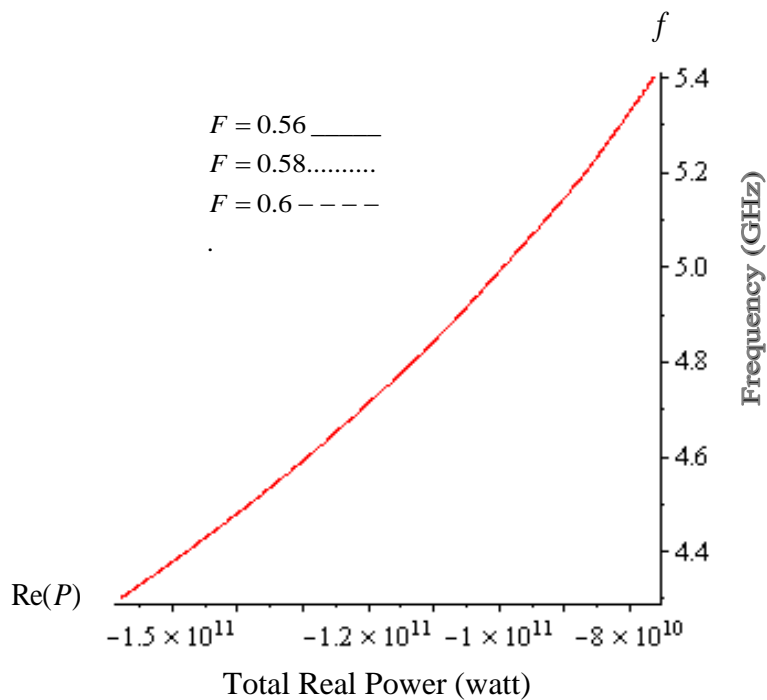


Figure 4.17: The total real part of the power flowing through the structure in TM mode versus the frequency with different values of fractional area F . Fiber parameter, $\mu_{cl}=1$, $C=1$, $\omega_p/2\pi = 10\text{GHz}$, $\omega_c/2\pi = 7\text{GHz}$, $v/2\pi = 3\text{GHz}$ and $a = 30\mu\text{m}$.

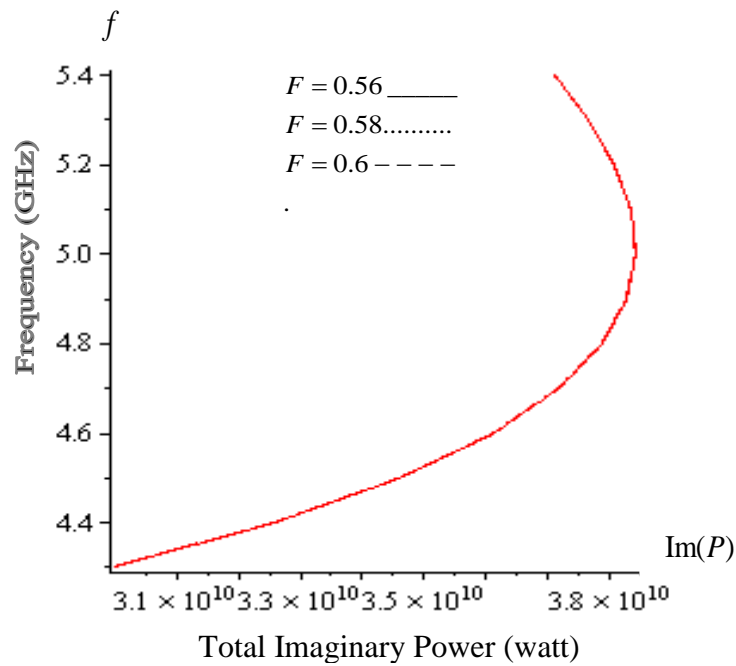


Figure 4.18: The total imaginary part of the power flowing through the structure in TM mode versus the frequency with different value of fractional area F . Fiber parameter $a = 30\mu m$, $\mu_{cl} = 1$, $C = 1$, $\omega_p/2\pi = 10GHz$, $\omega_c/2\pi = 7GHz$ and $\nu/2\pi = 3GHz$.

Figure 4.19 and figure 4.20 show the variation total $Re(P)$ and $Im(P)$ power versus the propagation constant β/k for different core radius a in case of TM polarization. As shown in figure 4.19, the total $Re(P)$ has negative value and has the peak value at specific value of β/k , the $Re(P)$ decreases as propagation constant decreases to specific value, the total $Re(P)$ decreases as the core radius increases and the $Re(P)$ curves exhibit different behaviors with different value core radius a . As we can see in figure 4.20, the total $Im(P)$ positive, the $Im(P)$ increases as propagation constant decreases until specific value of β/k and the effect of core radius appears where the $Im(P)$ power increases as a increases.

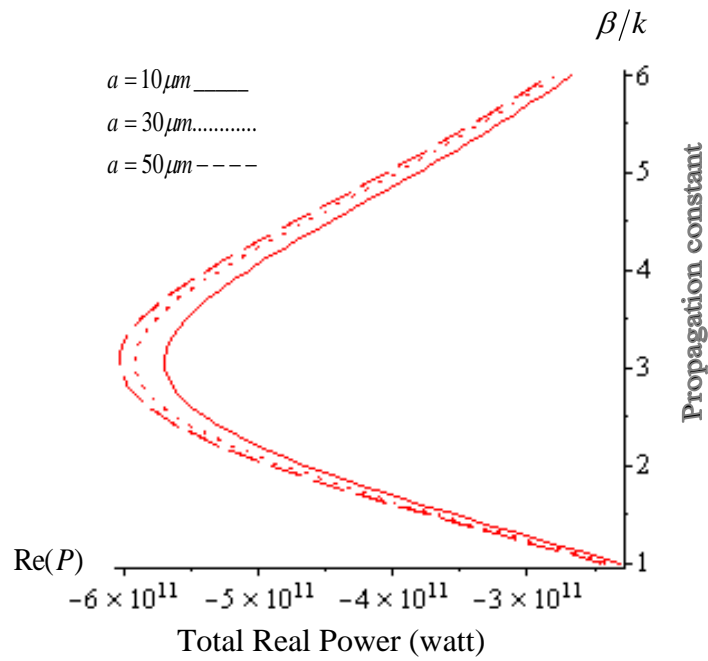


Figure 4.19: The total real part of the power flowing through the structure in TM mode versus the propagation constant with different values of core radius a . Fiber parameter $F = 0.56$, $\mu_{cl} = 1$, $A = 1$, $\omega_p/2\pi = 10\text{GHz}$, $\omega_c/2\pi = 7\text{GHz}$, $\nu/2\pi = 3\text{GHz}$ and $a = 30\mu\text{m}$.

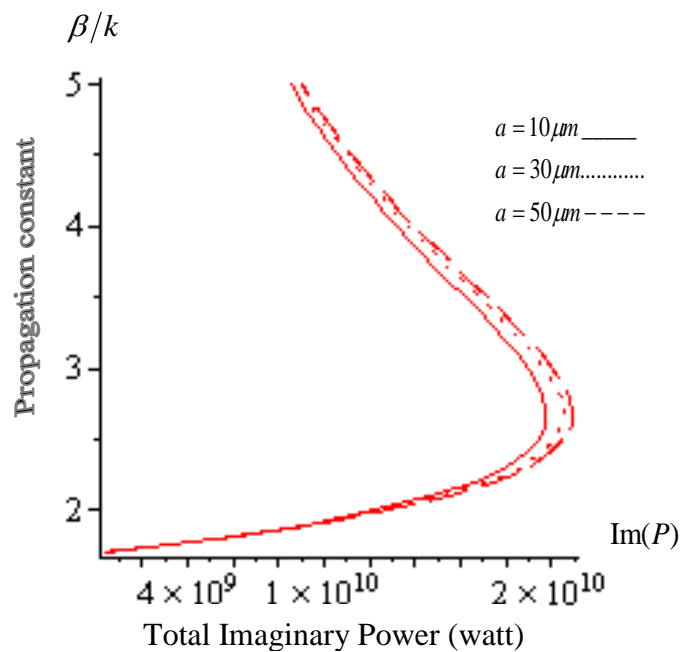


Figure 4.20: The total imaginary part of the power flowing through the structure in TM mode versus the propagation constant with different values of core radius a . Fiber parameter $F = 0.56$, $\mu_{cl} = 1$, $A = 1$, $\omega_p/2\pi = 10\text{GHz}$, $\omega_c/2\pi = 7\text{GHz}$, $\nu/2\pi = 3\text{GHz}$ and $a = 30\mu\text{m}$.

CHAPTER FIVE

MODES IN OPTICAL FIBER WITH LHM CORE AND SEMICNDUCTOR CLAD: SPECIAL CASE

In this chapter, a special case, is studied where the elements $\epsilon_{xx} = \epsilon_{yy} = \epsilon_{zz}$. The dispersion equations for TE, TM, HE and EH modes for the waveguide fiber will be presented in section 5.2. The total power flow in the structure for TE and TM polarization will be calculated in section 5.3. The dispersion curves are plotted for different parameters, core radius and fractional area unit cell in section 5.4.

5.1. Structure Analysis

In this chapter, we will limit our study to a special case. We consider that electromagnetic waves are propagating in the optical fiber along z- direction where LHM in the core with radius a which characterize by electric relative permittivity ϵ_{co} given by Eq. (2.1) and magnetic relative permeability μ_{co} given by Eq. (2.2). The LHM core of the fiber is bounded by a semiconductor material that is characterized by electric relative permittivity ϵ_{cl}^{zz} in the special case given from Eq. (3.13) and the magnetic relative permeability $\mu_{cl}=1$ this mean that:

$$\epsilon_{cl}^{zz} = \frac{\epsilon_{zz}}{\epsilon_0} = 1 - \frac{\omega_p^2 (\omega + i\nu)}{\omega \left((\omega + i\nu)^2 - \omega_c^2 \right)} \quad (5.1)$$

In this special case, the semiconductor permittivity tensor can be expressed:

$$\epsilon_{cl}(\omega) = \frac{1}{\epsilon_0} \begin{bmatrix} \epsilon_{zz} & 0 & 0 \\ 0 & \epsilon_{zz} & 0 \\ 0 & 0 & \epsilon_{zz} \end{bmatrix} \quad (5.2)$$

where $\epsilon_{cl}^{zz} = \frac{\epsilon_{zz}}{\epsilon_0}$ (5.3)

using Eq. (3.12) and comparing with Eq. (5.2) we get:

$$\epsilon_{xx} = \epsilon_{yy} = \epsilon_{zz} \quad (5.4)$$

And the *components* of ϵ_{xz} , ϵ_{zx} to be zero as in Eq. (4.5).

5.2. The Dispersion equations

5.2.1. TE and TM Modes

The dispersion relation for each mode has been derived in chapter three. We have to introduce the special case so that

$$\xi^2 = (\beta^2 - \mu_0 \epsilon_{zz} \omega^2) \quad (5.5)$$

where η and ξ are defined in chapter three.

From Eq. (5.6) and Eq. (5.7), we get:

$$\eta^2 = \xi^2 = (\beta^2 - \mu_0 \epsilon_{zz} \omega^2) \quad (5.6)$$

where η and ξ are define in Eq. (3.35) and Eq. (3.59).

Then using Eq. (3.37) , Eq. (3.61) and Eq. (5.6), we get:

$$W_1 = W_2 = W \quad (5.7)$$

Using Eq. (5.7) and substituting into Eq. (3.49) the dispersion equation for TE mode in this special case is rewritten as:

$$\left(\frac{1}{U} \frac{J'_m(U)}{J_m(U)} + \frac{1}{\mu_{co}} \frac{1}{W} \frac{K'_m(W)}{K_m(W)} \right) = 0 \quad \text{TE mode} \quad (5.8)$$

Using Eq. (5.7) and substituting into Eq. (3.73) the dispersion equation for TM mode in this special case is written as:

$$\left(\frac{1}{U} \frac{J'_m(U)}{J_m(U)} + \frac{\varepsilon_{zz}^{cl}}{\varepsilon_{co}} \frac{1}{W} \frac{K'_m(W)}{K_m(W)} \right) = 0 \quad \text{TM mode} \quad (5.9)$$

5.2.2. Hybrid Mode (HE and EH)

To obtain the dispersion equation for HE and EH modes, we use Eq. (5.4) and Eq. (4.5) then substituting into Eq. (3.88), we get the two type of hybrid mode as:

$$+ \sqrt{\left(\frac{1}{U} \frac{J'_m(U)}{J_m(U)} + \frac{1}{\mu_{co}} \frac{1}{W} \frac{K'_m(W)}{K_m(W)} \right) \left(\frac{1}{U} \frac{J'_m(U)}{J_m(U)} + \frac{\varepsilon_{zz}^{cl}}{\varepsilon_{co}} \frac{1}{W} \frac{K'_m(W)}{K_m(W)} \right)} = \frac{\beta k (\varepsilon_{co} \mu_{co} - \varepsilon_{zz}^{cl}) a^2}{W^2 U^2 \sqrt{\varepsilon_{co} \mu_{co}}} m \quad \text{EH mode} \quad (5.10)$$

$$- \sqrt{\left(\frac{1}{U} \frac{J'_m(U)}{J_m(U)} + \frac{1}{\mu_{co}} \frac{1}{W} \frac{K'_m(W)}{K_m(W)} \right) \left(\frac{1}{U} \frac{J'_m(U)}{J_m(U)} + \frac{\varepsilon_{zz}^{cl}}{\varepsilon_{co}} \frac{1}{W} \frac{K'_m(W)}{K_m(W)} \right)} = \frac{\beta k (\varepsilon_{co} \mu_{co} - \varepsilon_{zz}^{cl}) a^2}{W^2 U^2 \sqrt{\varepsilon_{co} \mu_{co}}} m \quad \text{HE mode} \quad (5.11)$$

5.3. Power Considerations

5.3.1. TE Mode

In this special case the total power transported between the core and clad for TE mode can be calculated by using equation (3.105).

From Eq. (5.7) and substituting into Eq. (3.104) we get:

$$P_{TE2} = \frac{\pi}{2} \beta \omega |C|^2 \mu_0 \frac{a^4}{W^2} \frac{J_0^2(U)}{K_0^2(W)} \left(K_0(W) K_2(W) - K_1^2(W) \right) \quad (5.12)$$

Using Eq. (3.98) and Eq. (4.12) then substituting into Eq. (3.105), we get:

$$TP_{TE} = \frac{\pi}{2} \beta \omega |C|^2 a^4 \mu_0 \left(\left(1 - \frac{F \omega^2}{\omega^2 - \omega_0^2} \right) \frac{1}{U^2} (J_1^2(U) - J_0(U) J_2(U)) + \frac{1}{W^2} \frac{J_0^2(U)}{K_0^2(W)} (K_0(W) K_2(W) - K_1^2(W)) \right) \quad (5.13)$$

where TP_{TE} is the total power in TE mode for a special case with

$$W = \eta a \quad (5.14)$$

5.3.2. TM Mode

Using Eq. (3.110), Eq. (3.115) and Eq. (5.7), then substituting into Eq. (3.116) the total power in TM mode becomes

$$TP_{TM} = \frac{\pi}{2} \beta \omega |A|^2 a^4 \varepsilon_0 \left(\left(1 - \frac{\omega_p^2}{\omega^2} \right) \frac{1}{U^2} (J_1^2(U) - J_0(U) J_2(U)) + \frac{1}{W^2} \left(1 - \frac{\omega_p^2 (\omega + i\nu)}{\omega ((\omega + i\nu)^2 - \omega_c^2)} \right) \frac{J_0^2(U)}{K_0^2(W)} (K_0(W) K_2(W) - K_1^2(W)) \right) \quad (5.15)$$

TP_{TM} is the total power in TM mode for a special case with

$$W = \xi a \quad (5.16)$$

5.4. Numerical Results :

In the analysis below we have assumed the core layer to be LHM with μ_{co} and ϵ_{co} are given by Eq. (2.1) and Eq. (2.2), and the cladding layer to be semiconductor material with $\mu_{cl}=1$ and ϵ_{cl} that given from Eq. (5.1). We considered the parameters $\omega_p/2\pi=10\text{GHz}$, $\omega_0/2\pi=4\text{GHz}$, $\nu/2\pi=2\text{GHz}$, and the cyclotron frequency $\omega_c/2\pi=1\text{GHz}$. The dispersion relation, for TE, TM, HE, and EH modes are solved numerically and the optical power are calculated using the above set of equations. Figures 3.1 shows the dispersion curves for fast and slow modes if the radius of the core LHM $a=50\mu\text{m}$ and $F=0.56$.

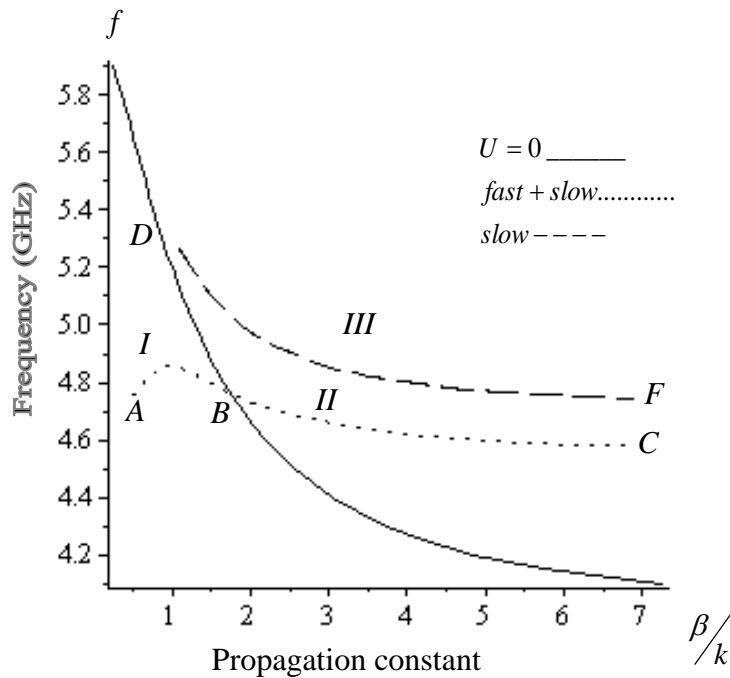


Figure 5.1: Dispersion curves describing the (fast- slow) mode curve AC ,fast mode with curve DF in the fiber. Fiber parameter $\mu_{cl}=1$, $a=50\mu\text{m}$, fractional area $F=0.56$, $\omega_p/2\pi=10\text{GHz}$, $\omega_c/2\pi=1\text{GHz}$ and $\nu/2\pi=2\text{GHz}$ that be divided in two region curves.

In Figure 5.1 there are three regions of modes in this case (I, II), and (III). In the first region (I) the condition $U^2 > 0$, this means $\epsilon_{co}\mu_{co} > \epsilon_{cl}\mu_{cl}$ and the fast mode exists. We can see only one type of the dispersion curves with fast mode lies in both regions I and II (AC curve), this curve partial from (AC curve) that (AB curve). Point B

divides the fast mode from the slow mode and satisfy that $U^2 = 0$. In region II and III the condition $U^2 < 0$ is satisfied, this means that only slow mode can exist. There are two dispersion curves of the slow mode one of them is completely in region III is the (DF curve) and the other in region II (BC curve). Figure 5.2 and 5.3 describe the modes TE, TM, HE and EH modes in the structure. In fact Figure 5.2 shows the (fast-slow) mode in regions (I) and (II) curve AC from figure 5.1, the modes polarization in this range arranged in the following way, if $m = 0$ there are two types TE and TM mode starting with TM mode have the largest propagation constant β/k and TE mode that exist with smallest propagation constant β/k . If $m > 0$ the two types of modes HE and EH exist, and have the same propagation constant β/k with the same frequency between TE and TM mode where HE dispersion curve is in agreement on EH dispersion curve. Figure 5.3 also shows the slow mode in region III (curve DF) from figure 5.1, the modes polarization in this range arranged as the same way in regions I and II.

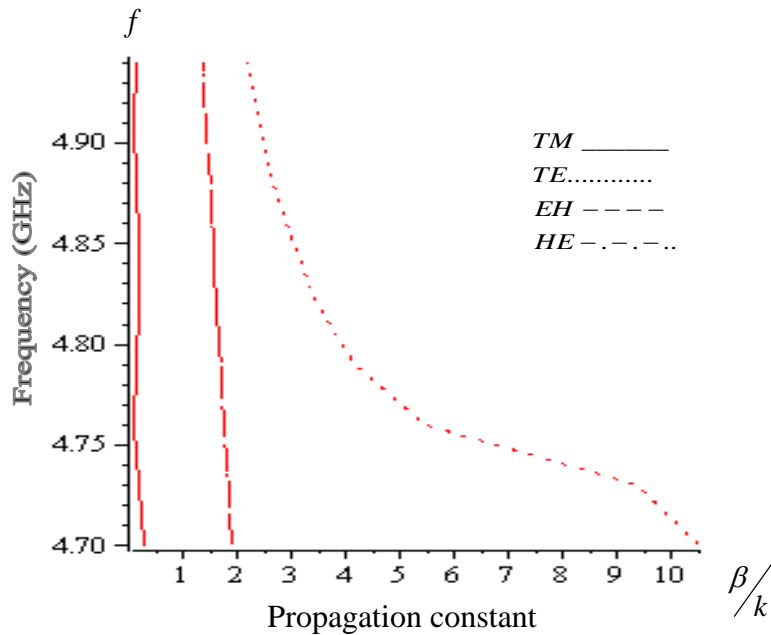


Figure 5.2: Fast-slow guided modes (desertion curve of AC type in Fig 2.2) at $m = 0,1$. Fiber parameter $\mu_{cl} = 1$, $a = 50\mu m$, fractional area $F = 0.56$, $\omega_p/2\pi = 10GHz$, $\omega_c/2\pi = 1GHz$ and $\nu/2\pi = 2GHz$.

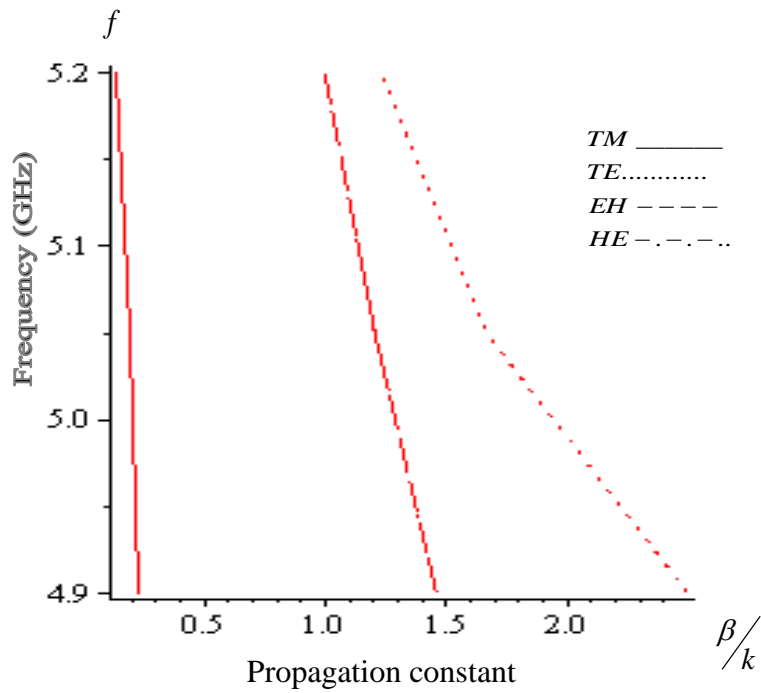


Figure 5.3 : Slow guided modes (desertion curve of DF type in Fig 2.2) at $m = 0,1$. Fiber parameter, $\mu_{cl}=1$, $a = 50\mu m$, fractional area $F = 0.56$, $\omega_p/2\pi = 10GHz$, $\omega_c/2\pi = 1GHz$ and $\nu/2\pi = 2GHz$.

Figure 5.4 shows the variation of the propagation constant β/k versus the frequency for various values of the fractional area F in TM mode polarization. As we can see in figure 5.4 the propagation constant β/k increases as the frequency decreases, and the dispersion curve have different behaviors for different values of F . Figure 5.5 shows the relation between propagation constant and frequency with differnt values of the core radius a in TM mode. As the figure shows, the propagation constant β/k decreases as the core radius increases, and the dispersion curves are starting at the same propagation constant for different value of the core radius.

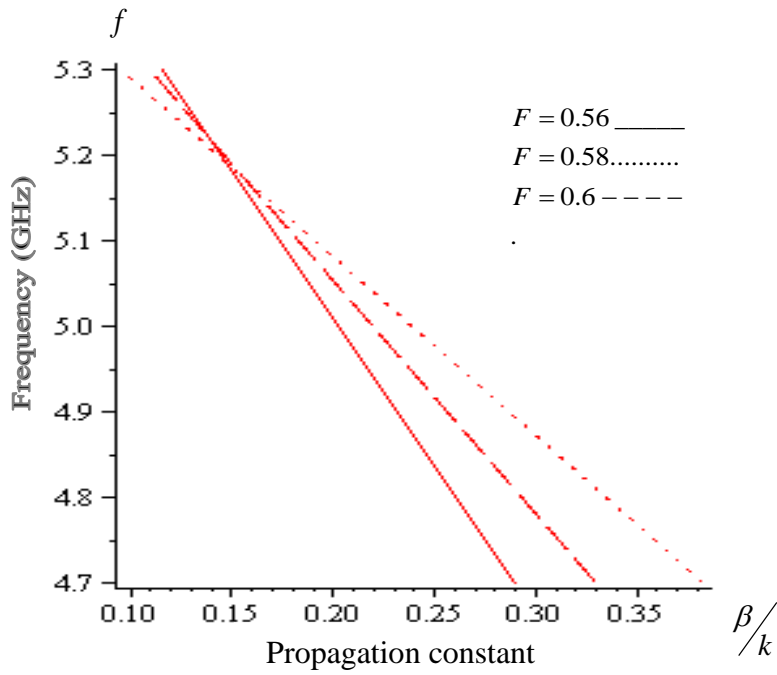


Figure 5.4: Dispersion relation for TM mode with different fractional area F . Fiber parameter $m = 0$, $\mu_{cl} = 1$, $a = 50\mu m$, $\omega_p/2\pi = 10GHz$, $\omega_c/2\pi = 1GHz$ and $\nu/2\pi = 2GHz$.

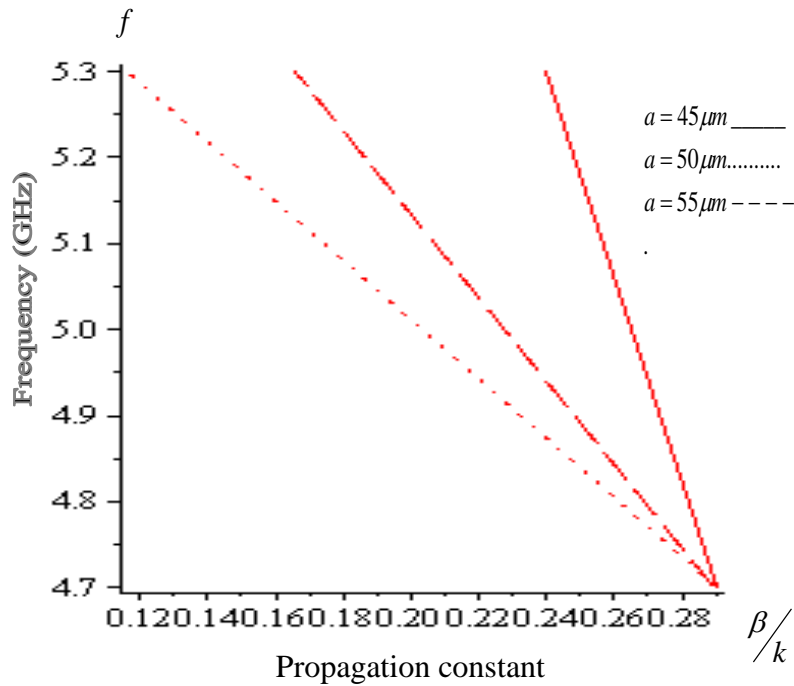


Figure 5.5 : Dispersion relation for TM mode with different core radius a , $m = 0$. Fiber parameter $\mu_{cl} = 1$, fractional area $F = 0.56$, $\omega_p/2\pi = 10GHz$, $\omega_c/2\pi = 1GHz$ and $\nu/2\pi = 2GHz$.

Figure 5.6 shows the effect of the fractional area unit cell for TE polarization. As we can see from the figure, there are two regions exist, (I) and (II), the propagation constant is plotted respectively versus to the frequency of the guided mode. In region (I), the propagation constant increases as the frequency increases, and there is cut of frequency at largest propagation constant and smallest F . In region (II) the β/k increases as the frequency decreases, the β/k have largest value at largest F , and the dispersion curve exhibit different behaviors for different values of F . The change between two regions I, II in figure 5.6 lead to the effective $\mu(\omega)$ and $\varepsilon(\omega)$ for the guided layer in the range of frequency. The dispersion curves are plotted in figure 5.7 for different core radius a . As shown in figure 5.7 the curves have the same as in figure 5.6 but the effect in core radius gives the same behaviors for different values of a .

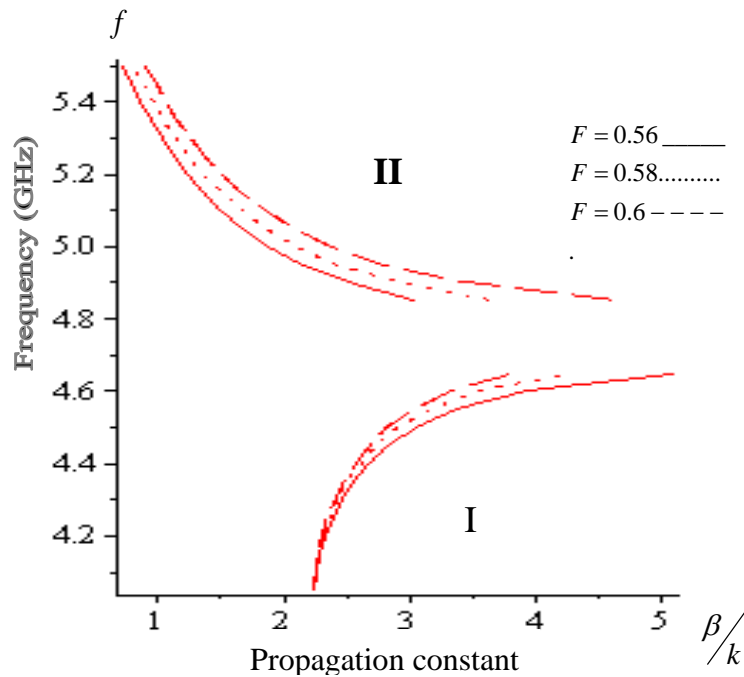


Figure 5.6: Dispersion relation for TE mode with different fractional area F , $m = 0$. Fiber parameter $\mu_{cl} = 1$, $a = 50 \mu m$, $\omega_p/2\pi = 10 GHz$, $\omega_c/2\pi = 1 GHz$ and $v/2\pi = 2 GHz$.

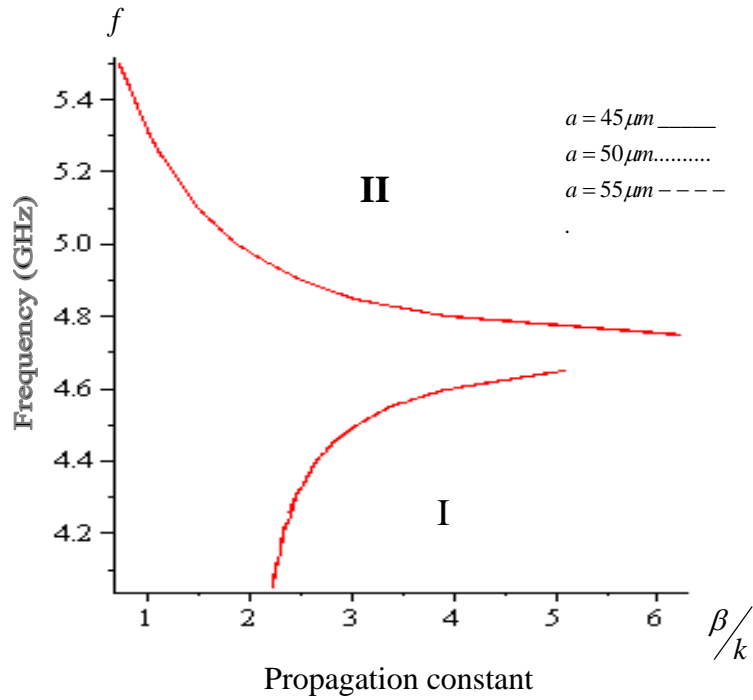


Figure 5.7: Dispersion relation for TE mode with different core radius a , $m = 0$. Fiber parameter $\mu_{cl} = 1$, fractional area $F = 0.56$, $\omega_p/2\pi = 10\text{GHz}$, $\omega_c/2\pi = 1\text{GHz}$ and $\nu/2\pi = 2\text{GHz}$.

In Figures (5.8, 5.9, 5.10 and 5.11) the dispersion curves are plotted for two types of hybrid mode, HE and EH mode with different values of F and core radius a . As shown in figure 5.8 and figure 5.10 with different F and given frequency in HE and EH polarization, the propagation constant decreases with increasing F , and the dispersion curves exhibit different behaviors for different values of F . Figure 5.9 and figure 5.11 show the relation between the propagation constant β/k with frequency and different values of core radius a for HE and EH polarization. As shown in the two figures, the propagation constant increases as the frequency decreases in both HE and EH polarization, and the curves are in agreement on each other having the same behaviors for different core radius.

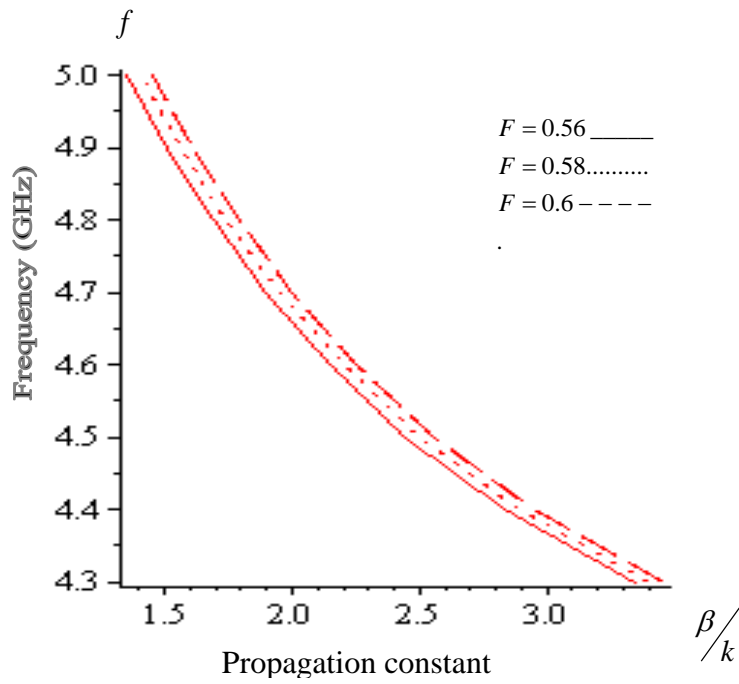


Figure 5.8 : Dispersion relation for HE mode with different fractional area F , $m = 1$.
 Fiber parameter $\mu_{cl}=1, a = 50\mu m, \omega_p/2\pi = 10GHz, \omega_c/2\pi = 1GHz$ and $v/2\pi = 2GHz$.

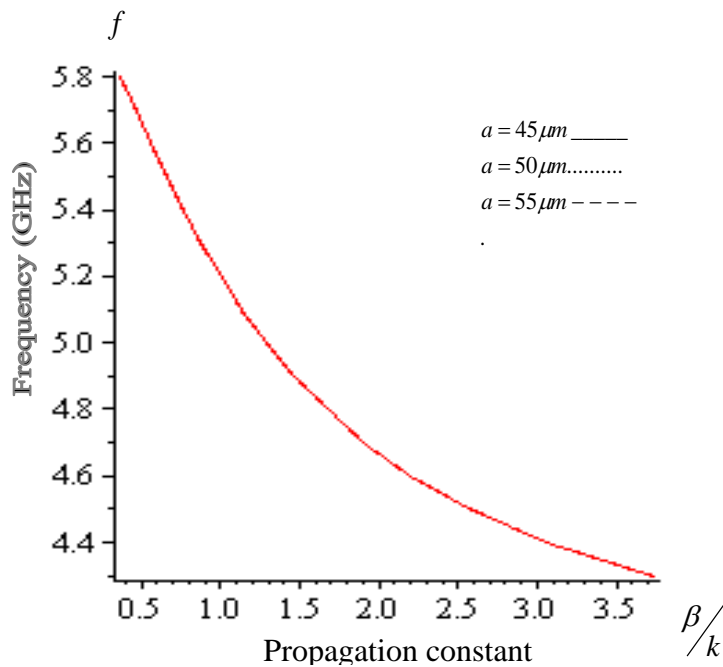


Figure 5.9: Dispersion relation for HE mode with different core radius a , $m = 1$.
 Fiber parameter $\mu_{cl}=1$, fractional area unit cell $F = 0.56, \omega_p/2\pi = 10GHz,$
 $\omega_c/2\pi = 1GHz$ and $v/2\pi = 2GHz$.

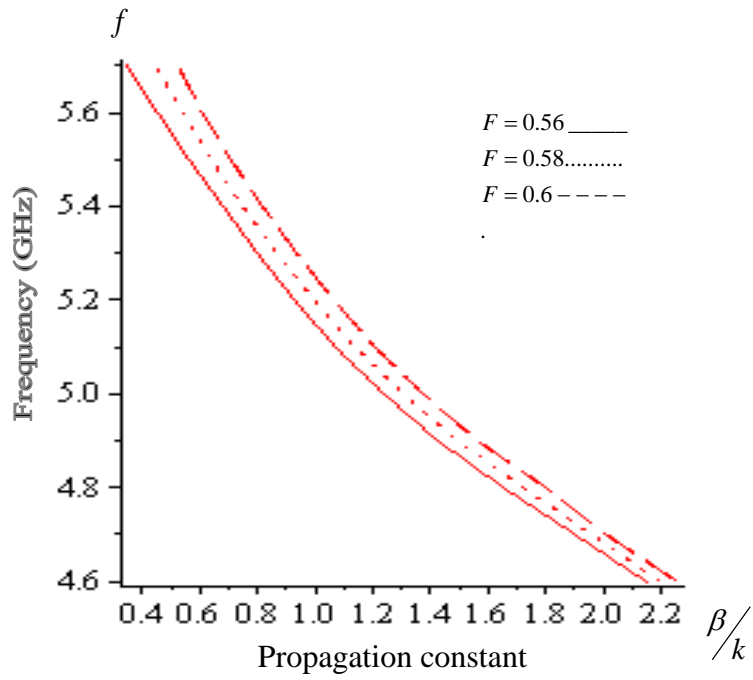


Figure 5.10: Dispersion relation for EH mode with different fractional area F , $m = 1$. Fiber parameter $\mu_{cl}=1$, $a = 50\mu m$, $\omega_p/2\pi = 10GHz$, $\omega_c/2\pi = 1GHz$ and $\nu/2\pi = 2GHz$.

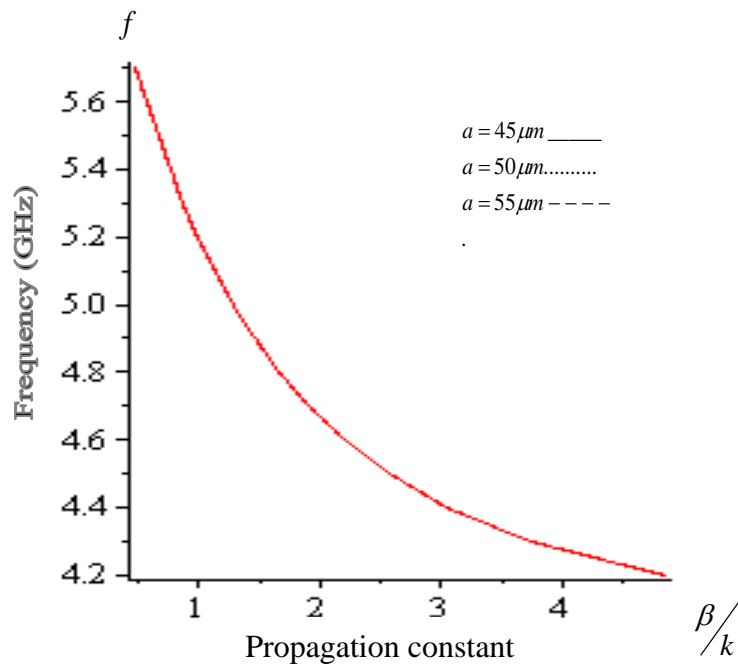


Figure 5.11: Dispersion relation for EH mode with different core radius a , $m = 1$. Fiber parameter $\mu_{cl}=1$, fractional area unit cell $F = 0.56$, $\omega_p/2\pi = 10GHz$, $\omega_c/2\pi = 1GHz$ and $\nu/2\pi = 2GHz$.

It is very important to calculate the total power carried by core and the clad, Eq. (5.13) solved to gives the total power in TE mode polarization. Figures 5.12 and 5.13 shows the total $\text{Re}(P)$ and $\text{Im}(P)$ respectively, with given frequency and different values core radius. As shown in figures 5.12 and 5.13, total $\text{Re}(P)$ and $\text{Im}(P)$ are positive, the total powers increases as the frequency increases and increasing core radius, and the power curves have different behaviors for different core radius. This means, the power in the clad region is very larg than power in the guided layer core (LHM) which is negative because the the vector \mathbf{S} and wave vector \mathbf{k} are in opposite directions.

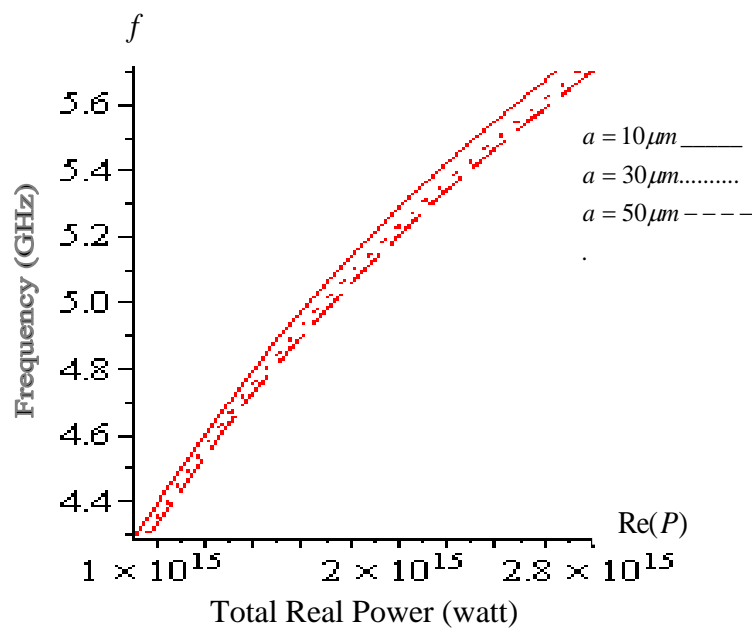


Figure 5.12: The total real part of the power flowing through the structure in TE mode versus the frequency with different values of core radius a . Fiber parameter $F = 0.56, \mu_{cl}=1, C=1, \omega_p/2\pi = 10GHz, \omega_c/2\pi = 1GHz$ and $\nu/2\pi = 2GHz$

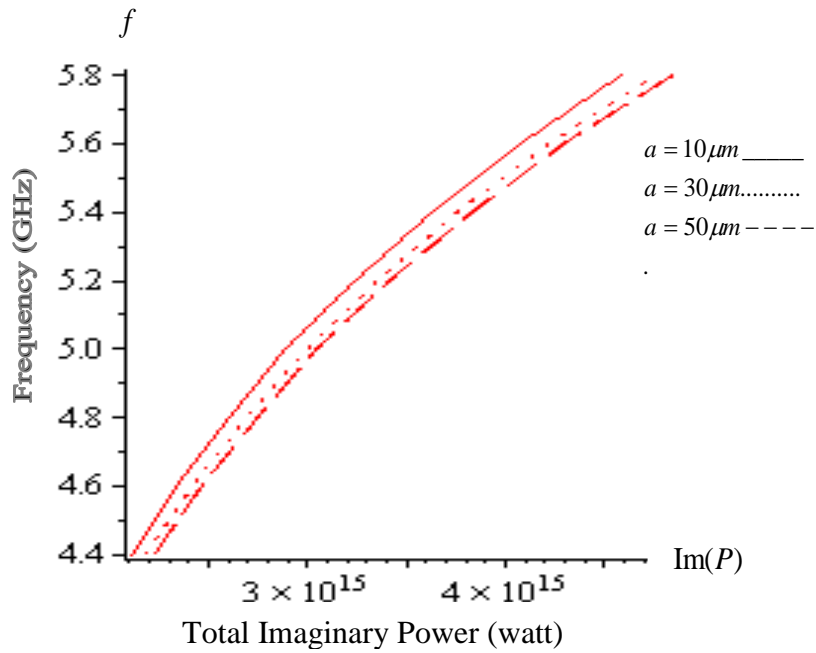


Figure 5.13: The total imaginary part of the power flowing through the structure in TE mode versus the frequency with different values of core radius a . Fiber parameter $F = 0.56$, $\mu_{cl} = 1$, $C = 1$, $\omega_p/2\pi = 10\text{GHz}$, $\omega_c/2\pi = 1\text{GHz}$ and $\nu/2\pi = 2\text{GHz}$.

The $\text{Re}(P)$ and $\text{Im}(P)$ and plotted respectively with β/k for different values core radius guided layer for TE polarization in figure 5.14 and figure 5.15. As shown in two figures, the total $\text{Re}(P)$ and $\text{Im}(P)$ positive, $\text{Re}(P)$ and $\text{Im}(P)$ increases as β/k decreases and increasing core radius and the power curves exhibit different behaviors for different core radius.

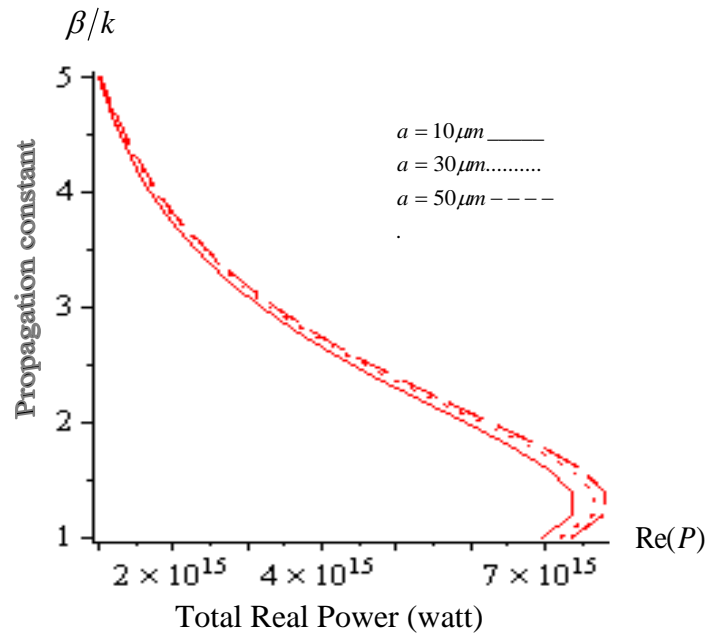


Figure 5.14: The total real part of the power flowing through the structure in TE mode versus the propagation constant with different value of core radius a . Fiber parameter $F = 0.56$, $\mu_{cl} = 1$, $C = 1$, $\omega_p/2\pi = 10\text{GHz}$, $\omega_c/2\pi = 1\text{GHz}$ and $\nu/2\pi = 2\text{GHz}$.

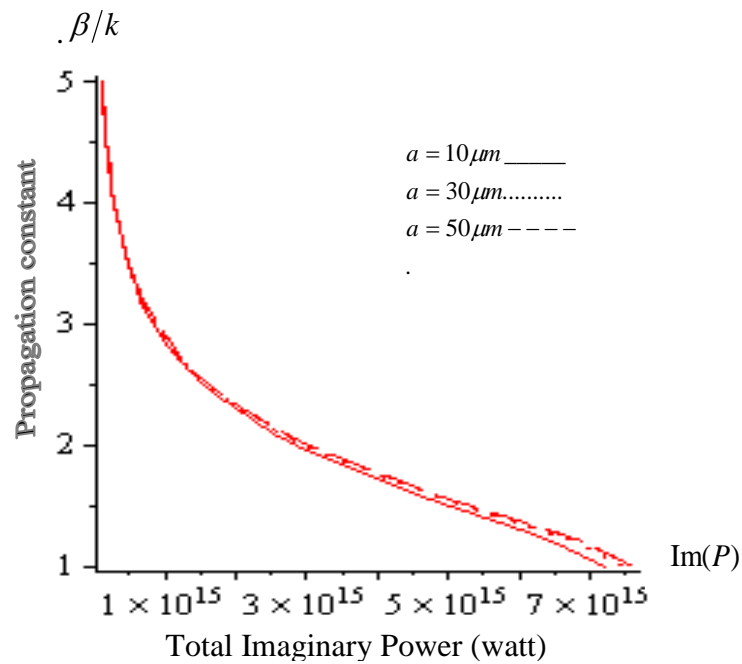


Figure 5.15: The total imaginary part of the power flowing through the structure in TE mode versus the propagation constant with different value of core radius a . Fiber parameter $F = 0.56$, $\mu_{cl} = 1$, $C = 1$, $\omega_p/2\pi = 10\text{GHz}$, $\omega_c/2\pi = 1\text{GHz}$ and $\nu/2\pi = 2\text{GHz}$.

To study the total power with different parameters for TM mode, Eq. (3.15) must be solved. Figure 5.26 and figure 5.17 respectively, show the total $\text{Re}(P)$, $\text{Im}(P)$ as given frequency and different values core radius. As shown in figure 5.16, the negative total $\text{Re}(P)$ means, the dependence of the vector \mathbf{S} in the core layer LHM in the opposite direction for vector \mathbf{k} , $\text{Re}(P)$ decreases as increasing a , and the effect core radius gives different behaviors. As shown in figure 5.17 the positive total $\text{Im}(P)$, means that, the $\text{Im}(P)$ is very large in the clad region, $\text{Im}(P)$ increases as the core radius increases, and the change in radius a exhibit different behaviors in the power curve.

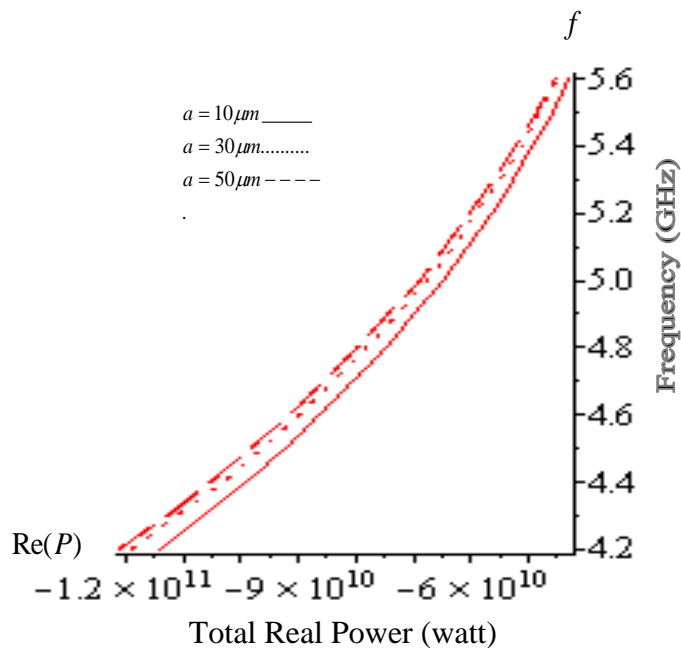


Figure 5.16: The total real part of the power flowing through the structure in TM mode versus the frequency with different value of core radius a . Fiber parameter $F = 0.56, \mu_{cl} = 1, A = 1, \omega_p/2\pi = 10\text{GHz}, \omega_c/2\pi = 1\text{GHz}$ and $\nu/2\pi = 2\text{GHz}$.

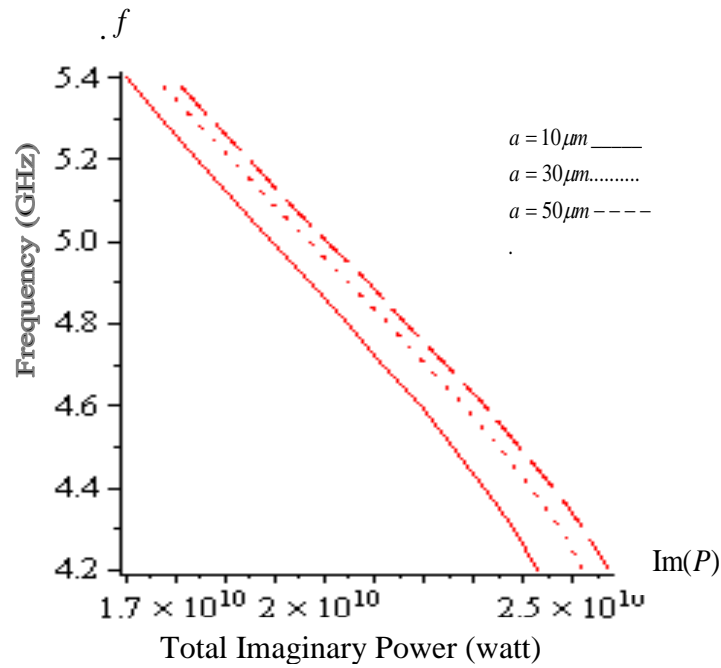


Figure 5.17: The total imaginary part of the power flowing through the structure in TM mode versus the frequency with different value of core radius a . Fiber parameter $F = 0.56$, $\mu_{cl} = 1$, $A = 1$, $\omega_p/2\pi = 10\text{GHz}$, $\omega_c/2\pi = 1\text{GHz}$ and $\nu/2\pi = 2\text{GHz}$.

Figures 5.18 and 5.19 represent respectively, the relation between, the total $\text{Re}(P)$, $\text{Im}(P)$ and the propagation constant with different core radius for TM polarization. As figure 5.18 shows, $\text{Re}(P)$, has the negative value, total $\text{Re}(P)$ decreases for increases core radius with given β/k and the increasing a gives different behaviors of $\text{Re}(P)$. As show in figure 5.19, $\text{Im}(P)$ is positive, $\text{Im}(P)$ has peak value at specific value of β/k , and $\text{Im}(P)$ increases with increasing core radius a .

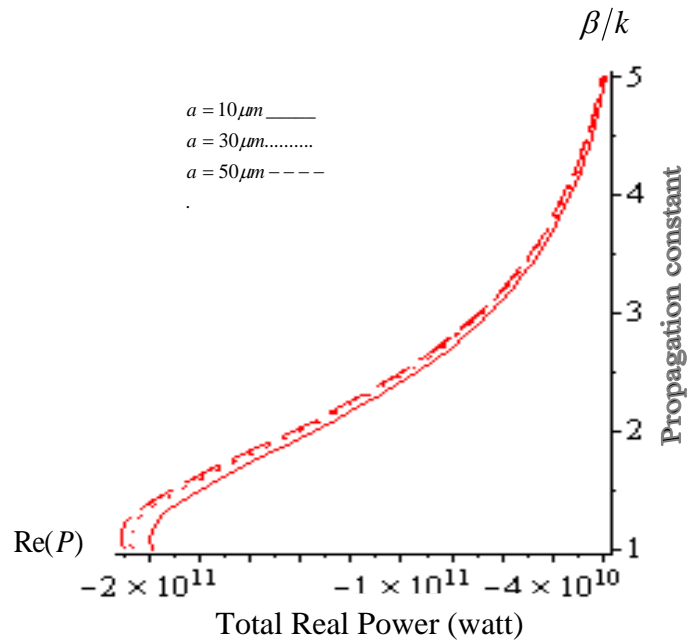


Figure 5.18: The total real part of the power flowing through the structure in TM mode versus the propagation constant with different value of core radius a . Fiber parameter $F = 0.56$, $\mu_{cl} = 1$, $A = 1$, $\omega_p/2\pi = 10GHz$, $\omega_c/2\pi = 1GHz$ and $\nu/2\pi = 2GHz$.

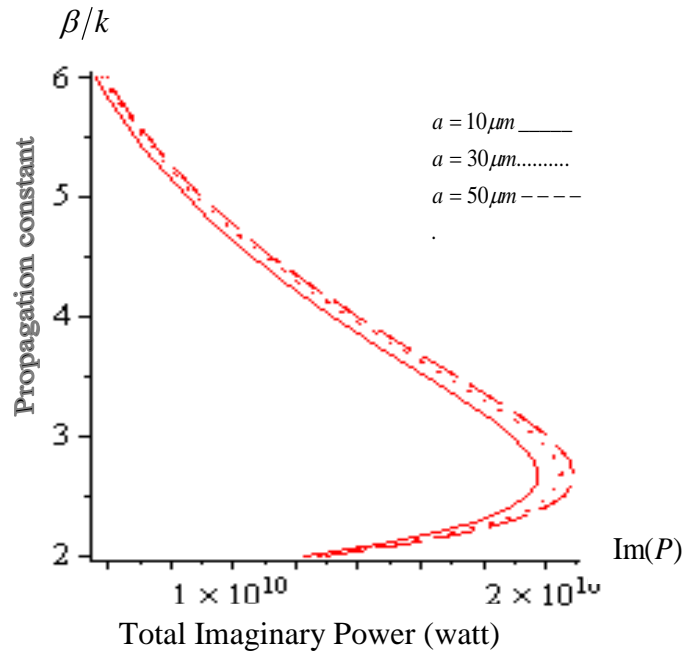


Figure 5.19: The total imaginary part of the power flowing through the structure in TM mode versus the propagation constant with different values of core radius a . Fiber parameter $F = 0.56$, $\mu_{cl} = 1$, $A = 1$, $\omega_p/2\pi = 10GHz$, $\omega_c/2\pi = 1GHz$ and $\nu/2\pi = 2GHz$.

In figures 5.20 and 5.21, we study respectively, the effect of the parameter F with frequency for plotted $\text{Re}(P)$ and $\text{Im}(P)$ in case TE mode. As shown in figure 5.20, the $\text{Re}(P)$ behave as the same in figure 5.12 but the power have same behaviors for different values F . As we can see in figure 5.21, the total $\text{Im}(P)$ described as in figure 5.13, and the effect of F does not appear which gives the same behaviors for different values F .

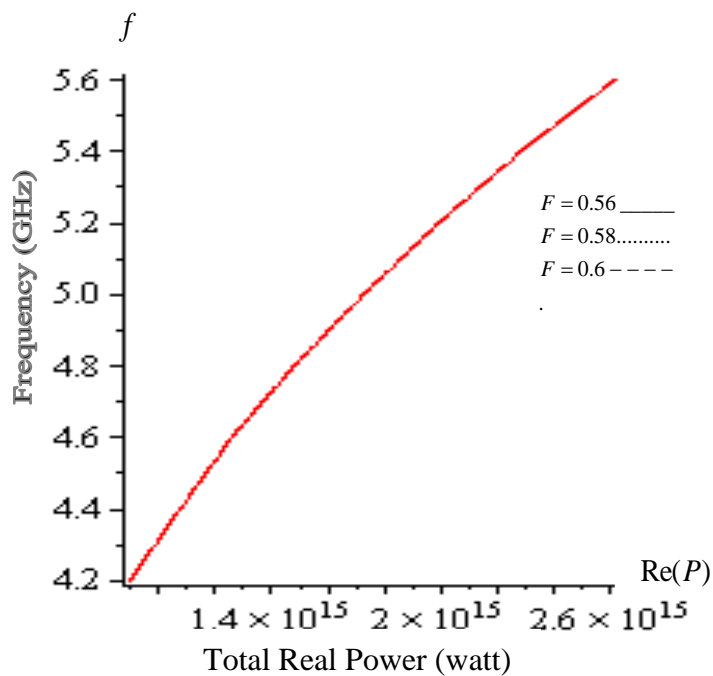


Figure 5.20: The total real part of the power flowing through the structure in TE mode versus the frequency with different values of F . Fiber parameter $a = 50\mu m$, $\mu_{cl} = 1$, $C = 1$, $\omega_p / 2\pi = 10\text{GHz}$, $\omega_c / 2\pi = 1\text{GHz}$ and $\nu / 2\pi = 2\text{GHz}$.

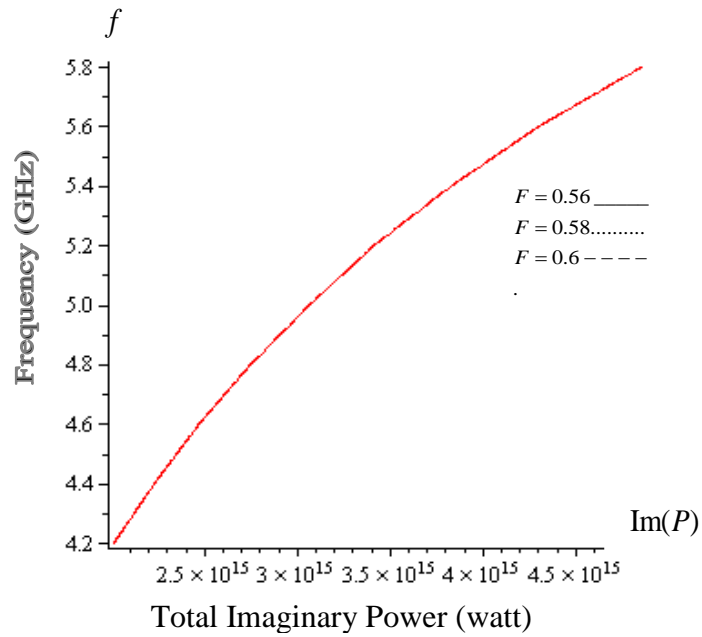


Figure 5.21: The total imaginary part of the power flowing through the structure in TE mode versus the frequency with different values of F . Fiber parameter $a = 50\mu m$, $\mu_{cl}=1$, $C=1$, $\omega_p/2\pi = 10GHz$, $\omega_c/2\pi = 1GHz$ and $\nu/2\pi = 2GHz$.

In figures 5.22 and 5.23, the total $Re(P)$ and $Im(P)$ are plotted respectively, versus the frequency for different values of F in case TM mode. As shown in figure 5.22, the $Re(P)$ described as in figure 5.16 and the curves exhibit the same behaviors for different values F . As we can see in figure 5.23 the $Im(P)$ have the same as in figure 5.17 but the curves are agreement to others with increasing F .

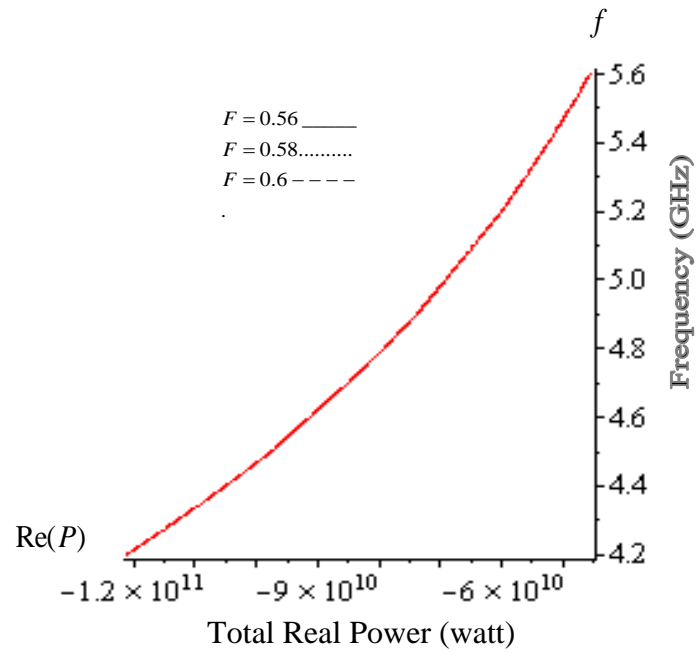


Figure 5.22:The total real part of the power flowing through the structure in TM mode versus the frequency with different values of fractional area F . Fiber parameter $a = 50\mu m$, $\mu_{cl} = 1$, $A = 1$, $\omega_p/2\pi = 10GHz$, $\omega_c/2\pi = 1GHz$ and $\nu/2\pi = 2GHz$.

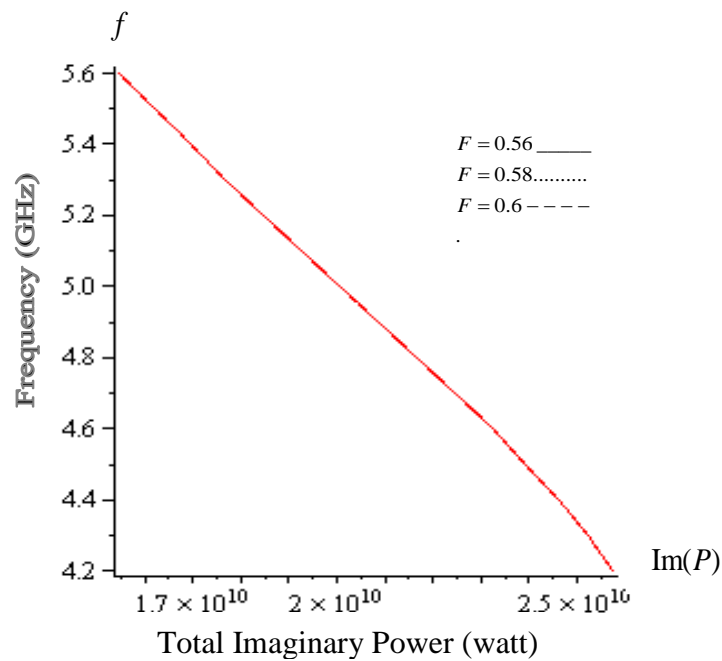


Figure 5.23:- The total imaginary part of the power flowing through the structure in TM mode versus the frequency with different values of fractional area F . Fiber parameter $a = 50\mu m$, $\mu_{cl} = 1$, $A = 1$, $\omega_p/2\pi = 10GHz$, $\omega_c/2\pi = 1GHz$ and $\nu/2\pi = 2GHz$.

CHAPTER SIX

CONCLUSIONS

In this thesis all modes have been analyzed in an optical fiber with core layer consisting of LHM and the cladding layer semiconductor material.

The dispersion curves are plotted and described for TE, TM, HE, and EH modes.

In this structure, it is significant to study the dispersion relation with changing core radius a and the fractional area F

With the dispersion TE, TM, HE and EH modes, the following observations are obtained:

- The dispersion curves in fast and slow mode for TE, TM, HE, and EH modes appear in the structure, TM mode has the smallest propagation constant, TE has largest propagation constant and dispersion curve for (HE, EH) mode agree on others.
- In case of TM mode, the dispersion curve exhibit different behaviors with different values of fractional area F . The propagation constant increases as the fractional area F increases with given frequency.
- In case of TM mode, the dispersion curve exhibit the same behaviors with different values of core radius a for given frequency.
- In case of TE mode, the dispersion curve exhibit different behaviors with different values of fractional area F . The propagation constant decreases as the fractional area F increases for given frequency and the largest propagation constant released at smallest fractional area.
- In the case of TE mode, the dispersion curve take the same behaviors agreement on each other as the core radius a increase with given frequency.
- In the case of HE and EH modes, dispersion curves exhibit different behaviors with different fractional area F and the propagation constant increases as the fractional area F increase.
- In the case of HE and EH modes, the dispersion curves take the same behaviors agreement to each other with different values of core radius a and given frequency.

The total carrying power transported in the core and the clad are described for both cases of TE and TM modes only with different variables values, fractional area F and the core radiuses a .

In the case TE mode the, the following observing are obtained

- The total carrying power $\text{Re}(P)$ and $\text{Im}(P)$ flow in the core and the clad has positive value and takes different behaviors with different core radius a for given frequency. The total power $\text{Re}(P)$ and $\text{Im}(P)$ increases as core radius a increase with given frequency.
- The total carrying power $\text{Re}(P)$ and $\text{Im}(P)$ that transported with in core and the clad has positive and take different behaviors with different core radius a for given propagation constant. The total $\text{Re}(P)$ and $\text{Im}(P)$ increase as core radius a increase as given propagation constant.
- The total power $\text{Im}(P)$ and $\text{Re}(P)$ transported in the core and the clad has positive value and exhibit the same behaviors agreement to others as increasing fractional area F for given frequency.
- The total power $\text{Im}(P)$ transported in the core and the clad are larger than total power $\text{Re}(P)$ as given frequency. The total power $\text{Im}(P)$ and $\text{Re}(P)$ are equal for given propagation constant.

In the case TM mode the, the following observing are obtained:

- The total carrying real power $\text{Re}(P)$ transported in the core and the clad has negative value and exhibit different behaviors as change in core radius a . The total power $\text{Re}(P)$ decreases as core radius a increase for given frequency and given propagation constant also.
- The total carrying power $\text{Im}(P)$ transported in the core and the clad has positive and exhibit different behaviors as change in core radius a . The total power $\text{Im}(P)$ increases as core radius a increase for given frequency and given propagation constant also.

- The total power $\text{Re}(P)$ transported in the core and the clad has negative values and exhibit the same behaviors in agreement to others as increasing fractional area F for given frequency.
- The total power $\text{Im}(P)$ transported in the core and the clad has positive values and exhibit the same behaviors in agreement to others as increasing fractional area F for given frequency.
- The total power $\text{Re}(P)$ transported in the core and the clad are smaller than total power $\text{Im}(P)$ for given frequency. The total power $\text{Im}(P)$ is larger than $\text{Re}(P)$ for given propagation constant.

Applications:

In this thesis, the fiber structure have many applications. One of most important as fiber-optics communications which transmission the data rates longer distance and higher bandwidth between two ends fiber than other forms of communications, it can be used as a media for telecommunication and computer networking. In the second application for this fiber used as fiber-optics sensors with different wavelength of light because no electrical power is needed at the location. In anther way it can be used also as fiber illumination application light guides, fiber lasers and imaging optics.

Advantages:

- 1- The amount of data rates transmission between two ends of the fiber has the same with different fiber core diameter because there is no change in the dispersion relation as change in the core radius.
- 2- In cases TM, HE and EH modes, the velocity that used to carry the information in the fiber increases, because the propagation increases when the fractional area F increases.
- 3- The core-clad fiber gives the same power to transmit data as increasing fractional area F .
- 4- In case of TM mode, core –clad fiber gives small power to carry data when increasing core radius.

Disadvantages:

- 1- In case of TE mode, the speed that carry data rates in the fiber decreases because the propagation decreases as fractional area increases.
- 2- The core –clad fiber gives large power to transmit data in the fiber when the core diameter increases for case TE mode

REFERENCES

- [1] K. Okamoto, Fundamentals of Optical Waveguides, Second Edition, Elsevier Academic Press, Elsevier, U. S. A (2006).
- [2] K. Iizuka, Elements Of Photonics. Volume II, For Fiber and Integrated Optics. Wiley Interscience Publication, New York, U. S. A (2002).
- [3] H. J. Eorn, Electromagnetic Wave Theory for Boundary-Value. Problems, Springer Publication, Germany (2004).
- [4] A. Lipson, S. G. Lipson and H. Lispon, Optical Physics, Fourth Edition. Cambridge University Press, New York, U. S. A (2010).
- [5] C. Chen, Foundation for Guided Wave Optics, First Edition, Wiley- Interference Publication, New Jersey, U. S. A (2007).
- [6] F. Pedrotti and L. Pedrotti, Introduction to Optics, Second Edition, Prentics Hall, addision wesley, New Jersey, U. S. A (1993).
- [7] J. Crisp, Introduction to Fiber Optics. 2nd Edition, Newnes Publication, Oxford, U. K (2001).
- [8] V. G. Veselago, The Electrodynamics of Substances With Simultaneously Negative Values of ϵ and μ , Sovtet Physics Uspekhi, Vo 10, No 4, 509-514, (1968).
- [9] C. Calzo and T. Itoh, Electromagmatic Metamaterials, Transmission Live Theory And Microwave Applications. Wiley Interscience Publication, United States of America, New Jersey, U. S. A (2006).
- [10] P. Markos and C. M. Soukoulis, Wave Propagation From Electrons to Photonic Crystals and Left-Handed Materials. Princeton University press, Oxford, U. K (2008).
- [11] A.V. Novitsky and L.M. Barkovsy, guided mode in negative refractive index fibers , J. Opt. A, Opt. 7, S51–S56, (2005).
- [12] L. F. Shen and Z. H. Wang, Guided mode in fiber with left – handed materials, , J. Opt. Soc. Am. Vol. 26, No 754-759, (2009).
- [13] A. W. Snyder and J. D. Love, Optical Waveguide Theory. Chapman and Hall Publication, London, U. K (1983).

- [14] L. F. Shen and Z. H. Wang, Surface Mode in a Hollow Optical Fiber Including negative refractive index, Microwave Conference, China-Japan Joint, vol, no, pp, 294,297, (10-Sept, 2008).
- [15] G. B. Arfen and Hans. J. Weber, Mathematical Methods for Physicists, 6th edition, Elsevier academic press, New York, U. S. A, (2005).
- [16] J. Pipre, Semiconductor Optoelectronic Devices- Introduction to Physics and Simulation, Academic Press Publication, California (1996).
- [17] D. K. Shroder, Semiconductor Material and Device Characterization. Third Edition, Wiley Interscience Publication, New Jersey, U. S. A (2006).
- [18] C. F. Klingshirn, Semiconductor Optics, Springer Publication, New York, U. S. A (1996).
- [19] W. L. Hwang and D. M. Bolle, Magnetoplasma Surface Wave Analysis For ANH- Guide Structure Contaning Semiconductor, International Journal of Infrared and Millimeter Wave, Vol 4, No 5 (819-830), (1983).
- [20] O. V. Shramova, Transmission Spectra in Ferrite- Semiconductor Periodic Structure , Progress In Electromagnetics Research M, Vol. 7, 71–85, (2009).
- [21] O. T. Jiang and Y. Feng, Slow-Light propgation in a cylindrical dielectric waveguide with metamaterial clading, J. Phy. D: Appl. Phys. 44, 1-6, (2011).
- [22] H. M. Mousa and M. M. Shabat, TE wave in a cylindrical superlattices (LANS) and left handed material (LHM) waveguide structure, Antenna Technology (iWAT), International Workshop on, Vol, no, pp.286-289, March- (2013).
- [23] H. M. Mousa and M. M. Shabat, TM waves in cylindrical superlattices (LANS) bounded by left-handed material (LHM), Applied Physics A, Vol. 111, Issue 4, pp. 1057- 1063, November- (2012).